



GEORGIA
DEPARTMENT OF NATURAL RESOURCES

ENVIRONMENTAL PROTECTION DIVISION

Final 2016 Ozone Exceedance Report for Atlanta, Georgia

Prepared by:
Data and Modeling Unit
Planning and Support Program
Air Protection Branch
Environmental Protection Division

July 5, 2017

Executive Summary

Ozone concentrations in Georgia have decreased over the past 25 years. On October 1, 2015, the 8-hour ozone National Ambient Air Quality Standard (NAAQS) was lowered from 75 ppb to 70 ppb. In 2016, six Metropolitan Statistical Areas (MSAs) experienced ozone exceedance days where the measured 8-hour average ozone concentration was above 70 ppb. For each ozone exceedance day, the Data and Modeling Unit developed an initial exceedance report with preliminary analyses of air quality, meteorological, and emission data to aid in determining the cause of the ozone exceedance. If ozone exceedances occur frequently, the design value (3-year average of 4th highest maximum daily 8-hour ozone concentrations) can exceed the ozone NAAQS, and EPA can classify the area as nonattainment. The recently certified 2016 ozone measurements show that Atlanta is the only area in Georgia currently violating the 2015 ozone NAAQS.

A final, in-depth ozone exceedance report was developed for the Metro Atlanta area to identify causes of the 2016 ozone exceedances. The report includes trend analysis of ozone concentrations and meteorological conditions in Atlanta during 1990-2016, multiple linear regression (MLR) analysis and classification and regression tree (CART) analysis to understand the relationship between ozone and environmental variables, Hybrid Single Particle Lagrangian Integrated Trajectory (HYSPLIT) back trajectory analysis to determine the origin of air masses, and establish source-receptor relationships on ozone exceedance days, and analysis of VOC and NOx measurements to understand the impacts of precursors on ozone formation.

In summary, the following factors likely contributed to 2016 ozone exceedances in Atlanta:

- 1) Low relative humidity in the afternoon;
- 2) High daily maximum air temperature;
- 3) Low cloud coverage;
- 4) High ozone on previous days;
- 5) Low wind speed;
- 6) NOx emissions, mainly from local on-road mobile sources;
- 7) VOC emissions, mainly from biogenic sources in the summer months with additional contributions from local on-road mobile sources in the evening and morning hours; and
- 8) Local transport of emissions from the Atlanta urban core to monitors outside the urban core.

This final ozone exceedance report can be used to guide future air quality management practices in Georgia to aid in preventing future ozone exceedances.

List of Acronyms

aNMOC	Anthropogenic Non-Methane Organic Carbon
AQI	Air Quality Index
AQS	Air Quality System
CAMD	Clean Air Markets Division
CART	Classification and Regression Tree
CAS	Chemical Abstract Service
CASTNET	Clean Air Status and Trends Network
CO	Carbon Monoxide
DMRC	Dekalb Mental Retardation Center
EBIR	Equal Benefit Incremental Reactivity
ENSO	El Niño–Southern Oscillation
EPA	U.S. Environmental Protection Agency
EPD	Environmental Protection Division
HYSPLIT	Hybrid Single Particle Lagrangian Integrated Trajectory
IR	Incremental Reactivity
LIDAR	Light Detection and Ranging
LT	Local Time
MAE	Mean Absolute Error
MB	Mean Bias
MDA8O3	Maximum Daily 8-hour Average Ozone Concentrations
MIR	Maximum Incremental Reactivity
MLR	Multiple Linear Regression
MOIR	Maximum Ozone Incremental Reactivity
MSAs	Metropolitan Statistical Areas
NAAQS	National Ambient Air Quality Standards
NAM	North American Mesoscale
NEI	National Emissions Inventory
NMB	Normalized Mean Bias
NME	Normalized Mean Error
NOAA	National Oceanic and Atmospheric Administration
NO _x	Oxides of Nitrogen
OMI	Ozone Monitoring Instrument
PAMS	Photochemical Assessment Monitoring Stations
PBL	Planetary Boundary Layer
QA	Quality Assurance
RH	Relative Humidity
RMSE	Root Mean Square Error
RWC	Reactivity-weighted concentrations
SEARCH	Southeastern Aerosol Research and Characterization
VOC	Volatile Organic Compounds

Table of Contents

Executive Summary	1
1. Introduction.....	4
2. Ozone Exceedance Trends in the Metro Atlanta Area during 1990-2016	8
3. Meteorological Conditions in Metro Atlanta area during 1990-2016.....	13
4. Ozone Regression Model	18
Correlation Analysis	18
Updated MLR Ozone Model.....	20
5. CART Analysis.....	22
Regression tree CART analysis	22
Classification tree CART analysis	25
High ozone day conditions.....	26
6. Meteorological Time Series Analysis	29
7. HYSPLIT back trajectory analysis	33
8. Ozone and NOx precursor.....	39
Diurnal patterns of NOx observations on ozone exceedance days	41
Day-of-Week patterns of NOx observations on ozone exceedance days.....	41
Monthly patterns of NOx observations on ozone exceedance days.....	41
Indicator analysis	50
NOx Trends Based on OMI Satellite Data.....	52
9. Ozone and VOCs precursors.....	55
Relationship between peak 8-hr ozone and anthropogenic VOC	55
Ozone-VOCs Time Series Analysis.....	65
10. Summary	71
11. References.....	73

1. Introduction

Ozone pollution can impair lung function and cardiovascular health. Ground-level ozone is formed in the atmosphere by chemical reactions of volatile organic compounds (VOCs) and oxides of nitrogen (NO_x) in the presence of sunlight. Sources of VOCs include fuel combustion, fuel evaporation, paints, solvents, and vegetation. NO_x emissions are primarily from the combustion of fuels. The U.S. Environmental Protection Agency (EPA) lowered the National Ambient Air Quality Standards (NAAQS) for ground-level ozone from 75 ppb (2008 ozone NAAQS) to 70 ppb (2015 ozone NAAQS) to better protect public health and welfare.

Ozone concentrations in Georgia have decreased over the years (Figure 1) in various Metropolitan Statistical Areas (MSAs). The Metro Atlanta area was the only area in Georgia designated nonattainment for the 2008 ozone standard, but was redesignated to attainment in June 2017. It is expected that EPA will complete designations for the 2015 ozone standard of 70 ppb in 2018.

In 2016, six MSAs experienced ozone exceedances where the measured 8-hour average ozone concentration was above 70 ppb (Figure 2). For each ozone exceedance day, the Data and Modeling Unit developed an initial exceedance report with a preliminary analysis of air quality, meteorological, and emission data to help understand the cause of the ozone exceedance. If ozone exceedances occur frequently the design value (3-year average of 4th highest maximum daily 8-hour ozone concentrations) can exceed the ozone NAAQS and EPA can classify the area as nonattainment. Based on 2014-2016 ozone data, Atlanta will likely be designated nonattainment for the 2015 ozone standard as five monitors are currently above 70 ppb.

The eleven ozone monitors in the Metro Atlanta area have altogether experienced 29 ozone exceedance days in 2016 (Figure 2). Detailed ozone exceedance days by monitor are displayed in Figure 3 and summarized by month in Table 1. In addition, ozone concentrations by ozone monitors in Atlanta on ozone exceedance days during 2016 are summarized in Table 2. Most of the 2016 ozone exceedances occurred at the Confederate Avenue monitor located in downtown Atlanta (Figure 3). In some cases, ozone exceedances occurred at several monitors on the same day, indicating a more regional pollution episode. Alternately, there were days when the ozone exceedance only occurred at one or two monitors which were likely caused by local production under specific meteorological conditions.

A final in-depth ozone exceedance report was developed for the Metro Atlanta area to identify causes of the 2016 ozone exceedances. The report includes trend analysis of ozone concentrations and meteorological conditions in Atlanta during 1990-2016, multiple linear regression (MLR) analysis and classification and regression tree (CART) analysis to understand the relationship between ozone and environmental variables, Hybrid Single Particle Lagrangian Integrated Trajectory (HYSPLIT) back trajectory analysis to determine the origin of air masses and establish source-receptor relationships on ozone exceedance days, and analysis of VOC and NO_x measurements to understand the impacts of precursors on ozone formation. This final ozone exceedance report can be used to guide future air quality management practices in Georgia to help prevent future ozone exceedances.

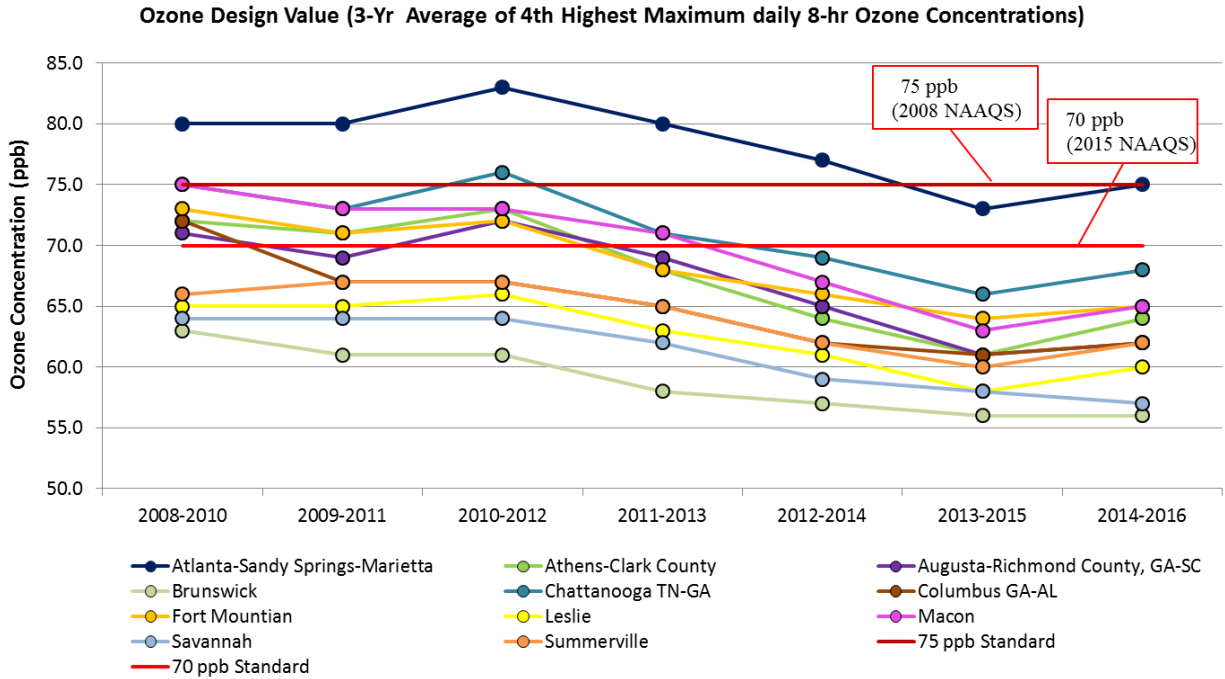


Figure 1. Trend of Ozone design values by various Metropolitan Statistical Areas (MSAs) in Georgia.

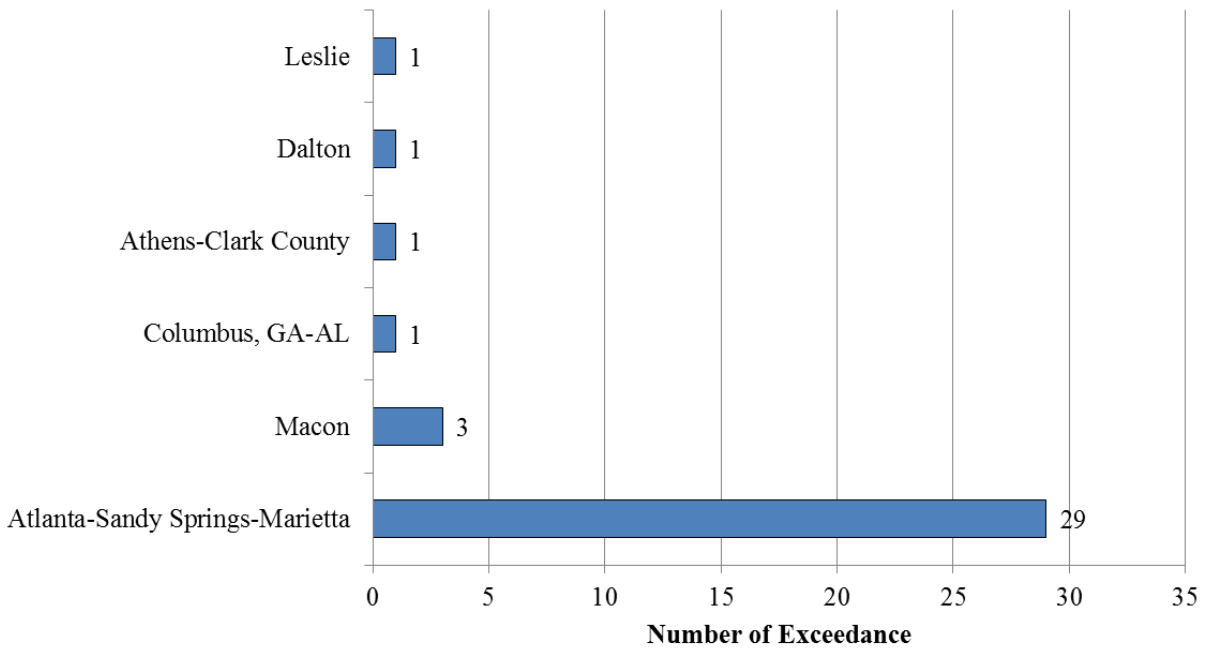


Figure 2. 2016 ozone exceedance days by MSAs in Georgia.

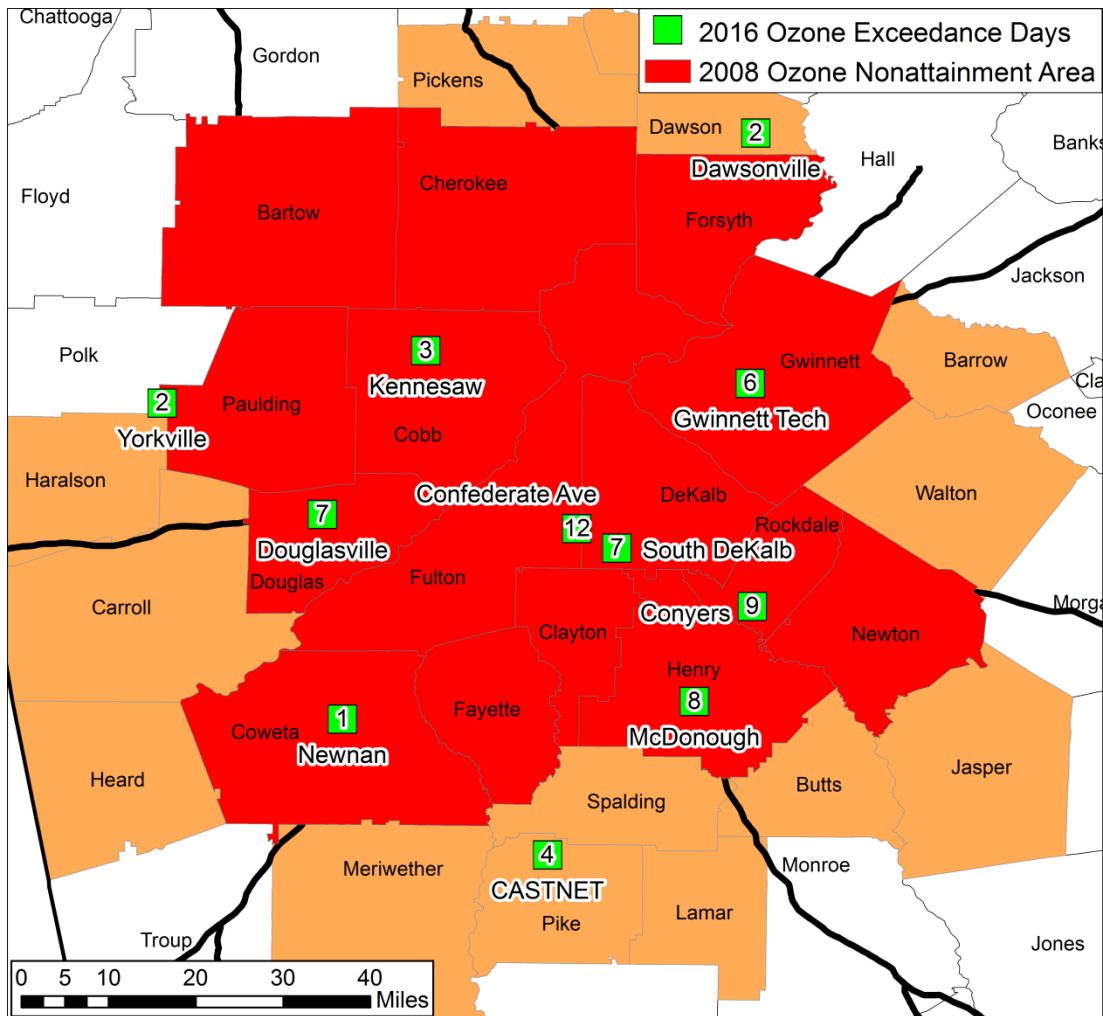


Figure 3. Locations of ozone monitors and number of 2016 ozone exceedance days in the Metro Atlanta area.

Table 1. Summary of 2016 ozone exceedances for eleven ozone monitors in Metro Atlanta area.

ID	Site Name	April	May	June	July	August	September	October	Total
131210055	Confederate Ave.	1	2	6	1	1	1		12
132470001	Conyers		2	4	2		1		9
131510002	McDonough		2	4	1	1			8
130970004	Douglasville		1	2	1		2	1	7
130890002	South DeKalb	1	1	4	1				7
131350002	Gwinnett Tech		3	3					6
132319991	CASTNET		1	2				1	4
130670003	Kennesaw			1	1	1			3
132230003	Yorkville		1	1					2
130850001	Dawsonville		1	1					2
130770002	Newnan			1					1
	Total	2	14	29	7	3	4	2	61

Table 2. Ozone concentrations (ppb) for eleven ozone monitors in Atlanta on exceedance days during 2016.

Month	Day	Confederate Avenue	Conyers	McDonough	Douglasville	South DeKalb	Gwinnett Tech	CASTNET	Kennesaw	Yorkville	Dawsonville	Newnan
April	29	78	64	63	59	74	66	54	59	54	54	55
May	23	67	69	74	64	61	64	68	66	62	58	63
May	24	74	82	78	66	74	73	67	70	63	64	69
May	25	69	71	70	65	68	72	71	69	64	78	65
May	26	65	64	58	54	61	78	55	59	55	56	56
May	28	55	54	50	71	52	53	49	64	71	48	57
May	31	71	48	49	60	65	59	58	63	58	52	63
June	8	64	70	78	61	60	55	67	59	60	49	60
June	9	74	65	65	75	70	67	78	65	60	58	87
June	10	88	77	70	86	82	82	75	105	78	76	69
June	11	66	68	60	54	78	82	54	54	50	58	56
June	13	75	75	89	58	74	59	62	68	55	50	56
June	21	62	73	68	58	63	60	62	54	54	50	61
June	25	64	70	72	58	63	53	56	57	52	52	52
June	27	74	57	52	52	64	80	50	54	50	50	51
June	29	71	76	84	62	67	57	70	63	62	51	59
June	30	85	61	70	62	83	59	47	64	59	65	63
July	1	68	77	73	57	66	67	61	65	61	58	59
July	2	64	73	63	50	64	57	59	54	56	52	60
July	20	Missing	60	61	74	71	59	58	76	53	50	61
July	25	72	49	48	44	62	53	38	51	36	46	42
August	3	66	63	71	53	62	54	59	48	49	39	51
August	23	75	51	54	54	65	55	44	71	36	42	49
September	7	74	68	61	57	59	64	51	59	54	52	55
September	8	61	72	58	51	60	66	58	51	47	53	54
September	15	57	51	49	71	51	54	51	62	69	52	55
September	25	55	49	44	71	52	53	46	60	67	50	50
October	3	63	51	48	71	56	57	60	60	53	53	65
October	13	58	65	64	61	Missing	54	74	59	60	51	60

2. Ozone Exceedance Trends in the Metro Atlanta Area during 1990-2016

Ozone exceedance trends in Atlanta during 1990-2016 were analyzed using ozone concentrations measured at the nine Georgia EPD ozone monitors located in the Atlanta nonattainment area (Table 3 and Figure 3). The 1990-2016 ozone data were downloaded from EPA Air Quality System (AQS). Note that the ozone measurements at Dawsonville and CASTNET monitors are not included in the following analysis since they are not in the Atlanta ozone nonattainment area.

Table 3. Nine Georgia EPD ozone monitors in the Atlanta nonattainment area.

ID	Site Name
130890002	South DeKalb
131210055	Confederate Avenue
131350002	Gwinnett Tech
132230003	Yorkville
132470001	Conyers
130970004	Douglasville
130770002	Newnan
131510002	McDonough
130670003	Kennesaw

Maximum daily 8-hour average ozone concentrations (MDA8O3) in Atlanta were calculated as the maximum MDA8O3 for the nine ozone monitors in Atlanta. The annual maximum, mean, and median MDA8O3 from April to October in 1990-2016 shows the inter-annual variability with a slight downward trend through the years (Figure 4). The annual mean MDA8O3 in 1999 is the highest at 71.8 ppb, and decreases to the lowest in 2013 with 47.6 ppb. This coincides with Georgia NOx emission reductions starting in 2003 and continuing to the present (Figure 5). The annual mean MDA8O3 increased slightly to 55.4 ppb in 2016, which was higher than the last four years from 2012-2015. Although the maximum MDA8O3 decreases through the years, the minimum MDA8O3 increased as a result of less ozone titration by NOx.

The MDA8O3 were compared with the 2015 ozone NAAQS (70 ppb) to identify ozone exceedance days. The number of exceedance days during the 1990-2016 ozone seasons shows a similar pattern. There were less than 20 ozone exceedance days during 2013-2015, but the number increased to 29 days in 2016. We see a high number of ozone days above 70 ppb in 1993, 1999, 2006, 2011, and 2016. There seems to be a 5-7 year period between these occurrences. It is similar to the 2-7 year period of El Niño–Southern Oscillation (ENSO), but not peaking in the same year. Further work is needed to determine if there is a potential connection between ozone concentrations and climate patterns.

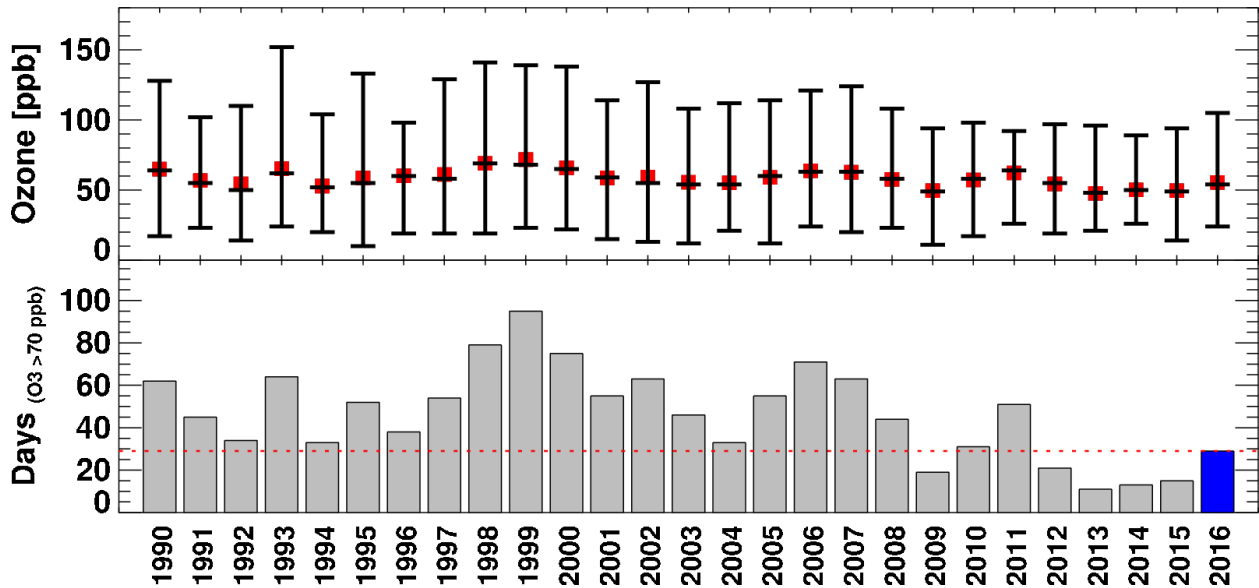


Figure 4. Annual mean MDA8O3 concentrations (top) and the number of days with ozone > 70 ppb (bottom) in April to October in 1990-2016 in Metro Atlanta area. 2016 is highlighted in blue.

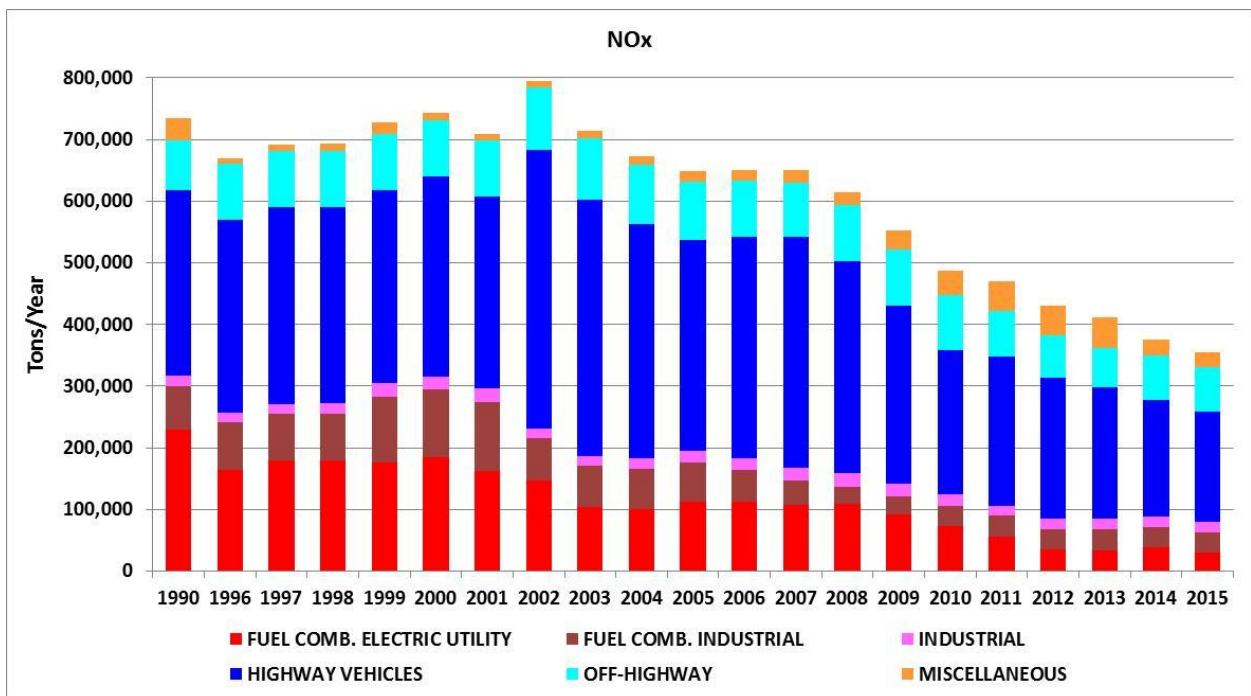


Figure 5. Georgia NOx emission trends by source sectors during 1990-2015 (data for 1991-1995 is not available). Data source: EPA 1990-2013 emission trend data, NEI2014, and 2015 CAMD data for 2015 inventory with emissions from other source sectors the same as 2014.

The monthly average ozone exceedance days and percentage of exceedance occurring in each month are summarized by different time periods during 1990-2016 in Metro Atlanta area (Figure 6). Typically, more than 70% of the ozone exceedances occur during June, July, and August when temperature is higher and sunlight is stronger, and less than 5% of the ozone exceedances occur in April and October when air temperature is relatively low. In 2016, ozone exceedances during June increased to 10 days and 35%, and more ozone exceedances occurred during May and September than during July and August. Close analysis of ozone exceedances during 2011-2016 (Figure 7) show strong year-to-year variation in the distribution of number of exceedance by months, but most exceedance still occurs during May to September.

Also, daily patterns of ozone exceedances were investigated (Figure 8). Generally, more ozone exceedances occur during weekdays than weekends, though the difference is small before 2010. Starting in 2011, many more ozone exceedances occur during weekdays than Sunday. Ozone exceedance on Saturdays is also high from 1990-1999.

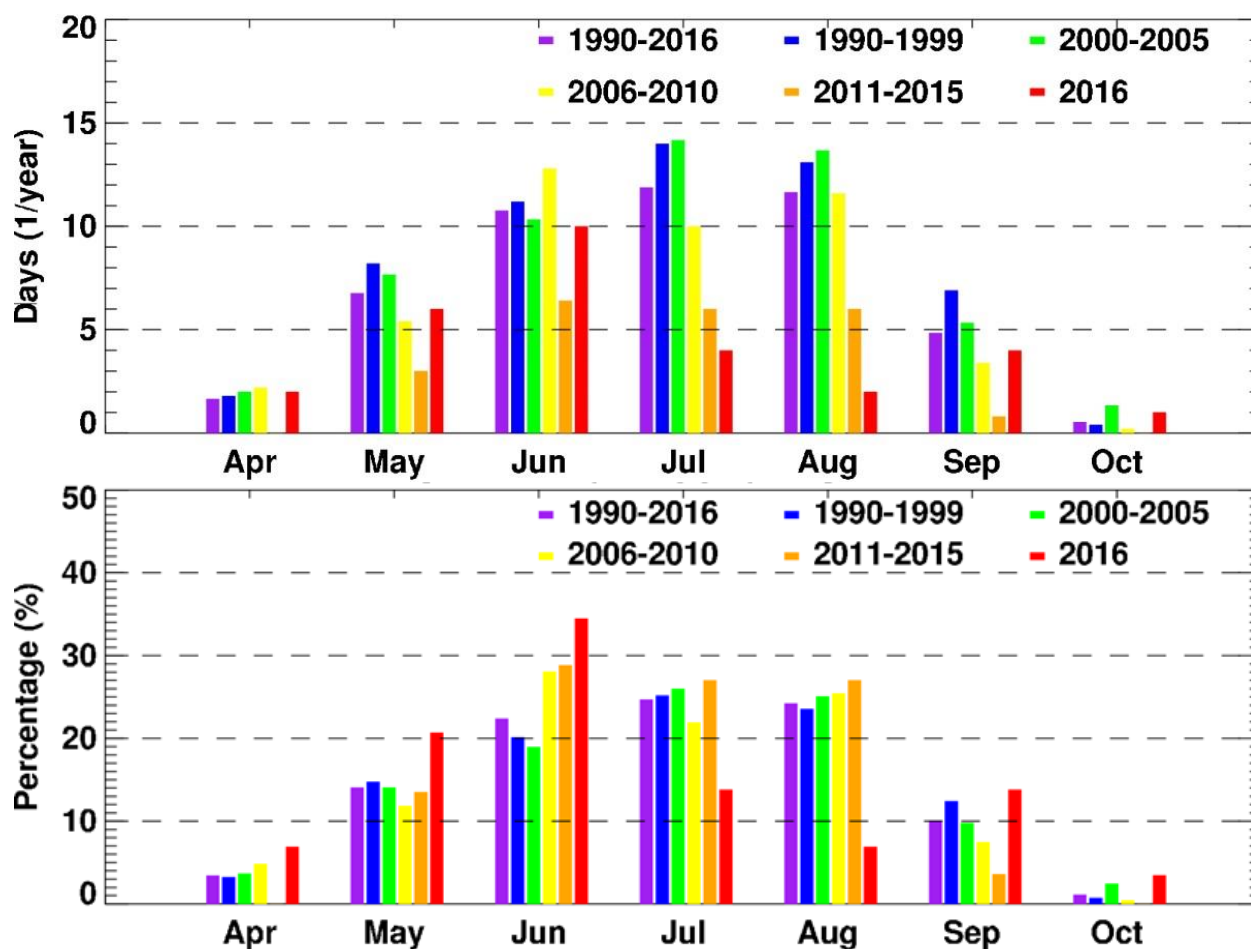


Figure 6. Monthly average number of ozone exceedance days (> 70 ppb) (top) and percentage of exceedances occurring in that month (bottom) in ozone season by different time periods during 1990-2016 in the Metro Atlanta area.

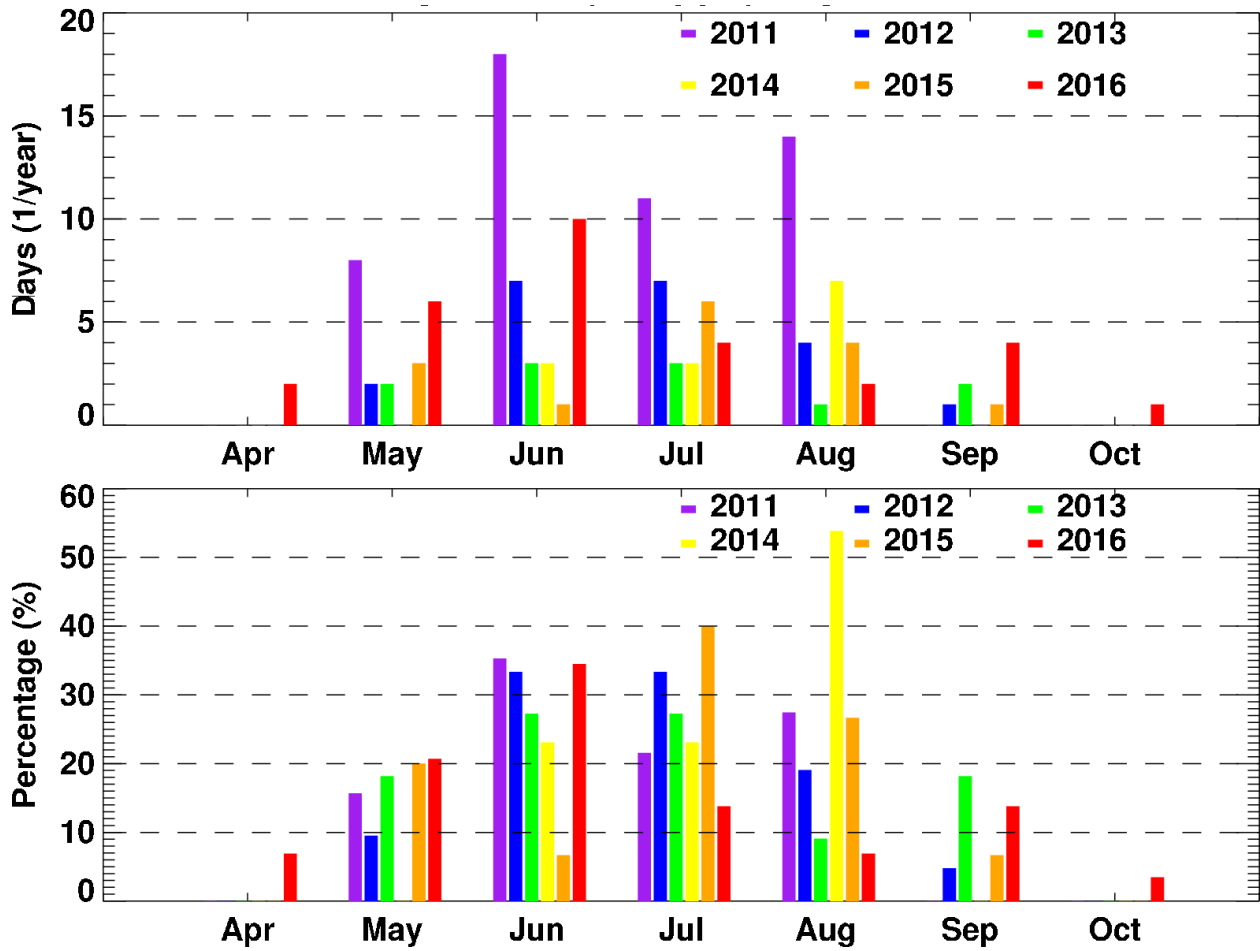


Figure 7. Monthly average number of ozone exceedance days (> 70 ppb) (top) and percentage of exceedances occurring in that month (bottom) in ozone season by different time periods during 2011-2016 in the Metro Atlanta area.

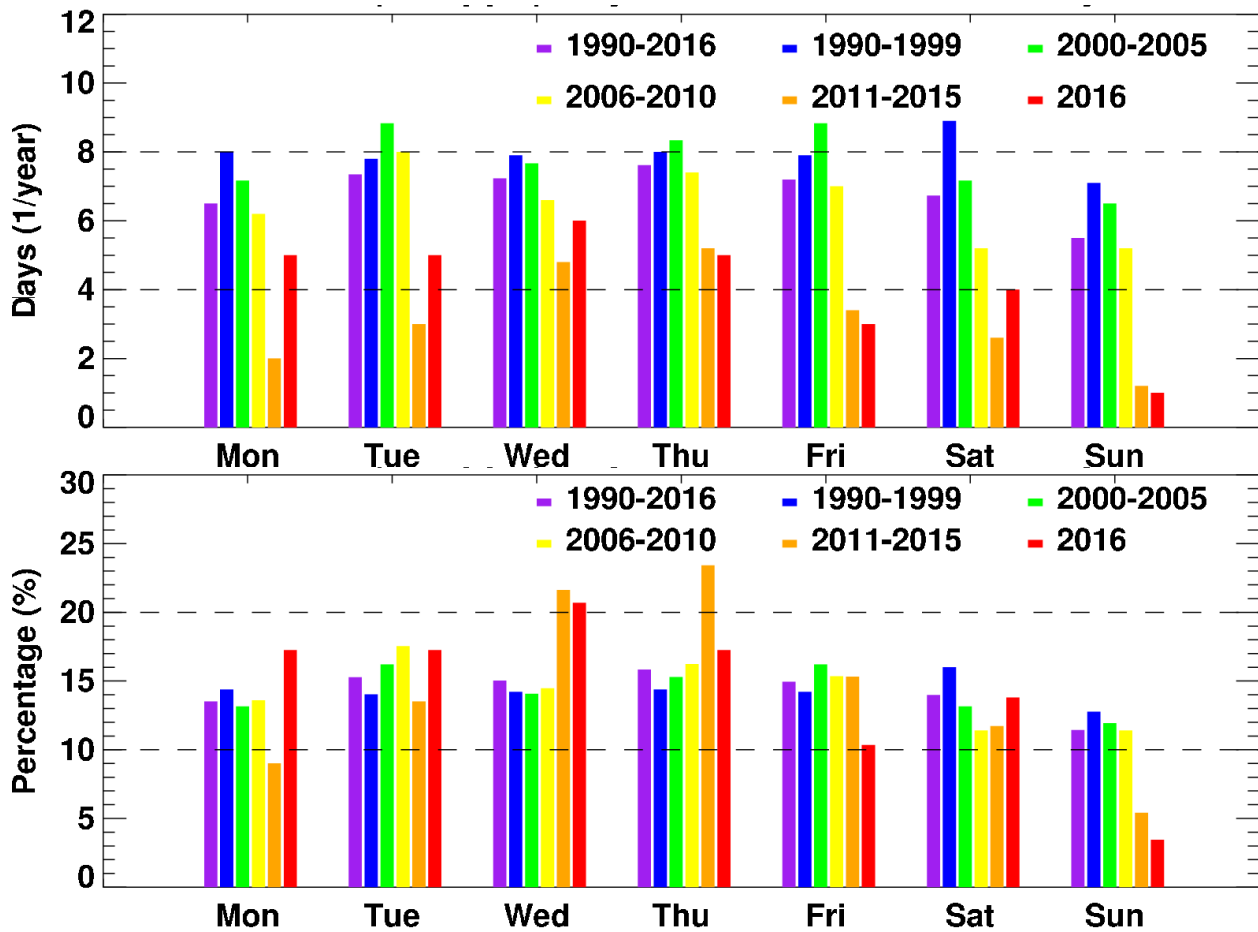


Figure 8. The number (top) and percentage (bottom) of ozone exceedance days (>70 ppb) by days of week for different periods during 1990-2016 in the Metro Atlanta area.

3. Meteorological Conditions in Metro Atlanta area during 1990-2016

Trends of meteorological conditions in Atlanta during 1990-2016 were analyzed using meteorological observations at Atlanta International Airport (Table 4) downloaded from https://mesonet.agron.iastate.edu/request/download.phtml?network=GA_ASOS. The observational intervals varied from one hour to several minutes depending on variables.

Table 4. Observed meteorological variables at Atlanta International Airport

Variables	Definition	Unit
tmpf	Air Temperature, typically @ 2 meters	degree of Fahrenheit
dwpf	Dew Point Temperature, typically @ 2 meters	degree of Fahrenheit
relh	Relative Humidity	%
drct	Wind Direction	degree from north
sknt	Wind Speed	knots
p01i	One hour precipitation for the period from the observation time to the time of the previous hourly precipitation reset.	
alti	Pressure altimeter	inches
mslp	Sea Level Pressure	millibar
vsby	Visibility	miles
gust	Wind Gust	knots
skyc1	Sky Level 1 Cloud Coverage	%
skyc2	Sky Level 2 Cloud Coverage	%
skyc3	Sky Level 3 Cloud Coverage	%
skyc4	Sky Level 4 Cloud Coverage	%

Ozone season means of the meteorological variables were calculated for each year and are shown in Figure 9, except pressure and wind direction which have insignificant inter-annual variations. For the period from April through October, 2016 is the warmest on record for Atlanta since 1878, according to NOAA/NCEI (Figure 10). The second warmest April through October period was in 2010 (NOAA/NCEI). The daily mean maximum temperature (T_{max}) in 2016 is 85.9°F, the daily mean average temperature (T_{avg}) in 2016 is 75.8°F, and the daily mean minimum temperature (T_{min}) in 2016 is 65.7 °F. 2016 also has the lowest cloud fraction, which is defined as the percentage of sky covered by clouds. Both AM and PM cloud fraction are less than 50%. In addition, 2016 AM relative humidity (RH) is 68.0%, the 3rd lowest following 2007 and 2011, and 2016 PM RH is 48.0%, the 2nd lowest following 2011. No significant deviation has been found for other meteorological variables in 2016. In summary, 2016 is one of the warmest and driest years on record with ample direct solar radiation. Such meteorological conditions are favorable for ground level ozone formation. Also, there have been higher ozone concentrations in additional years with similar meteorological conditions (Figure 4 and Figure 9).

The meteorological conditions for the 29 ozone exceedance days that occurred in 2016 are further investigated. The relative humidity, cloud fraction, wind speed in the morning and afternoon, and daily maximum and minimum temperatures on the day before and after each exceedance are compared to those on the exceedance day (Figure 11). For the days without observations, the data from two days before or after are used. Continuous exceedances lasting

more than one day are considered as one event. In general the ozone exceedance days feature relatively lower RH, less cloud coverage, lower wind speed, and higher daily max temperature. Other meteorological variables such as dew point temperature, pressure, and wind direction don't show a clear correlation with ozone exceedances. This is consistent with the analysis of meteorological and air quality data during the period from 1990-2016 mentioned above.

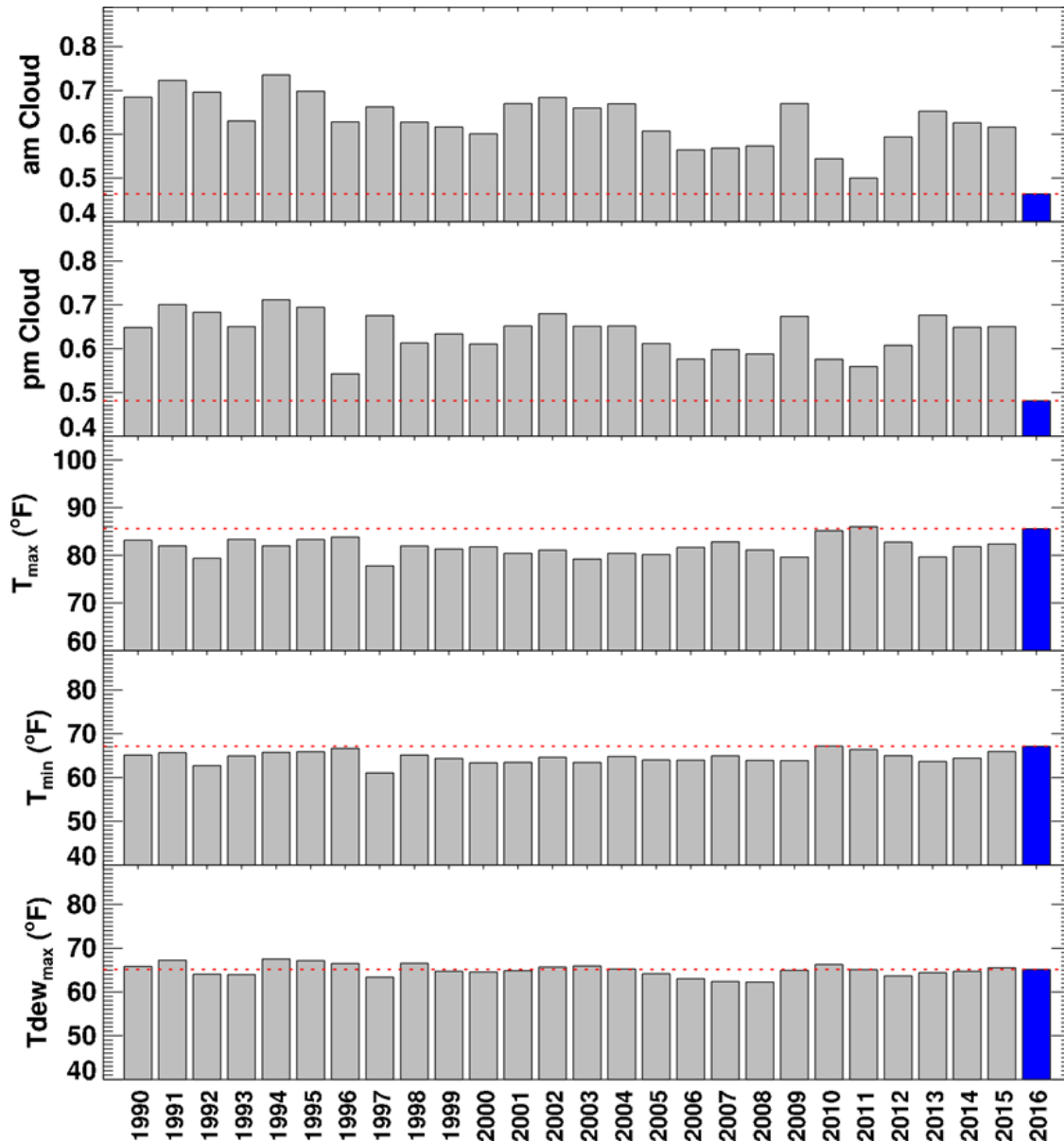


Figure 9. Atlanta ozone season mean meteorological conditions during 1990-2016. 2016 values are highlighted in blue and also represented by the red dotted line to facilitate comparison.

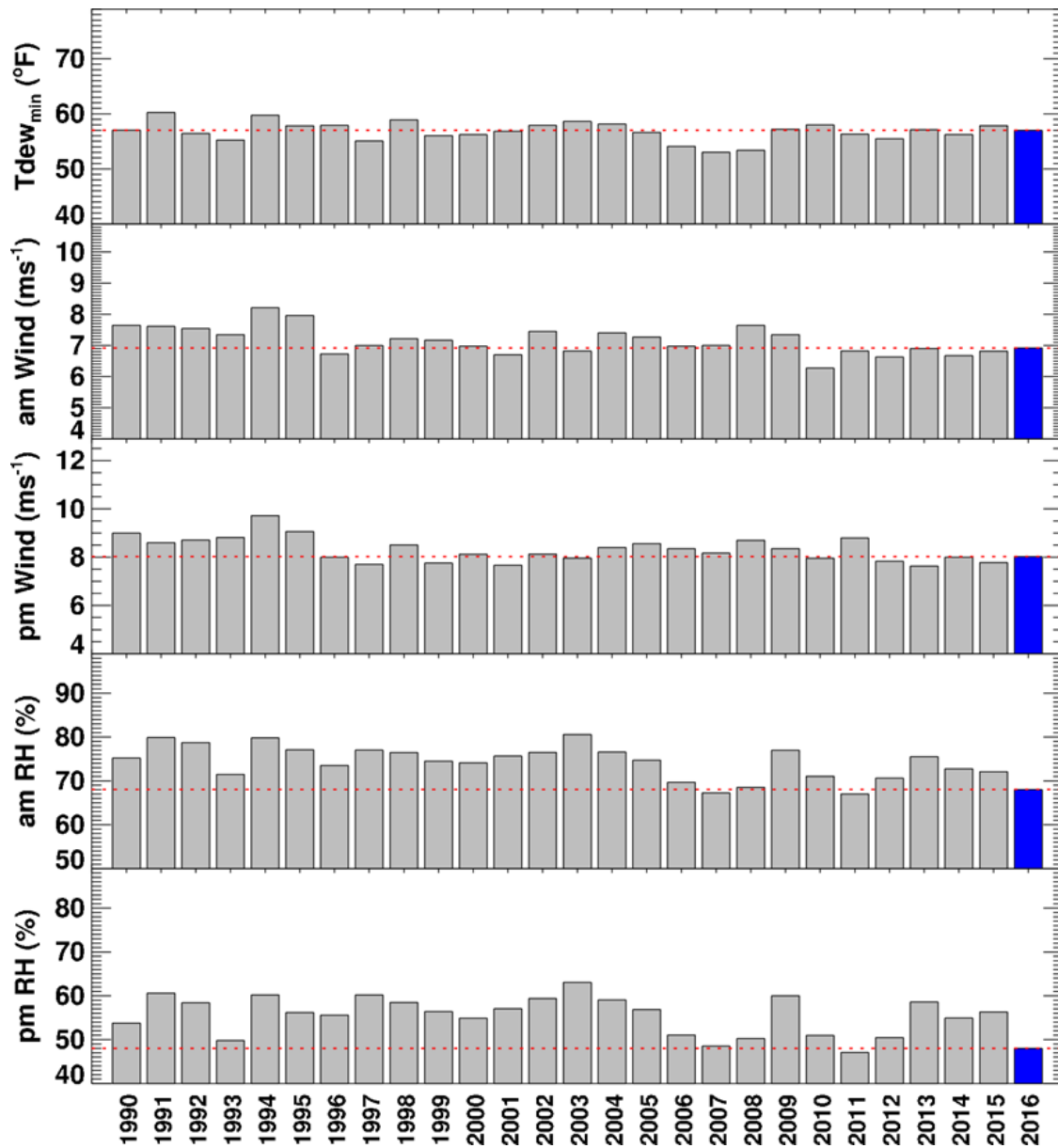


Figure 9. (continued). Atlanta ozone season mean meteorological conditions during 1990-2016. 2016 values are highlighted in blue and also represented by the red dotted line to facilitate comparison.

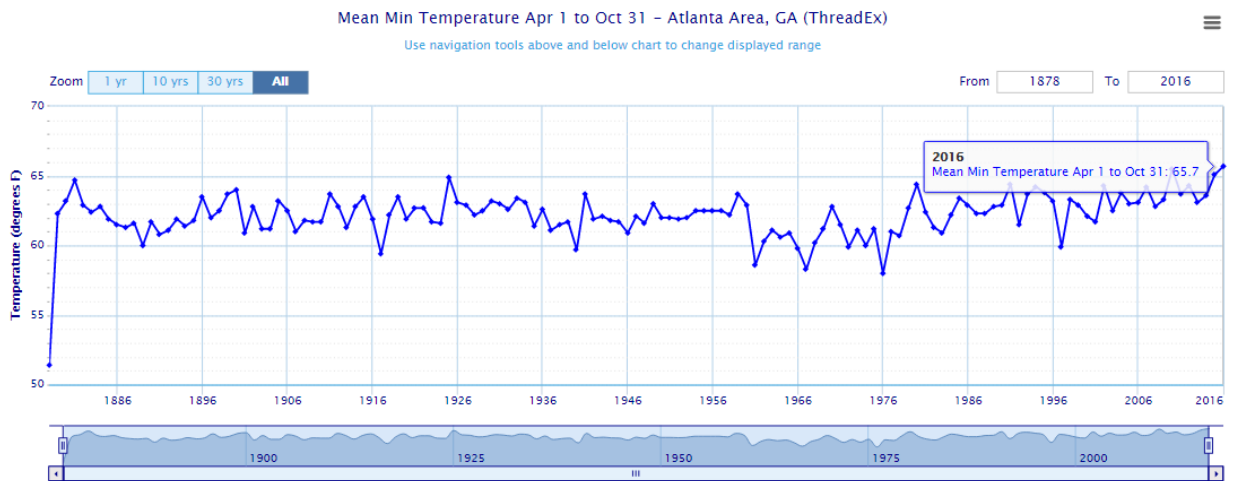
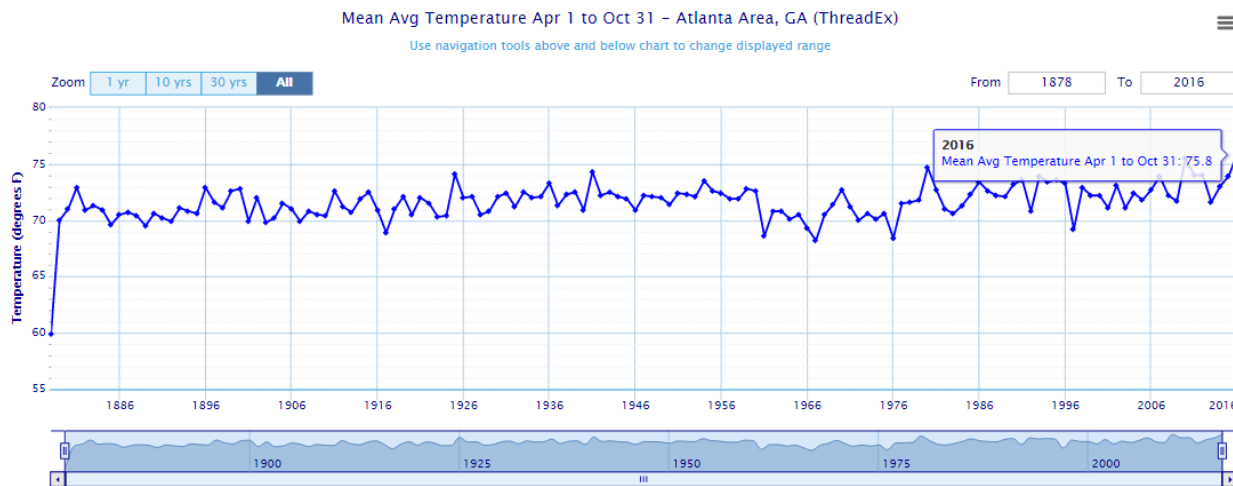
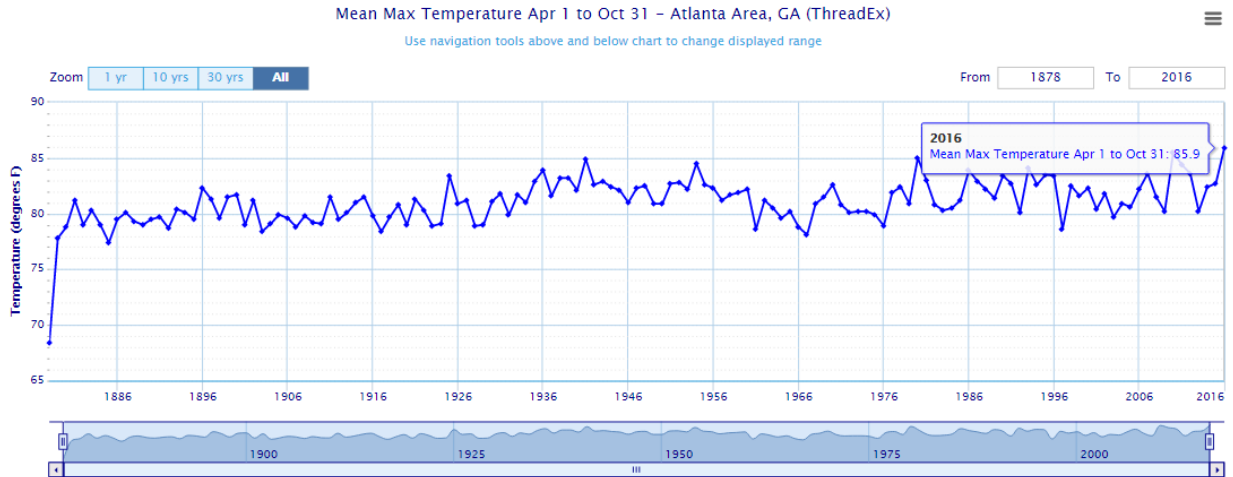


Figure 10. Mean maximum temperature (top), mean average temperature (middle), and mean minimum temperature (bottom) during the ozone season (April 1 – October 31) in Atlanta from 1878 to 2016.

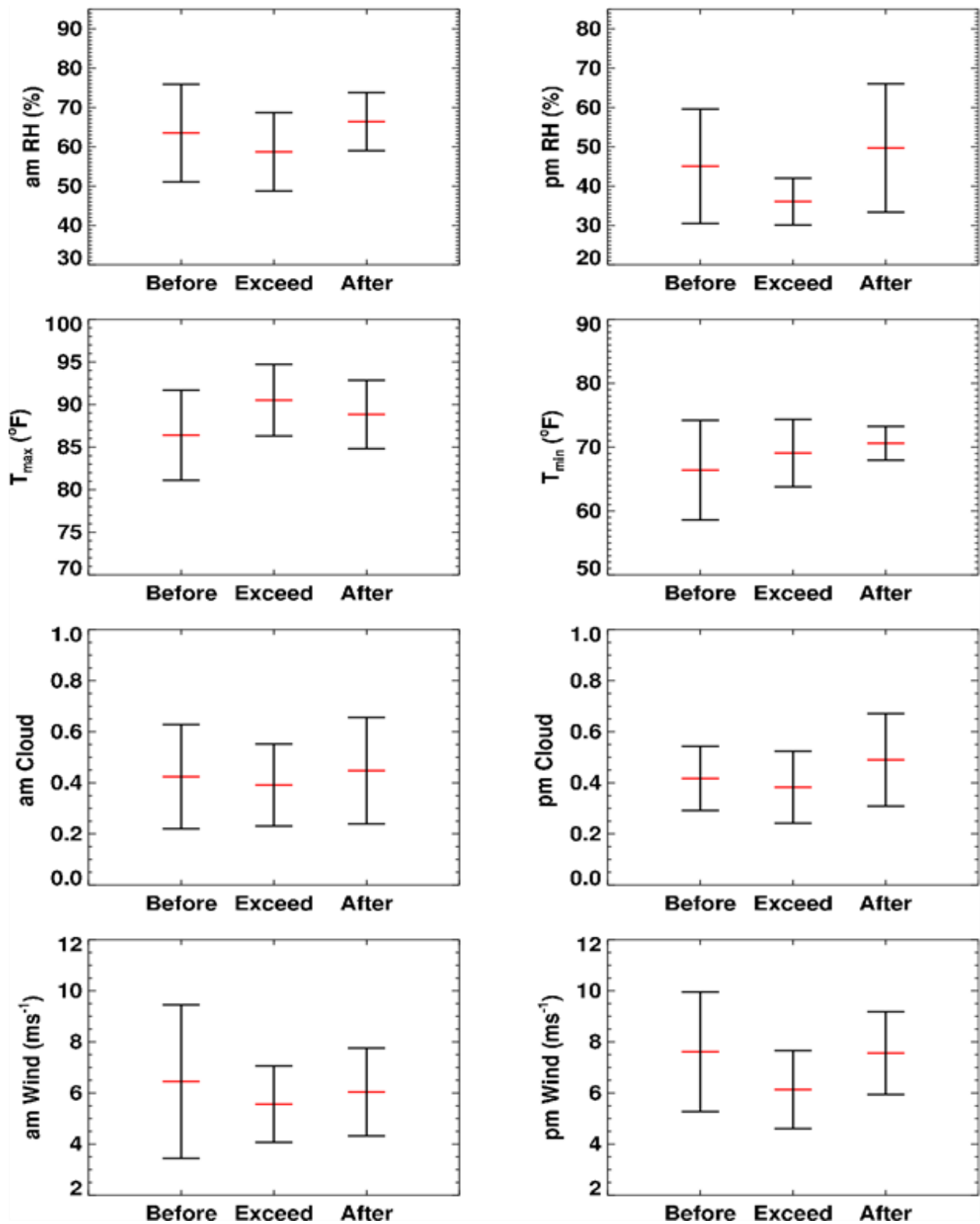


Figure 11. Comparison of meteorological variables in 2016 on the ozone exceedance day, and the day before and after the exceedance. The red bar is the mean, and the upper and lower bars (black) represent the standard deviations.

4. Ozone Regression Model

Multiple linear regression (MLR) analysis was used to quantify the relationship between Atlanta MDA8O3 and environmental variables in a previous study (Cardelino, 2011). In the 2011 study, 15 environmental variables (12 meteorological variables and 3 additional variables (i.e. O3-day2, weekday, and jday)) are used (Table 5). O3-day2 is used to represent chemical production background assuming slow changes, weekday for emission variation due to human activities, and jday to represent the seasonal variation of ozone formation. Daily data of MDA8O3 and 17 environmental factors are used in MLR to build a linear relationship of Atlanta MDA8O3 and environmental factors assuming independency among these environmental factors:

$y = \alpha_0 + \sum_{i=1}^{15} \alpha_i x_i$. Where y stands for MDA8O3, x_i stands for the environmental factor, α_0 is an adjustment factor, and α_i is a weighting factor. MLR analysis is updated in this study by including two new environmental variables (relh1 and relh2) according to findings identified in the “Meteorological Conditions in Atlanta during 1990-2016” section.

Table 5. Daily variables used for the MLR analysis

Name	Meaning	Unit
T _{max}	Daily maximum temperature	degree of Fahrenheit
T _{min}	Daily minimum temperature	degree of Fahrenheit
TD _{max}	Daily maximum dew point temperature	degree of Fahrenheit
TD _{min}	Daily minimum dew point temperature	degree of Fahrenheit
pres1	Mean surface pressure in the morning (6-12 am)	millibar
pres2	Mean surface pressure in the afternoon (12-6 pm)	millibar
wdir1	Mean wind direction in the morning (6-12 am)	degree from north
wdir2	Mean wind direction in the afternoon (12-6 pm)	degree from north
wsp1	Mean wind speed in the morning (6-12 am)	m/s
wsp2	Mean wind speed in the afternoon (12-6 pm)	m/s
sky1	Mean cloud coverage in the morning (6-12 am)	%
sky2	Mean cloud coverage in the afternoon (12-6 pm)	%
O ₃ -day2	Daily Maximum 8-hr average ozone two days ago	ppbv
weekday	Day of week	n/a
jday	Day of year (Julian day)	n/a
relh1*	Mean relative humidity in the morning (6-12 am)	%
relh2*	Mean relative humidity in the afternoon (12-6 pm)	%

Correlation Analysis

The correlation coefficients of MDA8O3 and the 17 environmental variables during ozone season were calculated by different time periods during 1990-2016 in Atlanta (Table 6 and Figure 12). Only data in a particular time period were used to calculate the corresponding correlation coefficients. The difference of correlation coefficients among different time period illustrates whether the relationship between Atlanta MDA8O3 and environmental variables change through the years. The ranking of correlation coefficients is similar for different time periods. The top 6 most correlated environment variables (i.e. variables with the top 6 highest absolute r) are AM and PM relative humidity, AM and PM cloud coverage, daily max

temperature, and ozone levels 2 days previous. Daily max temperature is the most correlated environmental variable before 2000, and PM relative humidity is the most correlated environmental variable after 2000. In 2016, daily max temperature is only the 6th most correlated variable, and PM wind speed replaced ozone 2 days previous, being one of the top 6 correlated environmental variables. This indicates the uniqueness of ozone production in 2016 compared to other years.

In general, the ozone exceedance days were associated with the following meteorological conditions:

1. Low relative humidity (dry)
2. High daily temperature (hot)
3. Low cloud coverage (high solar radiation)
4. High ozone on previous days (persistence)
5. Relatively low wind speed (calm)

The above meteorological conditions favor the chemical production of ozone in the lower troposphere. Low relative humidity may reduce the ozone loss through the reaction with water vapor (Seinfeld and Pandis, 1998). Ozone formation increases with higher temperatures and low cloud coverage due to higher solar radiation, leading to more active ozone production. High ozone on previous days might indicate that the ozone buildup was be a multiple-day process. Calm conditions correspond to poor dispersion and less long-range transport, indicating that the local ozone production is relatively more important for ozone exceedances in Atlanta.

Table 6. Correlation coefficients of MDA8O3 and environmental variables during ozone season by time periods during 1990-2016 in Metro Atlanta area.

Name	1990-2016	1990-1999	2000-2005	2006-2010	2011-2015	2016
O ₃ -day2	0.492	0.48	0.475	0.499	0.452	0.3
sky1	-0.512	-0.559	-0.565	-0.549	-0.55	-0.379
sky2	-0.476	-0.515	-0.498	-0.485	-0.523	-0.451
T _{max}	0.545	0.592	0.581	0.571	0.526	0.342
T _{min}	0.272	0.317	0.265	0.32	0.219	0.063
TD _{max}	0.076	0.136	0.04	0.057	0.003	-0.146
TD _{min}	0.066	0.128	0.043	0.035	-0.017	-0.126
jday	-0.119	-0.095	-0.101	-0.195	-0.184	-0.018
pres1	0.028	-0.027	0.09	0.059	0.018	0.152
pres2	0.005	-0.056	0.066	0.041	0.002	0.11
wdir1	0.139	0.231	0.11	0.056	0.132	0.026
wdir2	0.154	0.25	0.125	0.063	0.147	0.039
wspd1	-0.262	-0.316	-0.237	-0.333	-0.231	-0.271
wspd2	-0.235	-0.266	-0.206	-0.318	-0.206	-0.372
relh1	-0.473	-0.475	-0.545	-0.555	-0.577	-0.515
relh2	-0.567	-0.573	-0.627	-0.618	-0.641	-0.597
wkday	-0.027	-0.011	-0.019	-0.062	-0.013	-0.174

Note: Top 6 absolute values are highlighted in red. The highest absolute value is in bold.

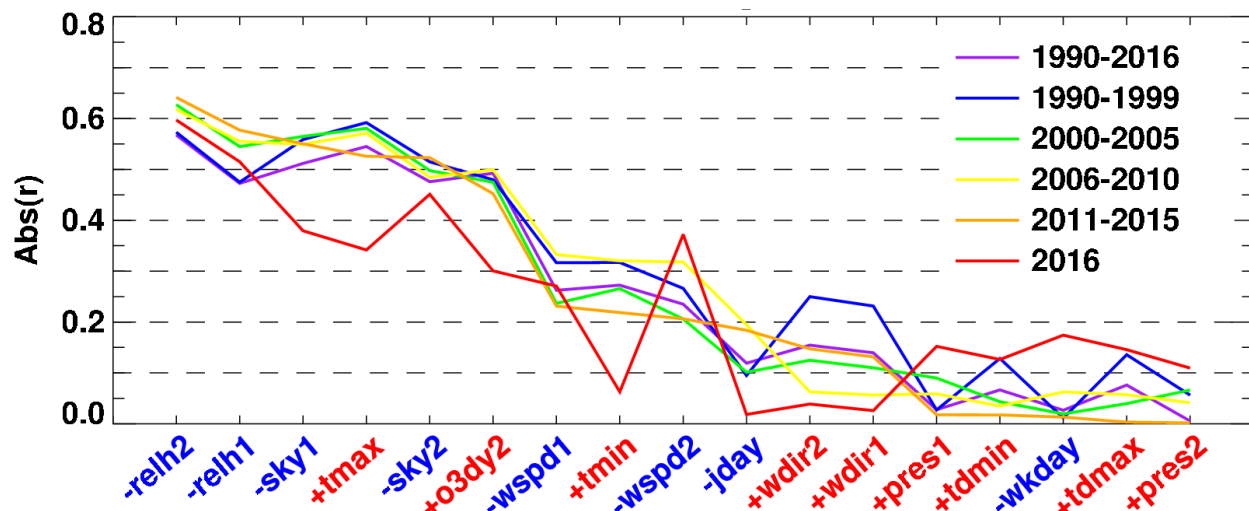


Figure 12. Correlation coefficients of MDA8O3 and environmental variables during ozone season by time periods during 1990-2016 in Atlanta. Variables with positive correlation with MDA8O3 are labeled in red, and variables with negative correlation are labeled in blue.

Updated MLR Ozone Model

The MLR ozone model developed by Cardelino (2011) employed data during 1987-1998 and tends to overestimate ozone concentrations by more than 5 ppb when it was used during Georgia EPD’s ozone forecasting in 2016. Therefore, an updated MLR ozone model (added RH as a new variable) was developed using data from 2011-2016 to capture the recent NOx emission reductions. The updated MLR model was then used to predict 2016 ozone. Performance of the updated MLR ozone models were evaluated by comparing the predictions with 2016 ozone observations (Table 7). The updated MLR ozone model can explain about 60% of the ozone variance (or R^2). The mean bias (MB) and normalized mean bias (NMB) decreases significantly by using recent data (i.e. MB and NMB for 2013-2015 are less than those for 2012-2015 and 2011-2015), while the Mean Absolute Error (MAE), Normalized Mean Error (NME), and Root Mean Square Error (RMSE) are similar among the updated MLR ozone models. The MLR model based on the data from 2011-2016 is recommended to be used for future ozone forecast. The coefficients of the MLR ozone model with 2011-2016 dataset are listed in Table 8.

Table 7. Performance of updated MLR ozone model using various datasets during 2011-2016.

Data range	R	R^2	MB ^a	MAE ^a	NMB ^a	NME ^a	RMSE ^a
2011-2015	0.764	0.584	2.395	6.813	4.3%	12.3%	8.889
2012-2015	0.768	0.590	1.86	6.726	3.4%	12.1%	8.742
2013-2015	0.762	0.581	1.556	6.797	2.8%	12.3%	8.761
2011-2016	0.784	0.615	1.784	6.488	3.2%	11.7%	8.45
2012-2016	0.788	0.621	1.327	6.426	2.4%	11.6%	8.337
2013-2016	0.788	0.621	1.06	6.441	1.9%	11.6%	8.312

^a MB is Mean Bias, MAE is Mean Absolute Error, NMB is Normalized Mean Bias, NME is Normalized Mean Error, RMSE is Root Mean Square Error.

Table 8. The coefficients of the MLR ozone model using dataset during 2011-2016.

Variable	Coefficient
Constant	456.14800
O ₃ -day2	0.19112
sky1	-2.69005
sky2	-4.77386
T _{max}	0.67914
T _{min}	0.09940
TD _{max}	-0.11265
TD _{min}	-0.19118
jday	-0.03037
pres1	-1.76369
pres2	1.36482
wdir1	-0.01127
wdir2	-0.00090
wspd1	-0.05748
wspd2	-1.06804
relh1	-0.18427
relh2	-0.25455
weekday	-0.46420

5. CART Analysis

Classification and regression tree (CART) analysis was used to understand the relationship between Atlanta MDA8O3 and environmental variables. CART (Breiman et al., 1984) is a non-parametric statistical tool which can estimate the hierarchs of the importance of each variable, especially when the relationship between these variables is complicated and nonlinear. Since linearity has been assumed in MLR ozone model as discussed above, CART analysis was performed to further investigate the causes of ozone exceedance using the CART package for R which is available online.

CART uses similar regression techniques as the MLR model, although it fits the model locally at each split instead of globally. A sequence of questions related to different variables (or attributes) are asked, and the answer is either “yes” or “no”. At each node, a large group is split into two distinct sub-groups based on a single variable. The recursive partition will divide a dataset into a binary tree chart. There are two types of trees, regression and classification trees. In regression trees, the response variable is continuous and the final nodes feature the mean values of the response variables. In classification trees, the response variable (i.e. MDA8O3) is categorical and the final nodes are assigned to different categories (classes). Both regression tree and classification tree analysis were conducted in this study.

The same 2011-2016 dataset used in MLR analysis was also used for both CART analyses. In comparison to the actual MDA8O3 concentrations used for regression CART analysis, MDA8O3 concentrations for the classification CART analysis were divided into 4 categories (Table 9) following the definition used in EPA’s air quality index (AQI) for the 2015 ozone NAAQS.

Table 9. Four ozone categories used for the classification CART analysis.

Category	Ozone (ppbv)
1	0-54
2	55-70
3	71-85
4	> 85

Regression tree CART analysis

The best split of regression tree CART analysis finds 32 nodes which represent ozone clusters grouped after a sequence of filters with various conditions. The mean ozone concentrations generally increase from left to right (Figure 13). There are four nodes with mean ozone concentrations higher than 70 ppb and nine nodes with mean ozone concentrations ranging from 60 to 70 ppb (Figure 14). Six “critical” nodes with mean ozone concentrations higher than 65 ppb were investigated to understand the patterns of environmental conditions on high ozone days (Table 10).

The six critical nodes are always associated with three environmental variables (i.e. PM relative humidity (RH), daily maximum temperature (T_{\max}), and PM wind), and five of the six nodes are associated with ozone concentrations on 2 days ago (O3 Day-2). PM pressure shows association in three nodes, and AM relative humidity (RH), AM pressure, Julian Day, and Week Day only

shows association in one node. The environmental variables with the higher number of associated nodes for high ozone days are more responsible for the high ozone days.

The PM RH is less than 43.86% for the six nodes except for node 25 in which the PM RH is 44-56%, indicating high correlation of high ozone days with low relative humidity (i.e. relatively dry conditions). This finding is consistent with the MLR analysis. The T_{\max} is higher than 83.48 °F for all six critical nodes, in particular T_{\max} is higher than 95.54 °F for node 31 which has the highest mean ozone concentration (87.9 ppb). Higher temperatures increase chemical reaction rates resulting in faster ozone production. Also, high solar radiation can enhance the photochemical production of ozone. The PM wind shows high ozone days can be associated with both high and low wind conditions. The higher ozone concentrations on 2 days ago are higher than 66.5 ppb for four of the six critical nodes, implying occurrence of consecutive high ozone conditions lasting more than one day. In summary, the ozone exceedance days are usually associated with dry and hot meteorological conditions.

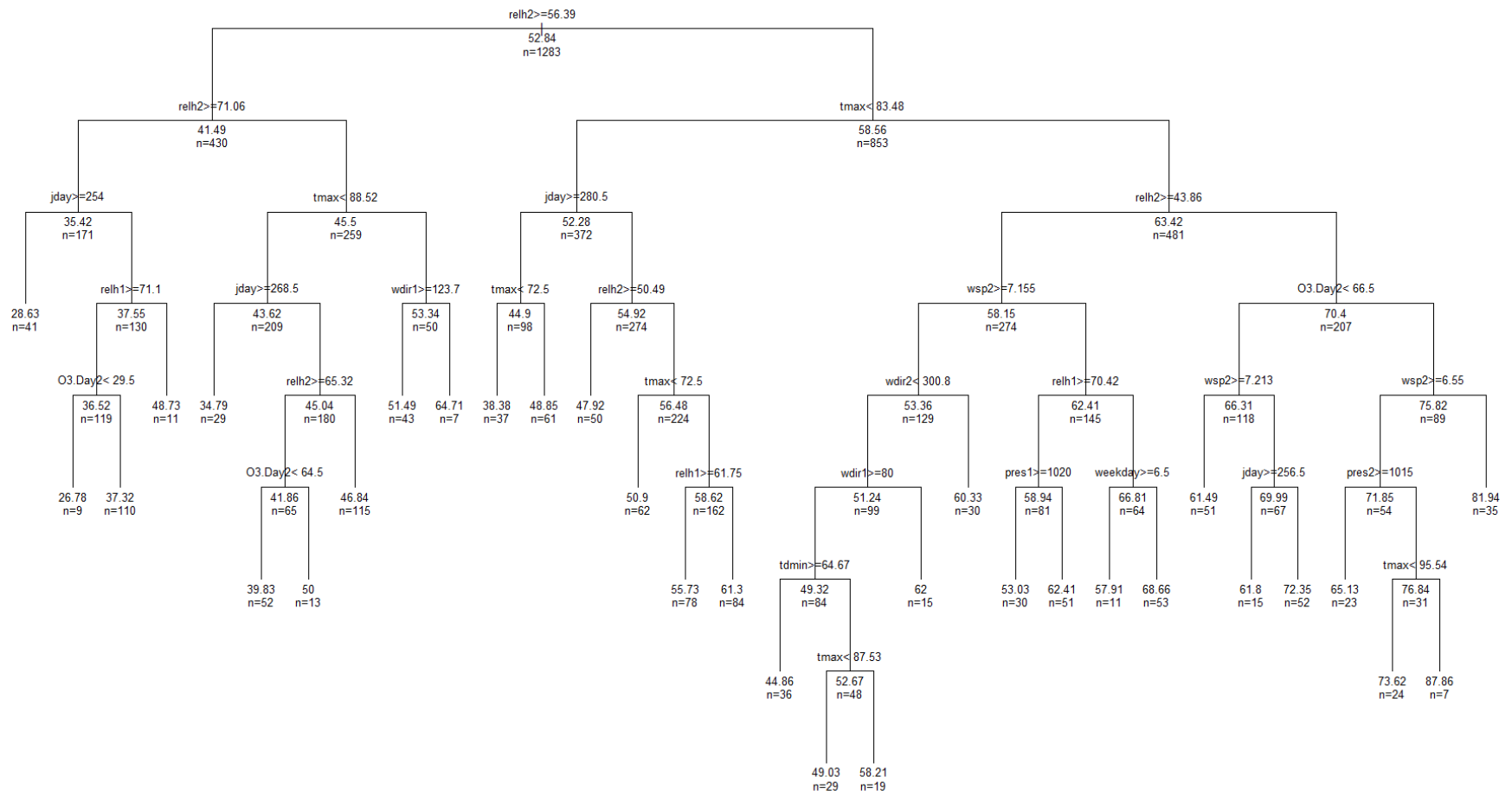


Figure 13. Best split for the regression tree CART analysis for Atlanta ozone during 2011-2016.

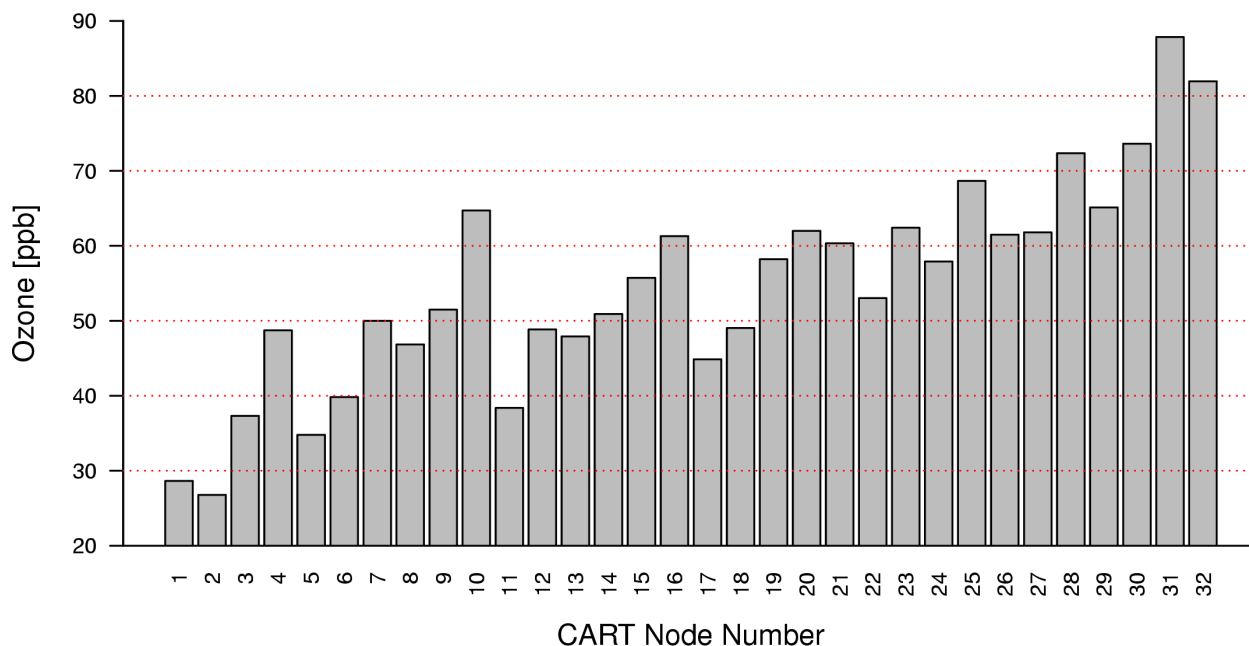


Figure 14. Mean ozone concentrations for 32 nodes found in the regression tree CART analysis.

Table 10. Conditions for top 6 high ozone nodes of the regression tree CART analysis

Node Number	29	25	28	30	32	31
Mean O ₃ (ppb)	65.1	68.7	72.4	72.6	81.9	87.9
PM RH (%)	< 43.86	43.86 - 56.39	< 43.86	< 43.86	< 43.86	< 43.86
AM RH (%)		< 70.42				
T _{max} (°F)	> 83.48	> 83.48	> 83.48	83.48 - 95.54	> 83.48	> 95.54
PM wind (m/s)	≥ 6.55	< 7.155	< 7.213	≥ 6.55	< 6.55	≥ 6.55
O ₃ Day-2 (ppb)	> 66.5		< 66.5	> 66.5	> 66.5	> 66.5
PM Pressure (mb)	< 1015			< 1015		< 1015
Julian Day			< 256.5			
Week Day		< 6.5				

Classification tree CART analysis

The best split of classification tree CART analysis finds 23 nodes which represent ozone clusters grouped after a sequence of filters with various conditions. The mean ozone concentrations generally increase from left to right (Figure 15). There are three nodes with mean ozone concentrations higher than 70 ppb and nine nodes with mean ozone concentrations ranging from 60 to 70 ppb (Figure 16). Six “critical” nodes with mean ozone concentrations higher than 65 ppb were investigated to understand the patterns of environmental conditions on high ozone days (Table 11), similar to the regression tree CART analysis conducted above. The mean ozone concentrations for the six critical nodes in the classification tree CART analysis are less than those in the regression tree CART analysis. This can be partially explained by the fewer number of ozone days in each node in the regression tree CART analysis due to more total nodes found in this analysis (32 vs. 23 nodes).

The six critical nodes in the classification tree CART analysis are always associated with two environmental variables (i.e. PM relative humidity (RH) and daily maximum temperature (T_{\max})). PM wind is associated with four of the six critical nodes in this analysis, compared to association with six nodes in the regression tree CART analysis. Four of the six critical nodes are also associated with daily minimum temperature (T_{\min}), which is not found in the regression tree CART analysis. AM relative humidity (RH), PM pressure and the maximum dew point temperature ($T_{d_{\max}}$) are respectively associated with three, two and one nodes, indicating less association with the nodes for high ozone days and thus less responsibility for the high ozone days.

The PM RH is less than 39.25% for the top four nodes and less than 51.42% for node 18 indicating that high ozone days are associated with low relative humidity (i.e. relatively dry conditions), though node 6 is associated with PM RH greater than 51.42%. The T_{\max} is higher than 83.48 °F for the six critical nodes, in particular, T_{\max} is higher than 87.89 °F for node 6. They are both consistent with the results in the regression tree CART analysis (i.e. the ozone exceedance days are usually associated with dry and hot meteorological conditions).

High ozone day conditions

Both regression and classification tree CART analyses have found that high ozone days are always associated with low PM RH and high T_{\max} , which are typical summer meteorological conditions in Atlanta due to high pressure systems. Under such conditions, local ozone formation would be largely enhanced. The large impact of the low RH and high air temperature on ozone formations has also been found in previous studies for the southeastern United States (Blanchard et al., 2014; Zhang and Wang, 2016). In addition, other factors such as PM wind, ozone concentrations on previous days, AM RH, and T_{\min} may also cause elevated ozone conditions though their impact levels may vary. Strong correlation of cloud coverage (sky1 and sky2) with ozone exceedance days was found in the MLR analysis, but not found in the CART analyses as cloud coverage is strongly correlated with RH.

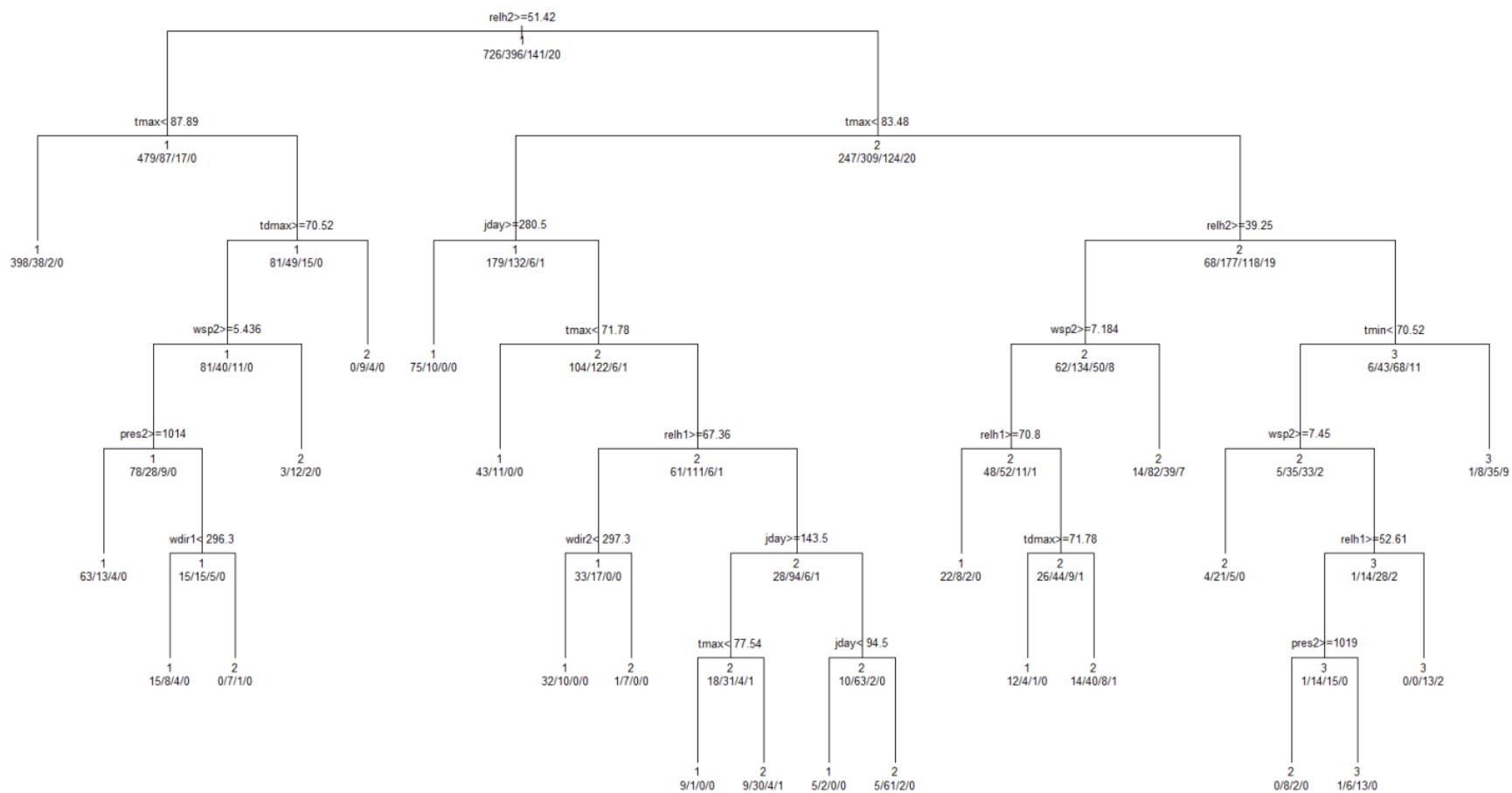


Figure 15. Best split for the classification tree CART analysis for Atlanta ozone during 2011-2016.

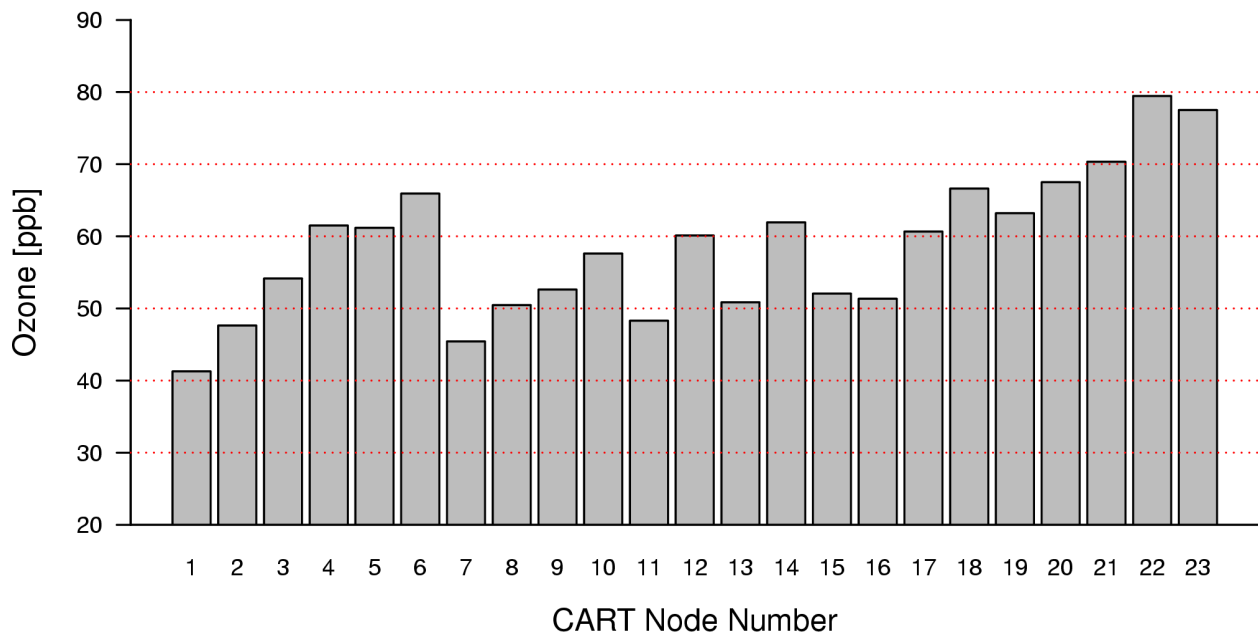


Figure 16. Mean ozone concentrations for 23 nodes found in the classification tree CART analysis.

Table 11. Conditions for top 6 high ozone nodes of the classification tree CART analysis

Node Number	6	18	20	21	23	22
Mean O ₃ (ppb)	65.9	66.6	67.5	70.3	77.5	79.5
PM RH (%)	> 51.42	39.25 - 51.42	< 39.25	< 39.25	< 39.25	< 39.25
AM RH (%)			> 52.61	> 52.61		< 52.61
T _{max} (°F)	> 87.89	> 83.48	> 83.48	> 83.48	> 83.48	> 83.48
T _{min} (°F)			< 70.52	< 70.52	> 70.52	< 70.52
PM wind (m/s)		< 7.184	< 7.45	< 7.45		< 7.45
PM Pressure (mb)			> 1019	< 1019		
Td _{max} (°F)	< 70.52					

6. Meteorological Time Series Analysis

Time series of hourly ozone and meteorological variables (temperature, relative humidity and solar radiation) during 2016 were developed for the Southeastern Aerosol Research and Characterization (SEARCH) monitor located at Jefferson Street in Atlanta (Figure 17 - Figure 27). The time series were developed for all exceedance days in Atlanta when there is at least one ozone monitor exceeding the NAAQS and include the data for at least one day before the exceedance event. Ozone exceedances tend to be associated with high temperature and low relative humidity, as well as high solar radiation as identified in the previous sections.

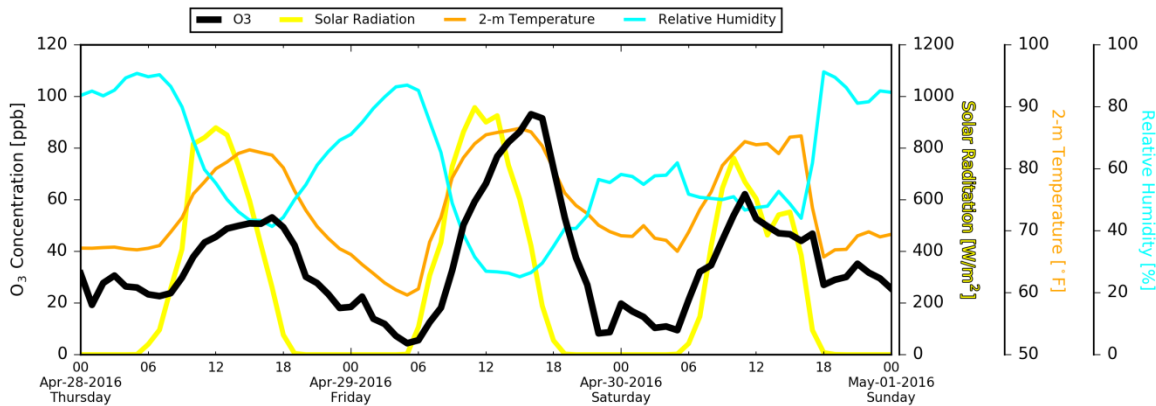


Figure 17. Time series of 1-hour ozone concentrations (left y-axis) and solar radiation (the first right y-axis), 2-m temperature (the second right y-axis), and relative humidity (the rightmost y-axis) for April 28-30, 2016.

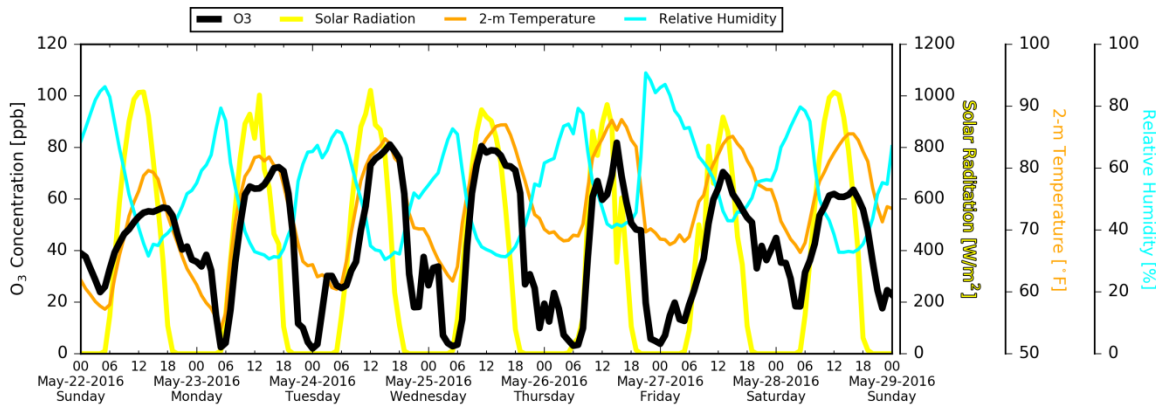


Figure 18. Time series of 1-hour ozone concentrations (left y-axis) and solar radiation (the first right y-axis), 2-m temperature (the second right y-axis), and relative humidity (the rightmost y-axis) for May 22-28, 2016.

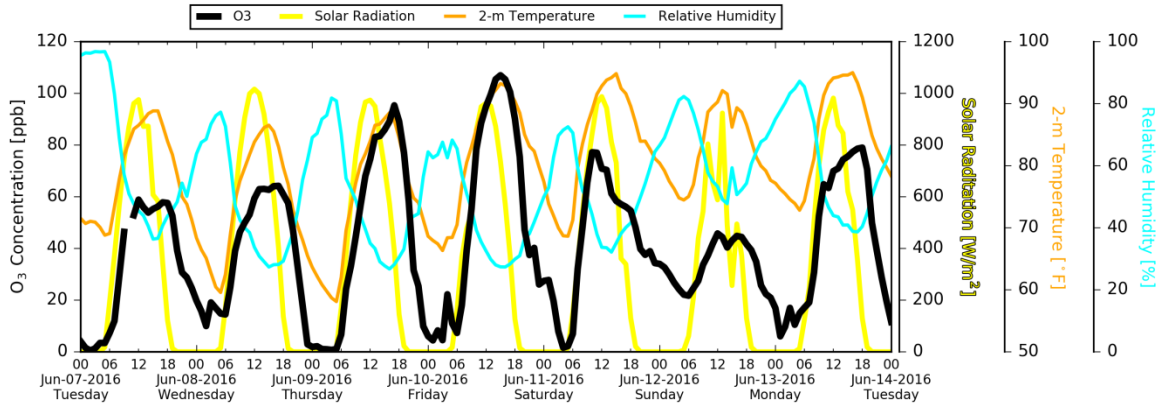


Figure 19. Time series of 1-hour ozone concentrations (left y-axis) and solar radiation (the first right y-axis), 2-m temperature (the second right y-axis), and relative humidity (the rightmost y-axis) for June 7-13, 2016.

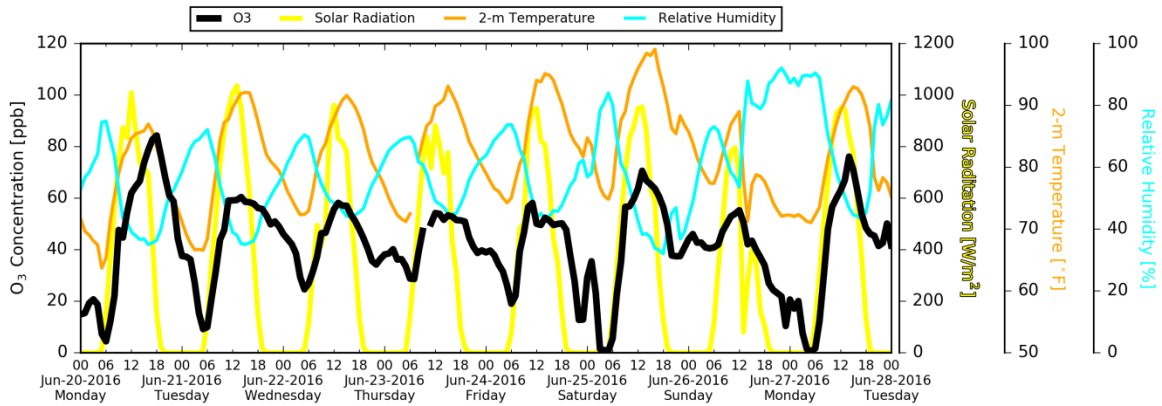


Figure 20. Time series of 1-hour ozone concentrations (left y-axis) and solar radiation (the first right y-axis), 2-m temperature (the second right y-axis), and relative humidity (the rightmost y-axis) for June 20-27, 2016.

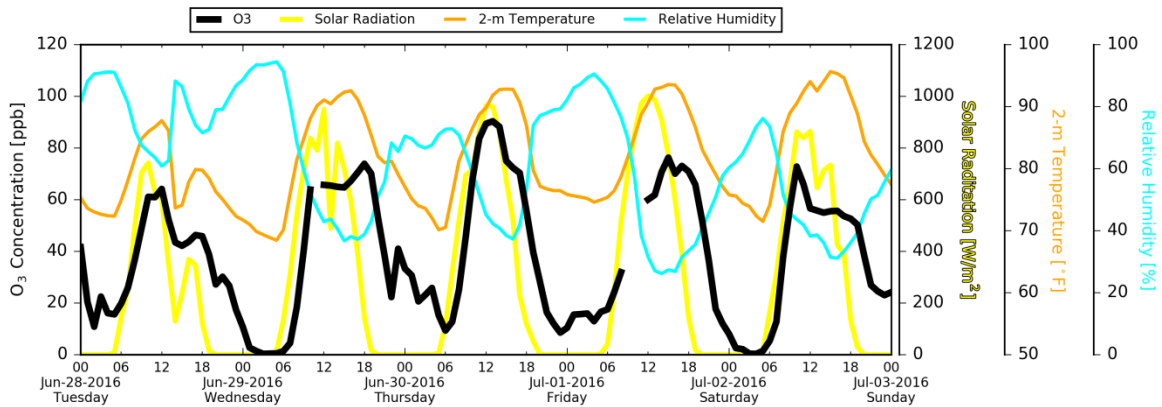


Figure 21. Time series of 1-hour ozone concentrations (left y-axis) and solar radiation (the first right y-axis), 2-m temperature (the second right y-axis), and relative humidity (the rightmost y-axis) for June 28-July 2, 2016.

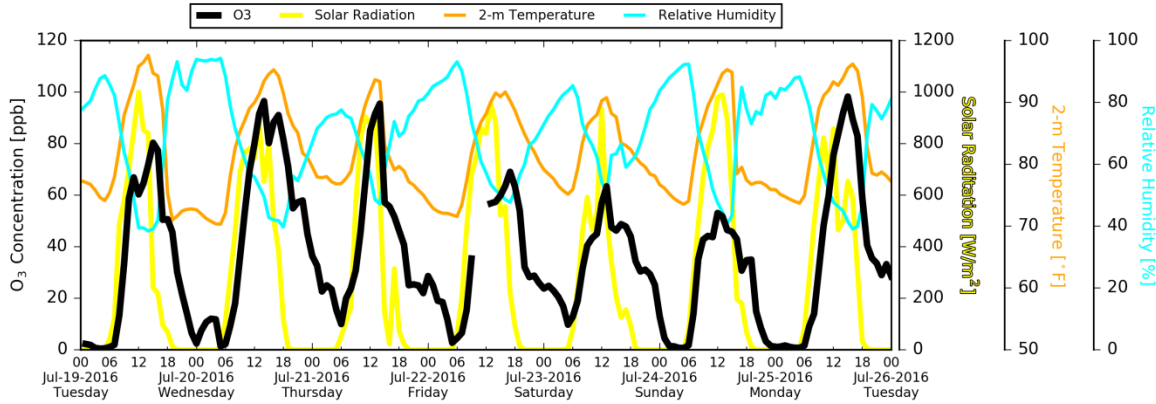


Figure 22. Time series of 1-hour ozone concentrations (left y-axis) and solar radiation (the first right y-axis), 2-m temperature (the second right y-axis), and relative humidity (the rightmost y-axis) for July 19-25, 2016.

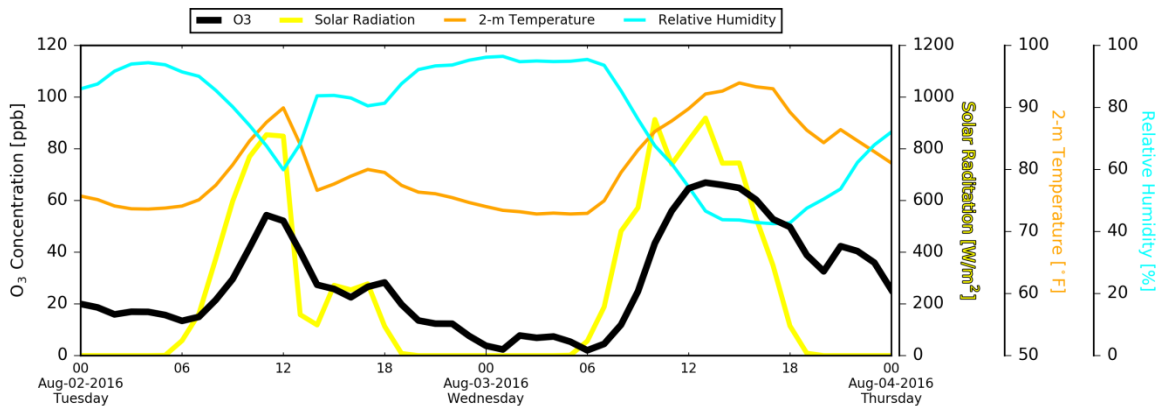


Figure 23. Time series of 1-hour ozone concentrations (left y-axis) and solar radiation (the first right y-axis), 2-m temperature (the second right y-axis), and relative humidity (the rightmost y-axis) for August 2-3, 2016.

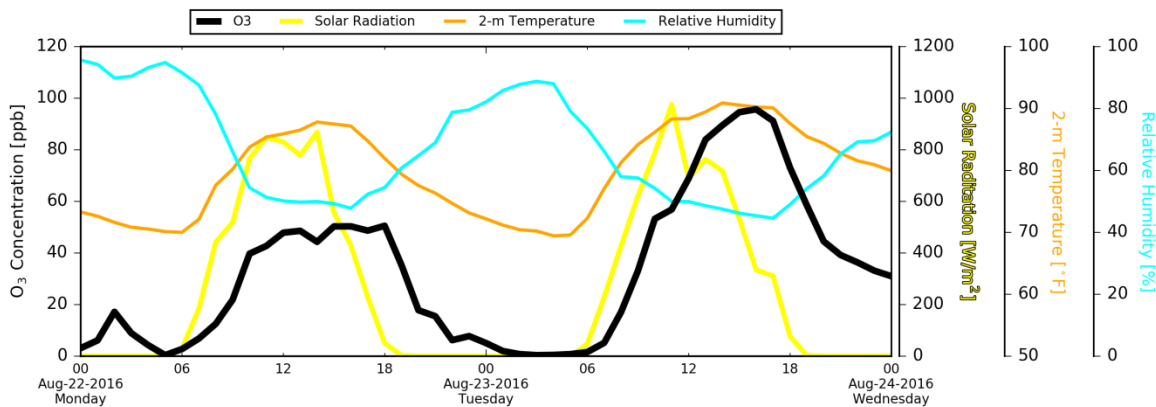


Figure 24. Time series of 1-hour ozone concentrations (left y-axis) and solar radiation (the first right y-axis), 2-m temperature (the second right y-axis), and relative humidity (the rightmost y-axis) for August 22-23, 2016.

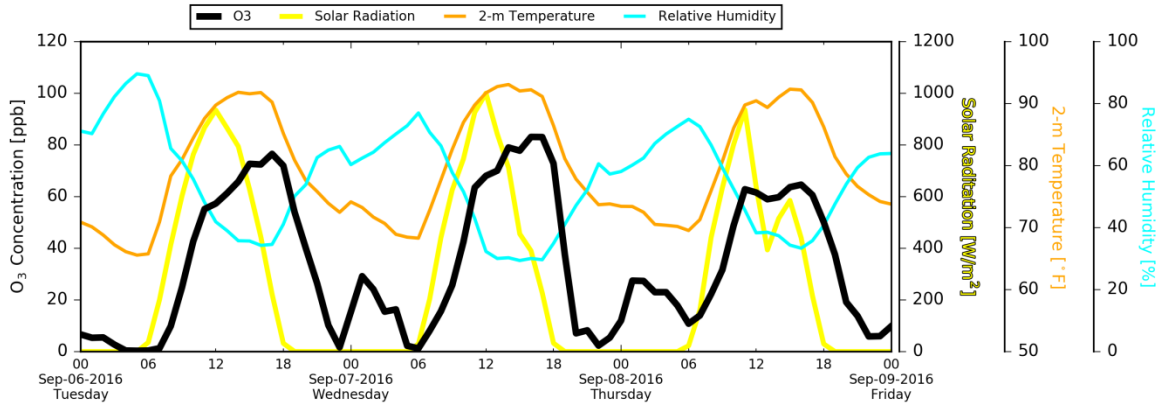


Figure 25. Time series of 1-hour ozone concentrations (left y-axis) and solar radiation (the first right y-axis), 2-m temperature (the second right y-axis), and relative humidity (the rightmost y-axis) for September 6-8, 2016.

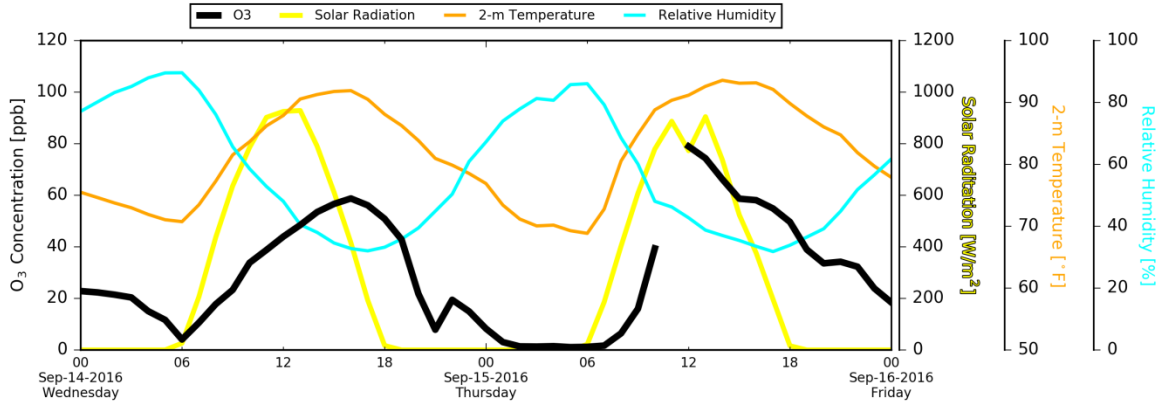


Figure 26. Time series of 1-hour ozone concentrations (left y-axis) and solar radiation (the first right y-axis), 2-m temperature (the second right y-axis), and relative humidity (the rightmost y-axis) for September 14-15, 2016.

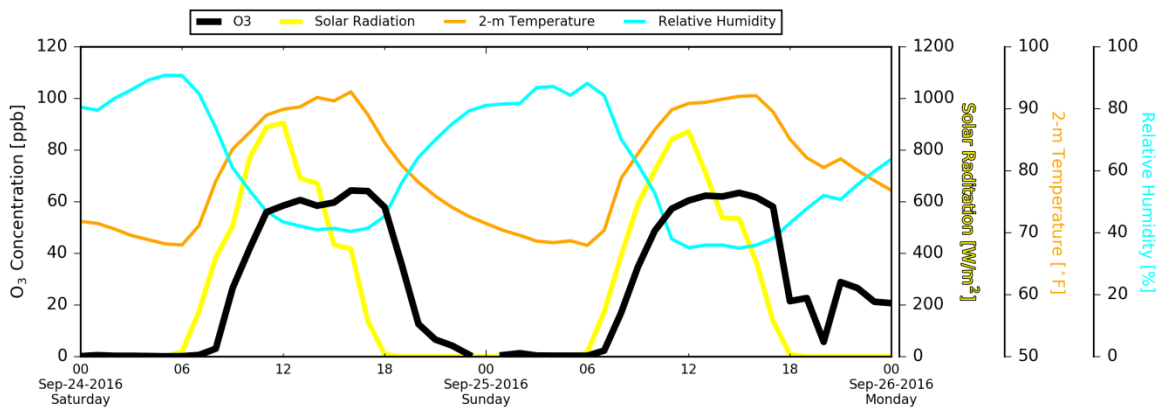


Figure 27. Time series of 1-hour ozone concentrations (left y-axis) and solar radiation (the first right y-axis), 2-m temperature (the second right y-axis), and relative humidity (the rightmost y-axis) for September 24-25, 2016.

7. HYSPLIT back trajectory analysis

The Hybrid Single Particle Lagrangian Integrated Trajectory (HYSPLIT, http://www.arl.noaa.gov/HYSPLIT_info.php) back trajectory analysis was conducted to determine the origin of air masses and establish source-receptor relationships on ozone exceedance days. The HYSPLIT model is one of the most extensively used atmospheric transport and dispersion models in the atmospheric sciences community. In this analysis, HYSPLIT 24-hour back-trajectories were computed for each ozone exceedance in 2016 at every Atlanta ozone monitor using North American Mesoscale (NAM) meteorological data, which is available at a 12-km resolution, from National Oceanic and Atmospheric Administration (NOAA). For each 2016 ozone exceedance at a monitor, three back-trajectories are computed for air parcels ending at heights of 100m, 500m and 1000m at the time of the 8-hr peak ozone.

HYSPLIT trajectories for five monitors whose 2014-2016 design values are above 70 ppb (i.e. 2015 Ozone NAAQS) are shown in Figure 28 - Figure 32. The long trajectories are associated with higher wind speed and indicate more opportunities for transport impacts, while short trajectories are associated with lower wind speed and indicate stagnant conditions and more opportunities for local impacts. The trajectories for the height of 100m at these five monitors are mostly short indicating a strong local impact. These trajectories at the Confederate Avenue (Figure 28) and South DeKalb (Figure 29) monitors (i.e. two monitors located inside the Atlanta urban core) may come from any directions. The trajectories at the Gwinnett Tech (Figure 30), McDonough (Figure 31), and Conyers (Figure 32) monitors mainly come from the south, north, and west directions respectively, where the Atlanta urban core is located. However, there are a few trajectories originating from other areas.

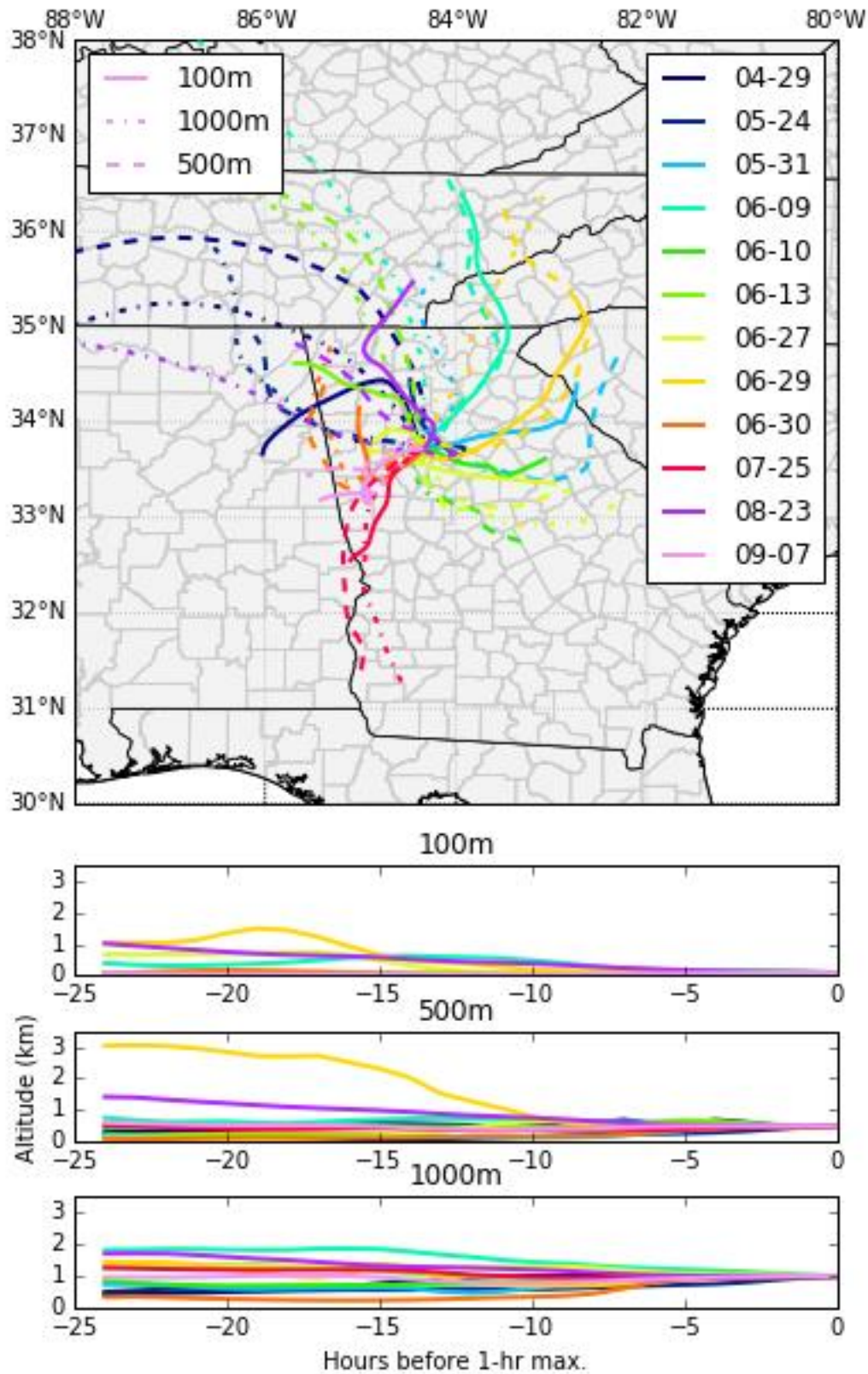


Figure 28. HYSPLIT 24 hour back-trajectories for exceedances at the Confederate Avenue monitor and trajectory path heights (bottom).

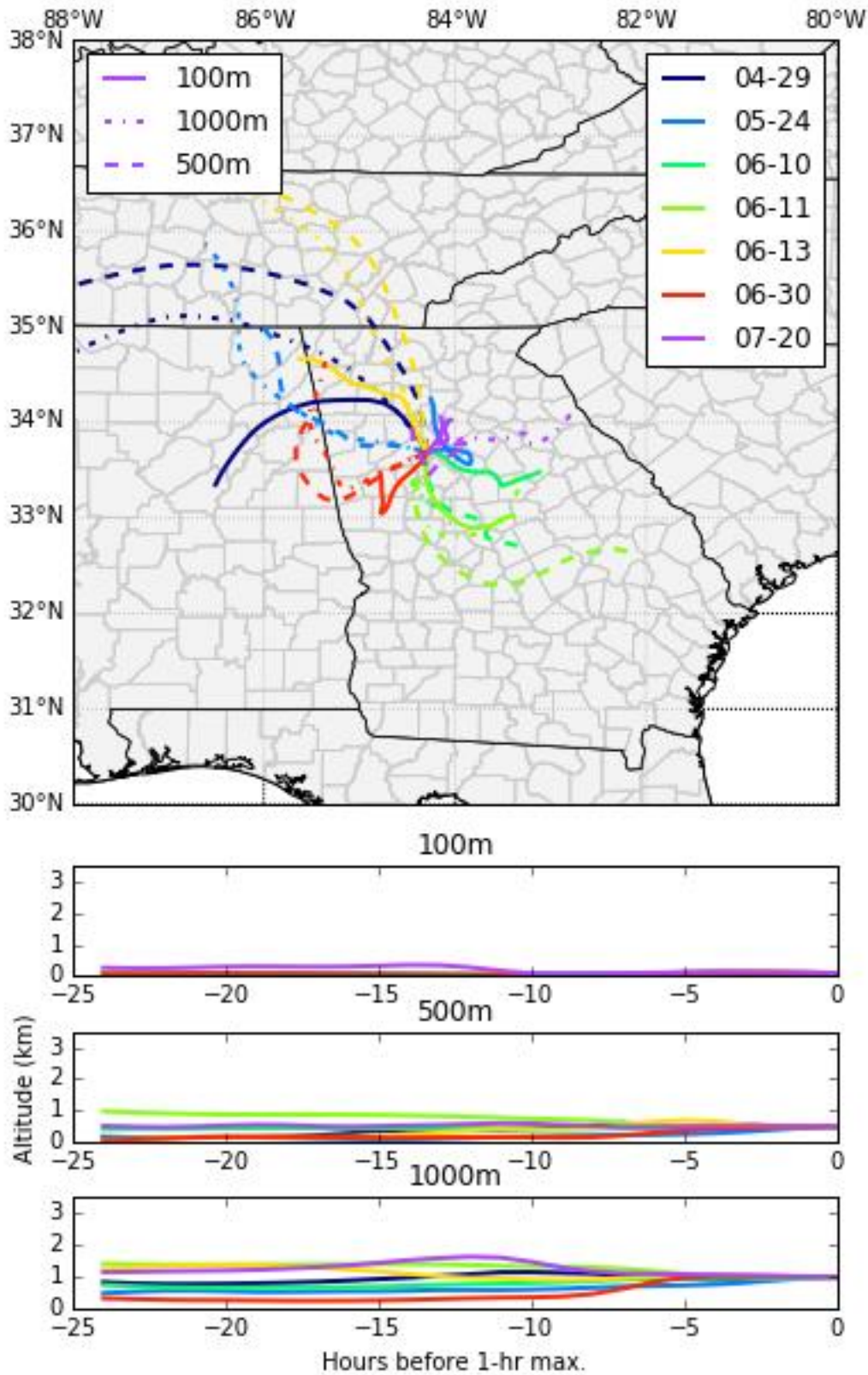


Figure 29. HYSPLIT 24 hour back-trajectories for exceedances at the South DeKalb monitor and trajectory path heights (bottom).

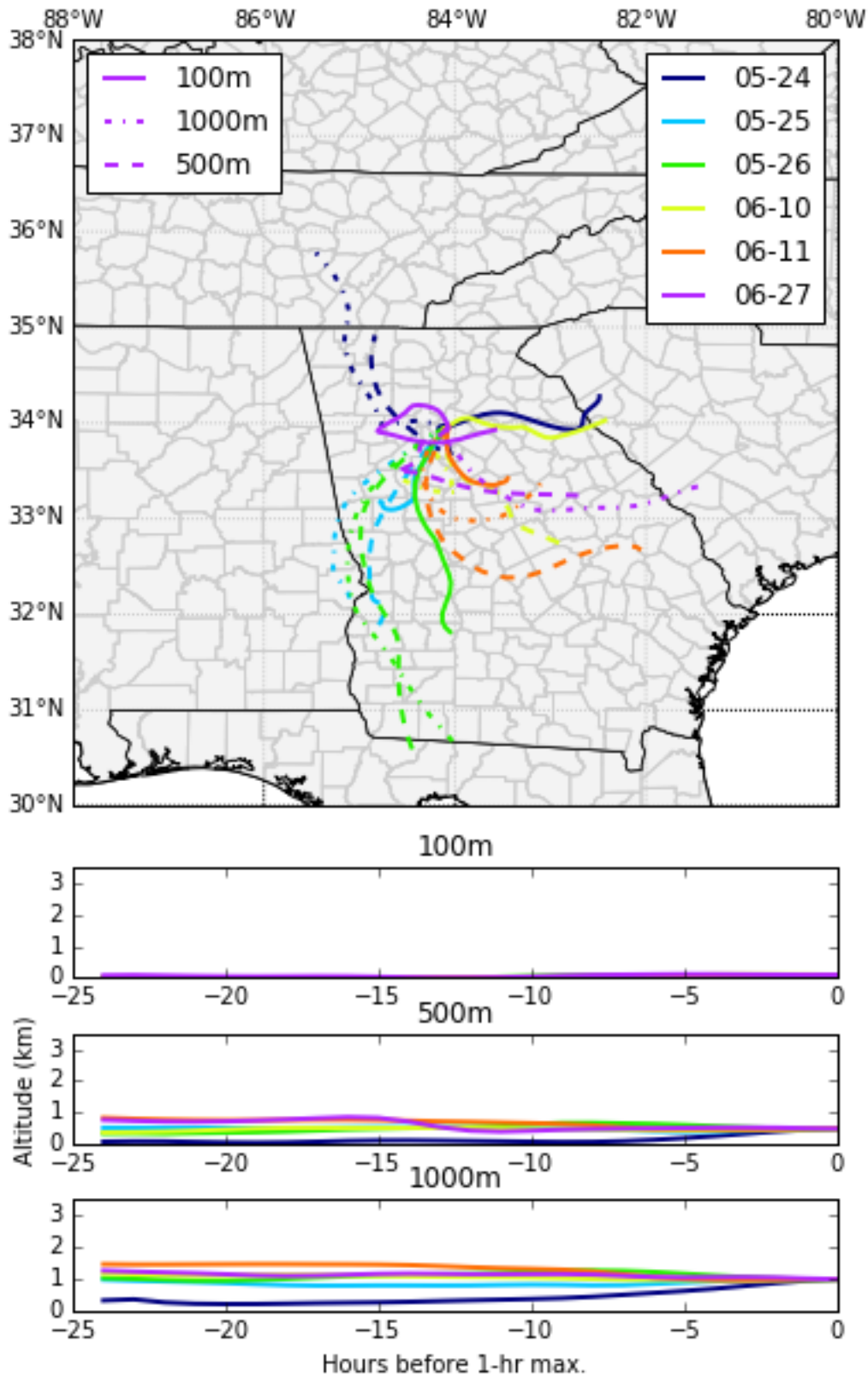


Figure 30. HYSPLIT 24 hour back-trajectories for exceedances at the Gwinnett Tech monitor and trajectory path heights (bottom).

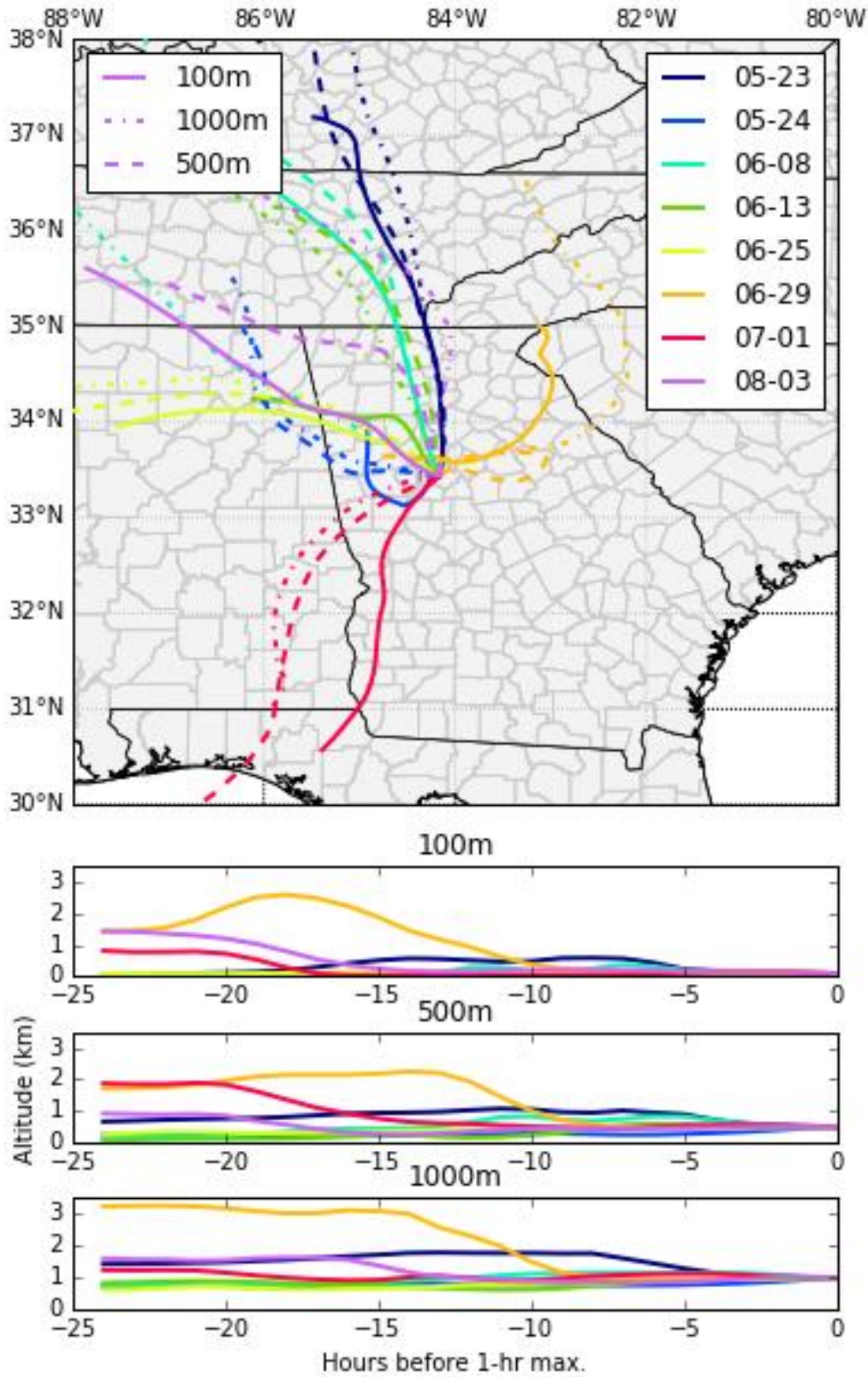


Figure 31. HYSPLIT 24 hour back-trajectories for exceedances at the McDonough monitor and trajectory path heights (bottom).

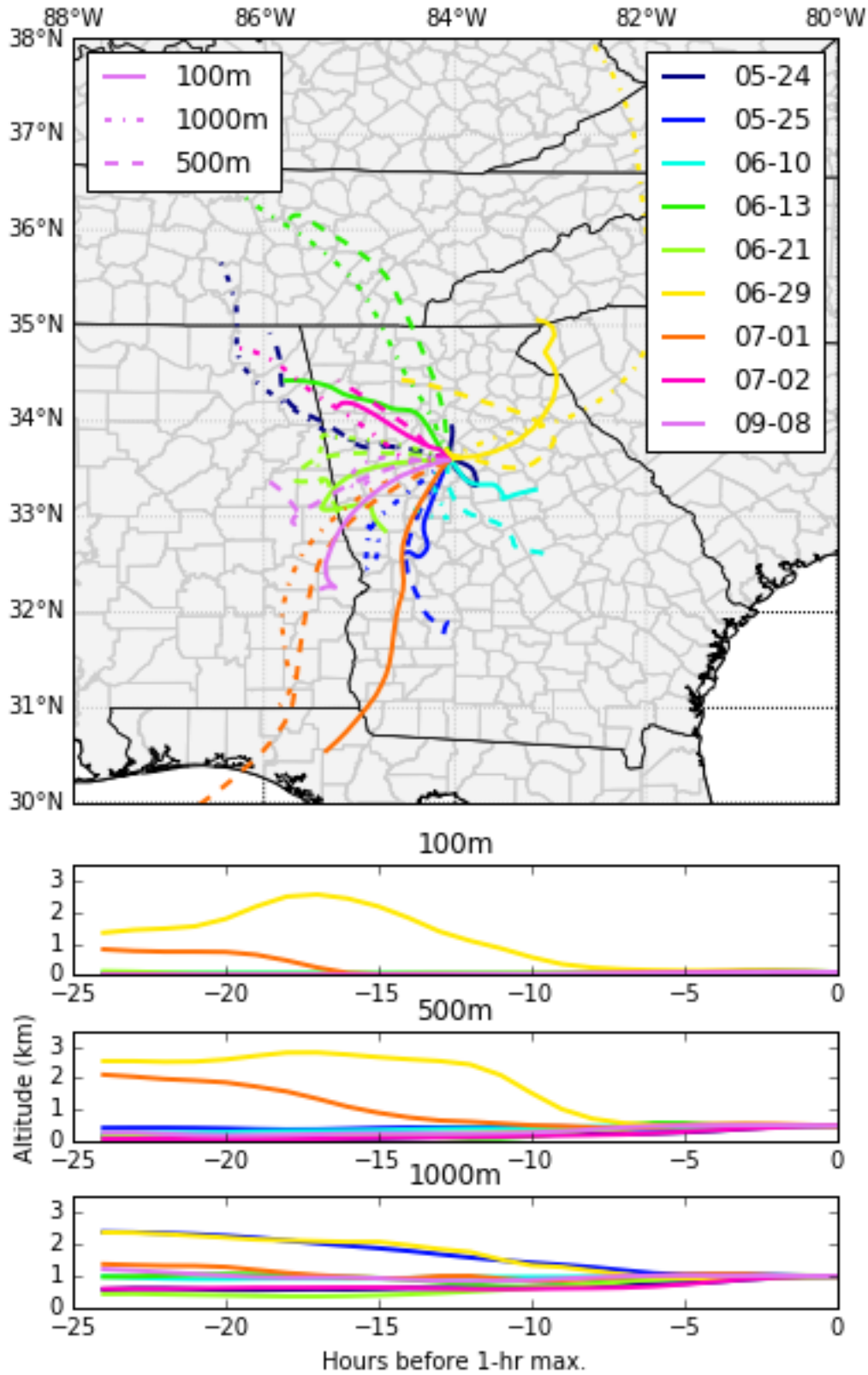


Figure 32. HYSPLIT 24 hour back-trajectories for exceedances at the Conyers monitor and trajectory path heights (bottom).

8. Ozone and NOx precursor

Ozone is not emitted directly into the air, but is formed by the reaction of volatile organic compounds (VOCs) and nitrogen oxides (NOx) in the presence of heat and sunlight. The relationship of ozone and NOx precursor is very nonlinear since NOx can not only help ozone formation, but also deplete ozone through titration. NOx can be emitted from automobiles, trucks and various non-road vehicles (e.g., construction equipment, boats, etc.) as well as industrial sources such as power plants, industrial boilers, cement kilns, and turbines. In the Metro Atlanta area during 2014, approximately 58% of NOx emissions were from on-road mobile sources and 20% from non-road mobile sources (Figure 33). In this study, the impacts of local NOx on ozone exceedances are investigated by analyzing NOx observations at the South DeKalb monitor and two roadside monitors (DMRC and Georgia Tech) located adjacent to major interstates during multiple ozone seasons (Figure 34). The two roadside monitors are investigated to identify impacts from on-road mobile NOx emissions. Scatter plots of MDA8O3 and NOx measurements at 8 AM and 4 PM (Figure 35) imply that high ozone concentrations generally occur when NOx concentrations are within a specific window. When NOx concentrations are low, ozone concentrations are also low since not enough radicals are propagated. However, when NOx concentrations are too high (>150 ppb at 8:00 AM or >11 ppb at 4:00 PM), the excess NOx removes ozone via NOx titration. Figure 35 shows that high ozone concentrations in Atlanta are highly correlated with low relative humidities (i.e. dry conditions).

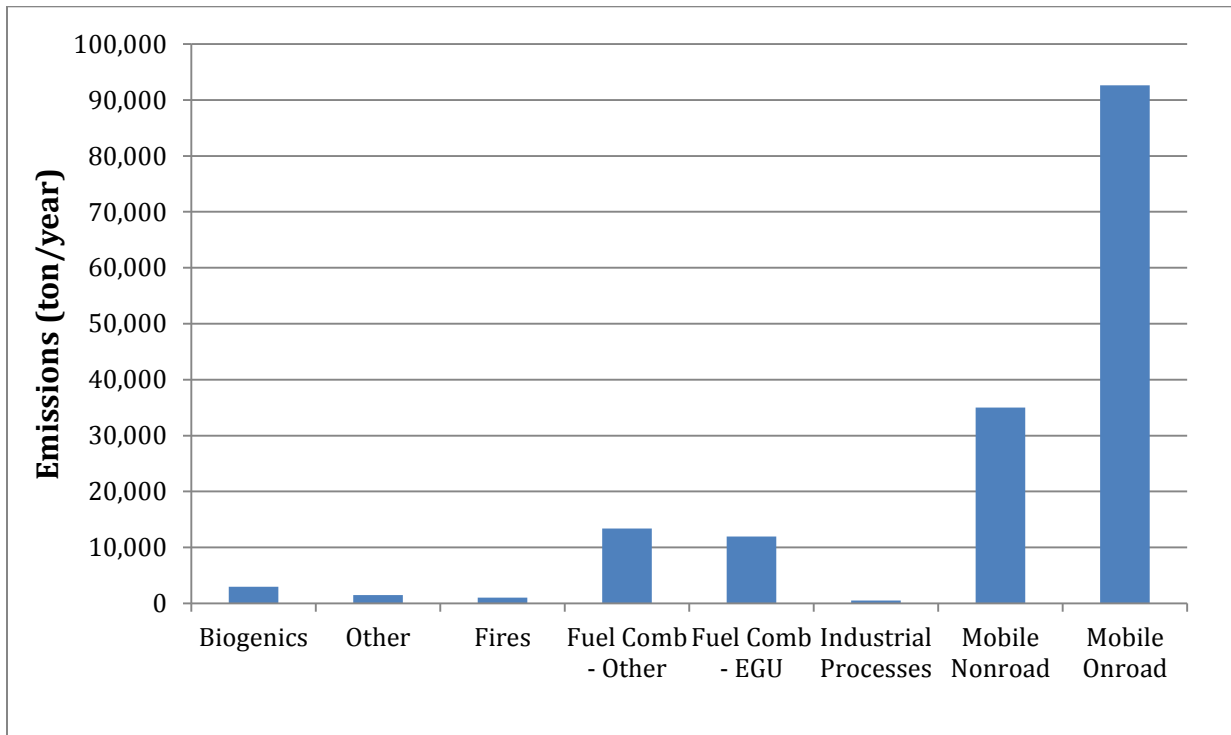


Figure 33. 2014 NOx emissions (tons/year) by source sectors in Metro Atlanta area.

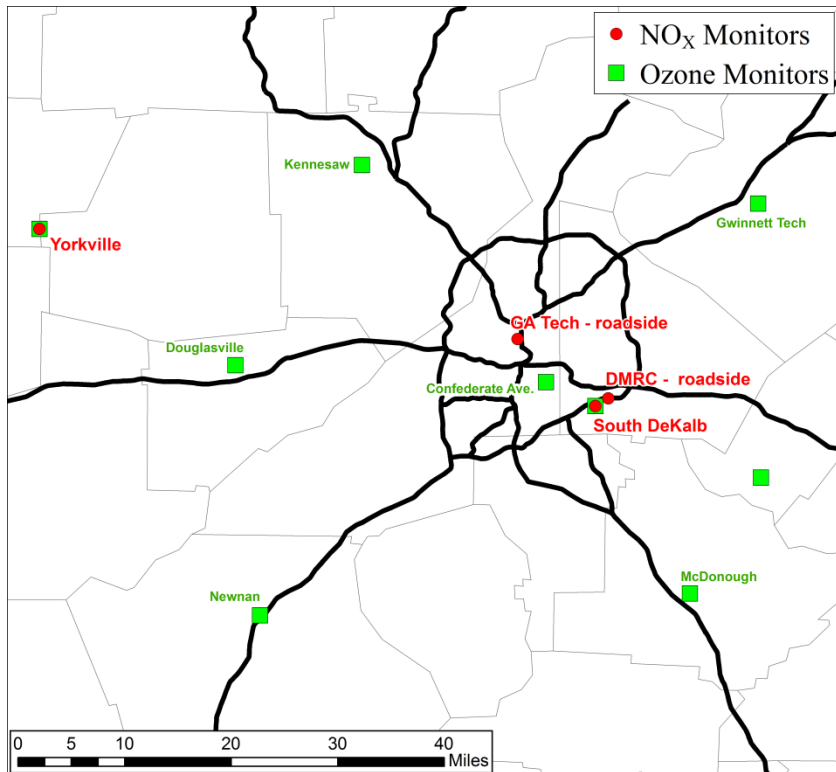


Figure 34. Locations of ozone and NO_x monitors in the Metro Atlanta area.

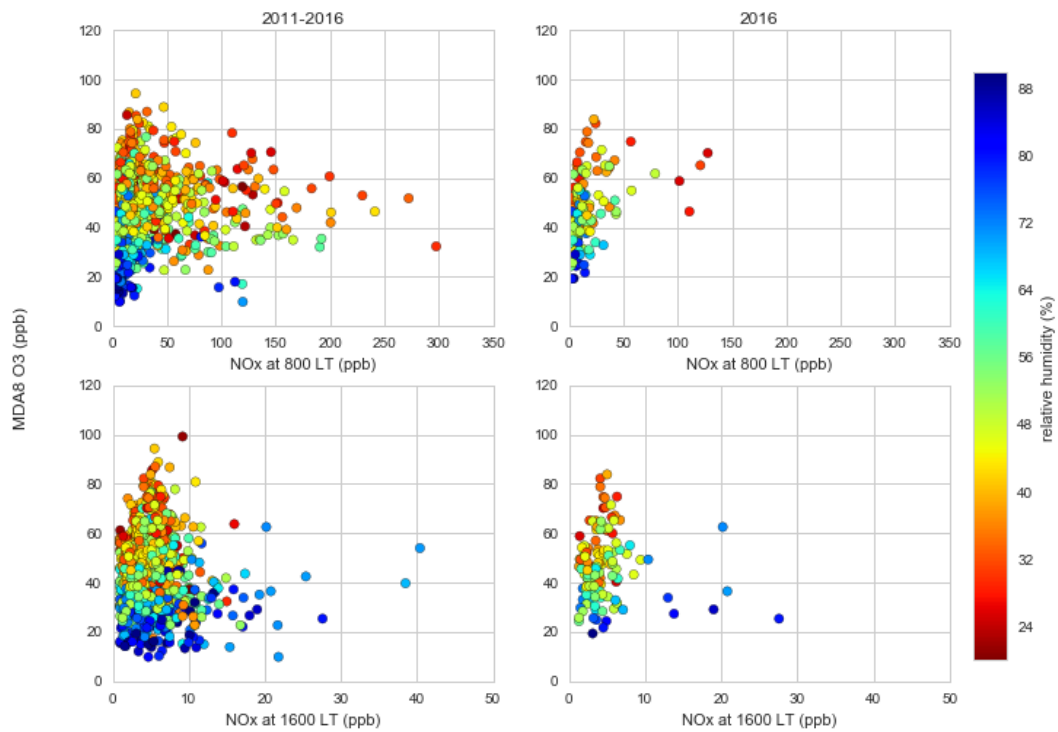


Figure 35. Scatter plots of MDA8O3 and NO_x at 8 AM (top row) and 4 PM (bottom row) at the South DeKalb monitor. The color of dots reflects afternoon relative humidity levels.

Diurnal patterns of NO_x observations on ozone exceedance days

The boxplots showing the statistics (i.e. mean, 10th, 25th, 75th, and 90th percentiles) are developed by hour of day for NO_x observations during the 2016 ozone season at the three NO_x monitors. These boxplots are overlaid with NO_x observations on ozone exceedances for the Confederate Avenue (Figure 36), South DeKalb (Figure 37), Gwinnett Tech (Figure 38), McDonough (Figure 39) and Conyers (Figure 40) monitors. NO_x observations at the two roadside monitors are higher than those at the South DeKalb monitor, indicating large impacts from mobile sources. There is also a clear diurnal variation in NO_x observation, peaking in the morning when NO_x emissions are high due to commuter traffic and NO_x emissions are trapped at low altitudes as the planetary boundary layer (PBL) is still quite low. NO_x observations then rapidly decrease when the PBL expands and photochemistry becomes stronger during the day, and increase again at night when the PBL collapses. On ozone exceedance days, morning time NO_x observations tend to be higher than the average NO_x observations, especially from 6 AM to 8 AM when traffic volumes are highest, though no clear patterns have been found for NO_x observations during evening/nighttime. However, there are also occasions when morning time NO_x is not high compared to typical values at multiple monitors on ozone exceedance days such as the period from June 27 to July 1, 2016. These morning time NO_x observations tend to be very low compared to the mean, especially at the South DeKalb NO_x monitor. As identified by the HYSPLIT modeling analysis, ozone exceedances during this episode are impacted by air parcels traveling down from high altitudes, which may likely cause the relatively lower NO_x observations during this period.

Day-of-Week patterns of NO_x observations on ozone exceedance days

Variation of NO_x observations by day of week is analyzed by developing similar boxplots for NO_x observations at 8 AM at the three NO_x monitors (Figure 41). The NO_x observations at 8 AM are chosen since they are likely correlated with high ozone levels as identified in the diurnal pattern analysis for the NO_x observations. The NO_x observations are higher on weekdays than the weekends, corresponding to similar traffic patterns (i.e. heavier commuter traffic during weekdays than weekend). Sunday morning NO_x is typically lower than Saturday morning. Friday morning NO_x also tends to be slightly lower than other weekday NO_x at the South DeKalb and the DMRC roadside monitors. The boxplots are overlaid with NO_x observations on ozone exceedance day labeled as red circles. The size of the circle indicates the number of ozone monitors that exceeded 70 ppb on a particular day. At all three NO_x monitors, NO_x observations usually tend to be higher on ozone exceedance days with minimal exceptions. Most ozone exceedance days occur during the weekdays. There is one ozone exceedance event that occurred on a Sunday when observed NO_x was relatively higher compared to most Sundays.

Monthly patterns of NO_x observations on ozone exceedance days

Variation of NO_x observation by month is then analyzed by developing similar boxplots for NO_x observations at 8 AM at the three NO_x monitors (Figure 42). The mean morning time NO_x observations at the two roadside monitors range between 25 and 60 ppb, usually higher than the South DeKalb monitor. The mean morning time NO_x observations at the South DeKalb monitor tend to be less than 20 ppb throughout most of the ozone season except in October. NO_x begins to increase through the winter because there is less photochemistry to remove atmospheric NO_x. NO_x observations at the DMRC roadside monitor also starts to increase in October; however, this trend is not observed for the Georgia Tech monitor. The boxplots are overlaid with NO_x

observations on ozone exceedance days (labeled as red circles). The size of the circle indicates the number of ozone monitors that exceeded 70 ppb on a particular day. Most exceedances took place in May and June with one day in June having ozone exceedances at nine monitors. Usually, morning time NO_x observations on an ozone exceedance day are higher than the mean NO_x observations in a month when the exceedance took place. At the Georgia Tech roadside monitor, any exceedance day with more than one exceeding monitor, morning time NO_x is much higher than the mean, reaching over 120 ppb on June 10, 2016 which is the day when nine monitors exceeded the ozone standard.

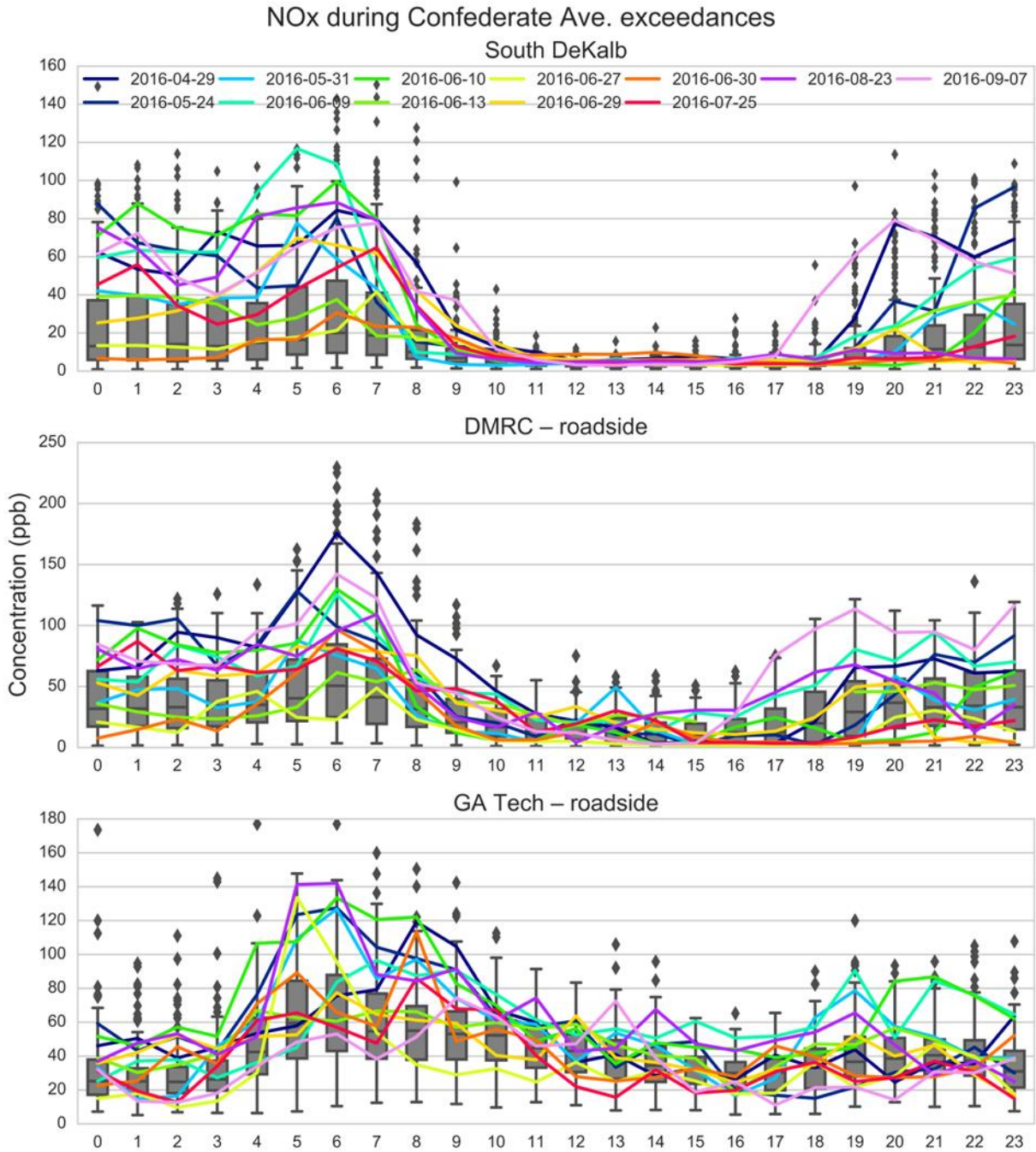


Figure 36. Boxplots by hour of day for NOx observations during 2016 ozone seasons at three NOx monitors. Colored lines are NOx observations on ozone exceedance at Confederate Avenue.

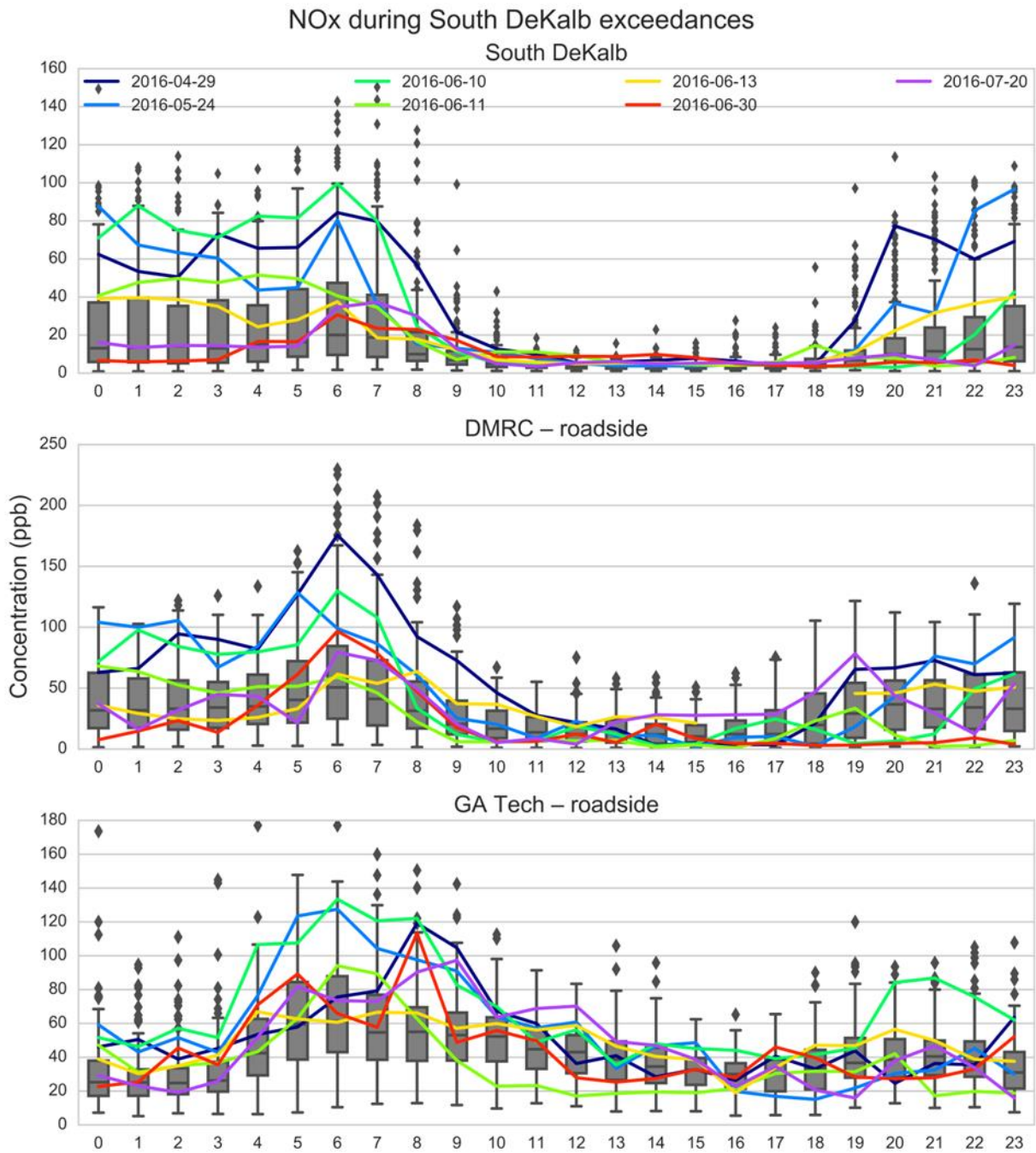


Figure 37. Boxplots by hour of day for NOx observations during 2016 ozone seasons at three NOx monitors. Colored lines are NOx observations on ozone exceedance at South DeKalb.

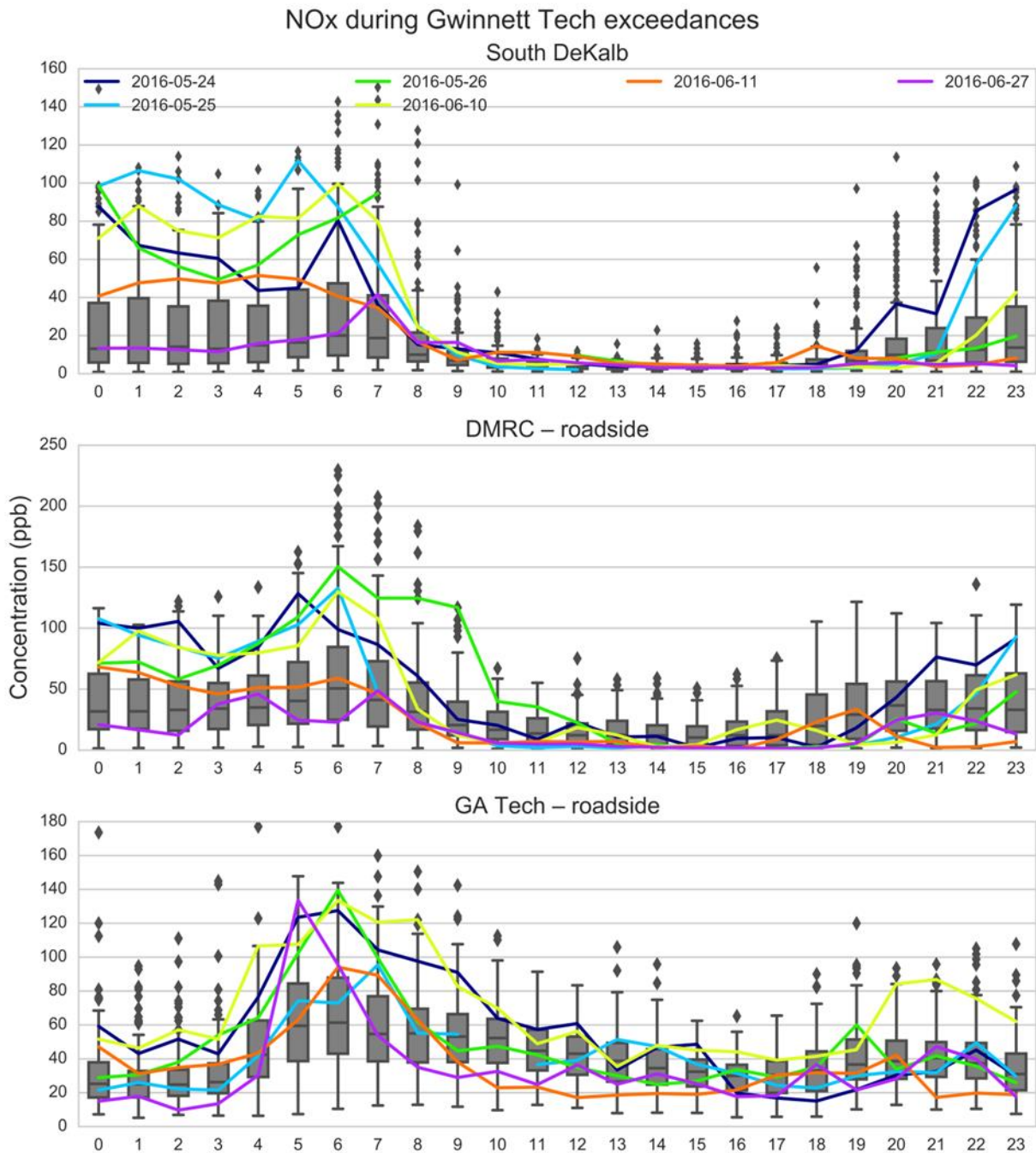


Figure 38. Boxplots by hour of day for NOx observations during 2016 ozone seasons at three NOx monitors. Colored lines are NOx observations on ozone exceedance at Gwinnett Tech.

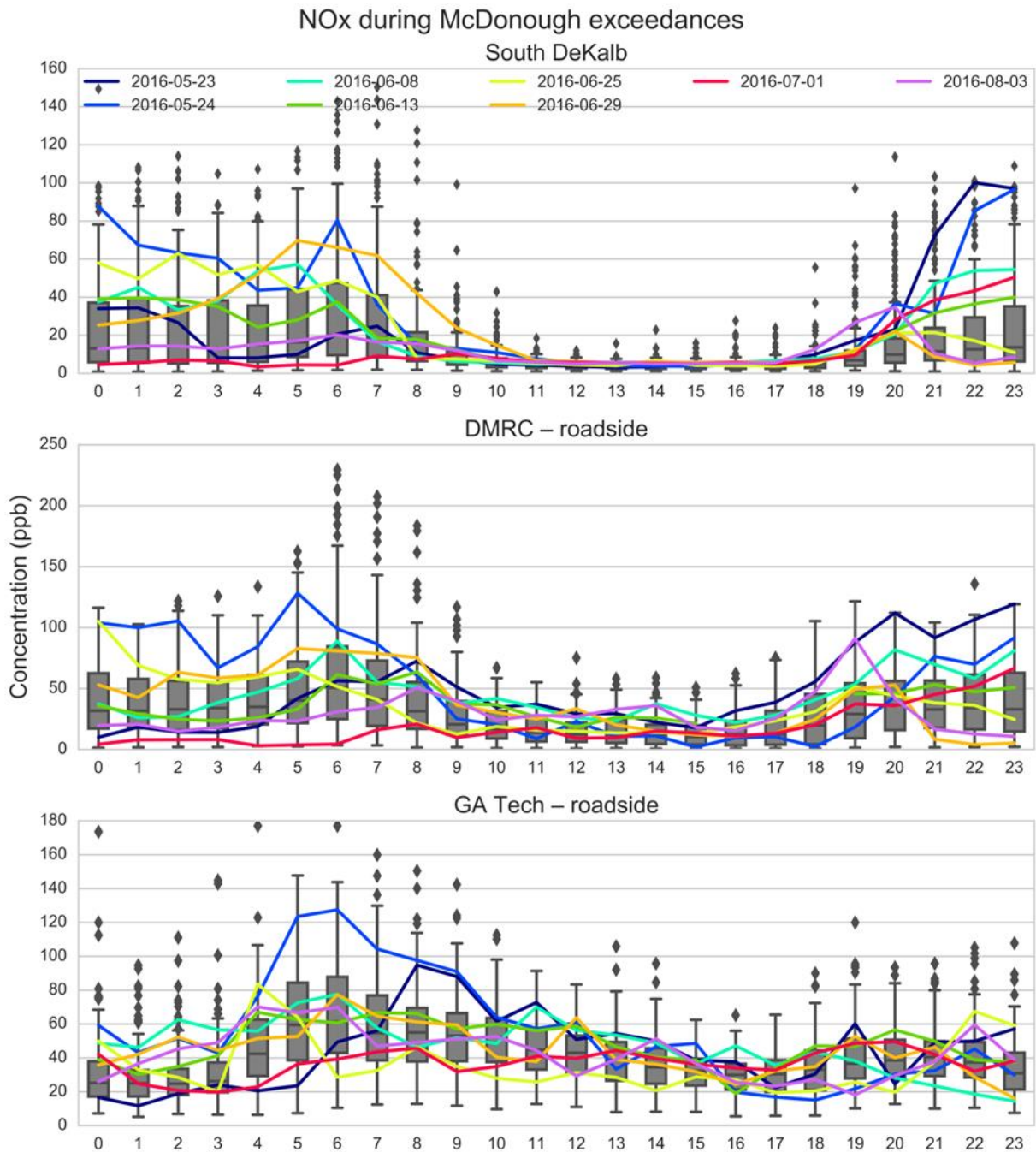


Figure 39. Boxplots by hour of day for NOx observations during 2016 ozone seasons at three NOx monitors. Colored lines are NOx observations on ozone exceedance at McDonough.

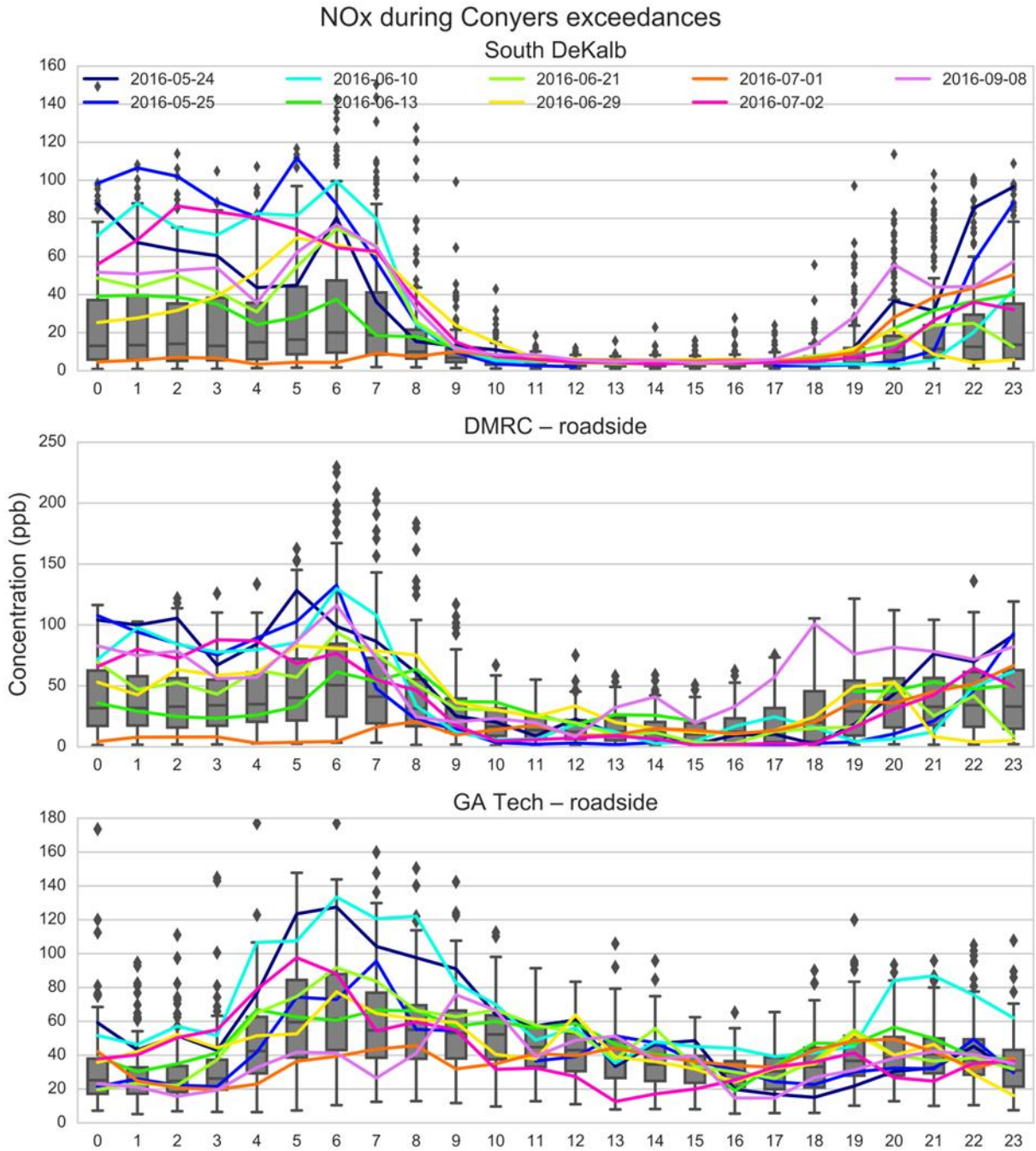


Figure 40. Boxplots by hour of day for NOx observations during 2016 ozone seasons at three NOx monitors. Colored lines are NOx observations on ozone exceedance at Conyers.

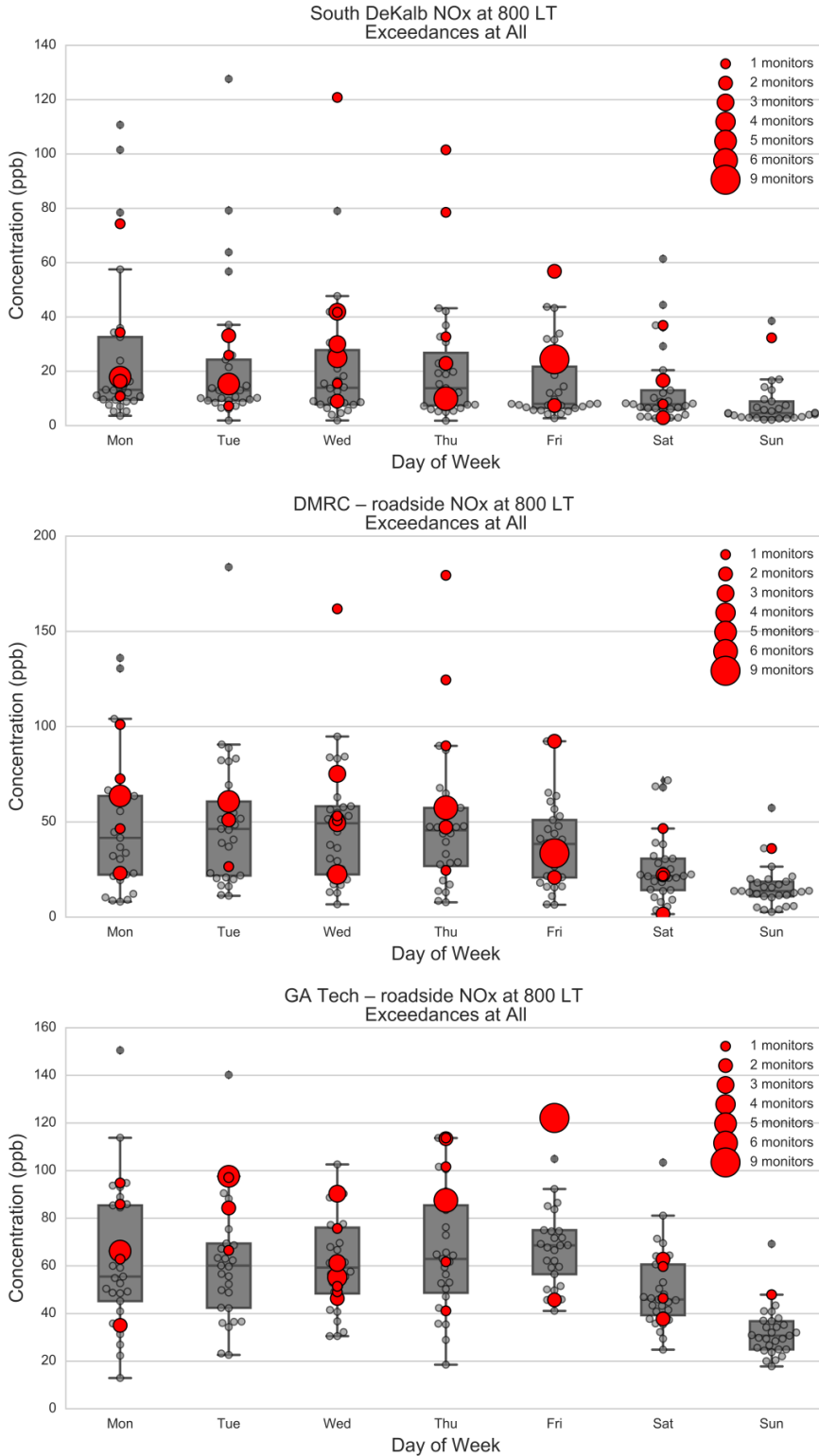


Figure 41. Boxplots by day of week for NOx observations at 8 AM during the 2016 ozone seasons at three NOx monitors. Red dots are average NOx observations on ozone exceedance days in Georgia. The size of red dots refers to the number of monitors exceeding the 2015 ozone NAAQS.

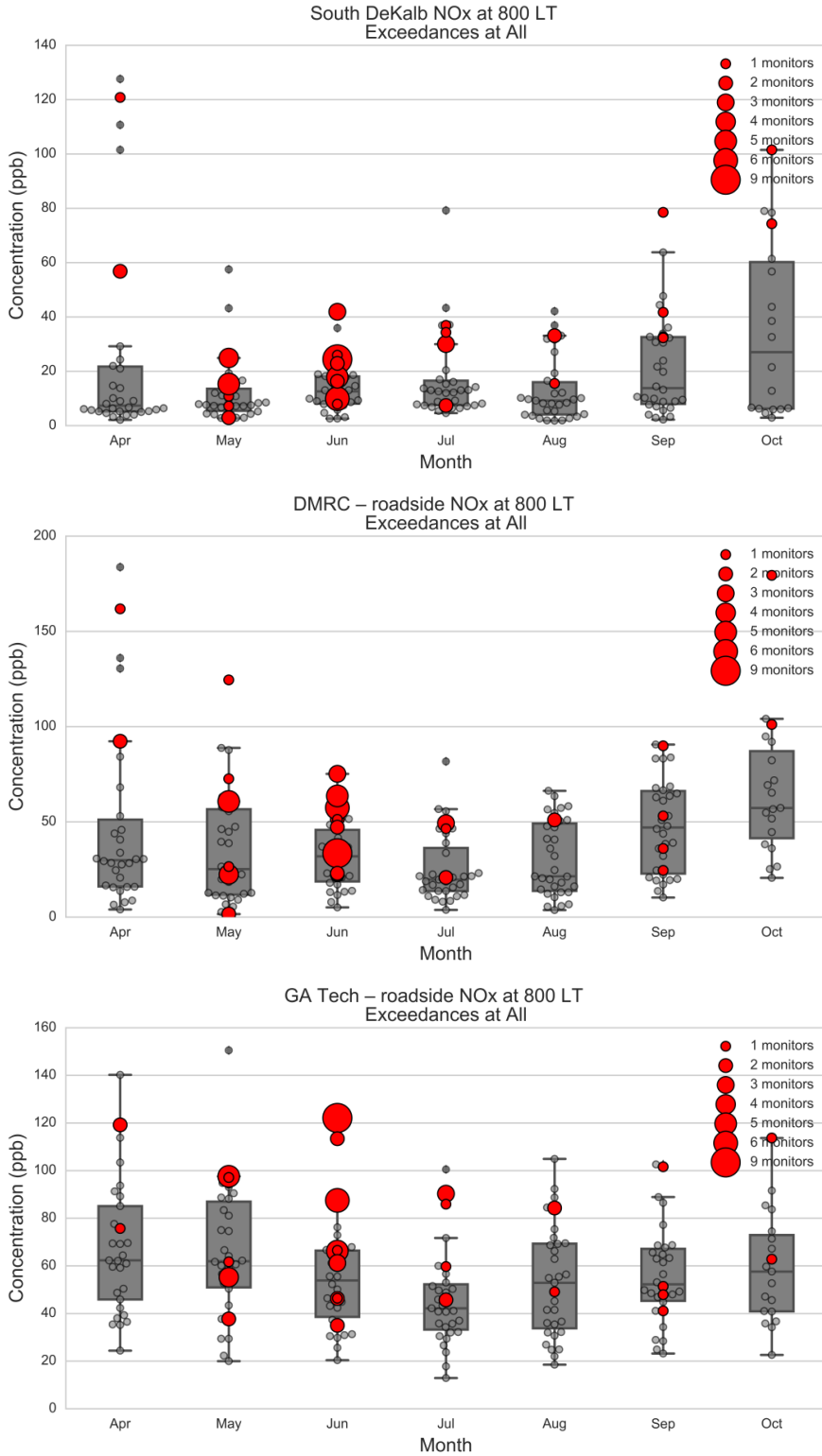


Figure 42. Boxplots by month for NOx observations at 8 AM during the 2016 ozone seasons at three NOx monitors. Red dots are average NOx observations on ozone exceedance days in Georgia. The size of red dots refers to the number of monitors exceeding the 2015 ozone NAAQS.

Indicator analysis

The ratio of O_3 to NO_x is calculated for 2011-2016 data at the South DeKalb monitor in this study as an indicator of local O_3 production efficiency (Tonnesen et al., 2000). When the ratio of O_3 to NO_x is high, radical propagation is reduced and thus O_3 is not produced efficiently; while when the ratio of O_3 to NO_x is low, NO can remove O_3 through titration. In the 2010 Tonnesen study, O_3 is produced most efficiently with the ratio of O_3 to NO_x being ~ 8 during a morning period (0900 to 1000 LT), the ratio being ~ 15 during noon (1200 to 1300 LT), and the ratio being 16 to 20 during an afternoon period (1600 to 1700 LT).

Diurnal profiles of median O_3 and NO_x for each ozone season and exceedance days during 2011-2016 (Figure 43 and Figure 44) have shown that NO_x concentration decreases when O_3 increases and vice versa. In addition, NO_x concentrations during low-ozone hours are much higher on ozone exceedance days. The ratios of O_3 to NO_x calculated here are compared with the ratios suggested in the 2010 Tonnesen study (Figure 45). In the morning period (0900 to 1000 LT), the ratios of O_3 to NO_x for ozone exceedance days are lower than Tonnesen's ratio for peak O_3 production and there is no clear difference between the ozone exceedance days and the average conditions during the ozone season. During noon (1200 to 1300 LT), the ratios of O_3 to NO_x for ozone exceedance days are mostly higher than those for the average conditions during ozone season. Such ratios are lower than Tonnesen's ratio for peak O_3 production (i.e. ~ 15), except for the ratios corresponding to exceedance days in 2011 and 2014. In the afternoon period (1600 to 1700 LT), the ratios of O_3 to NO_x for ozone exceedance days are mostly higher than those for the average conditions during the ozone season. The ratios for exceedance days during 2011, 2014, and 2016 are close to Tonnesen's ratio for peak O_3 production (i.e. 16-20). In general, the ratio of O_3 to NO_x is still a good indicator for high ozone days, implying a strong impact of NO_x on ozone formation.

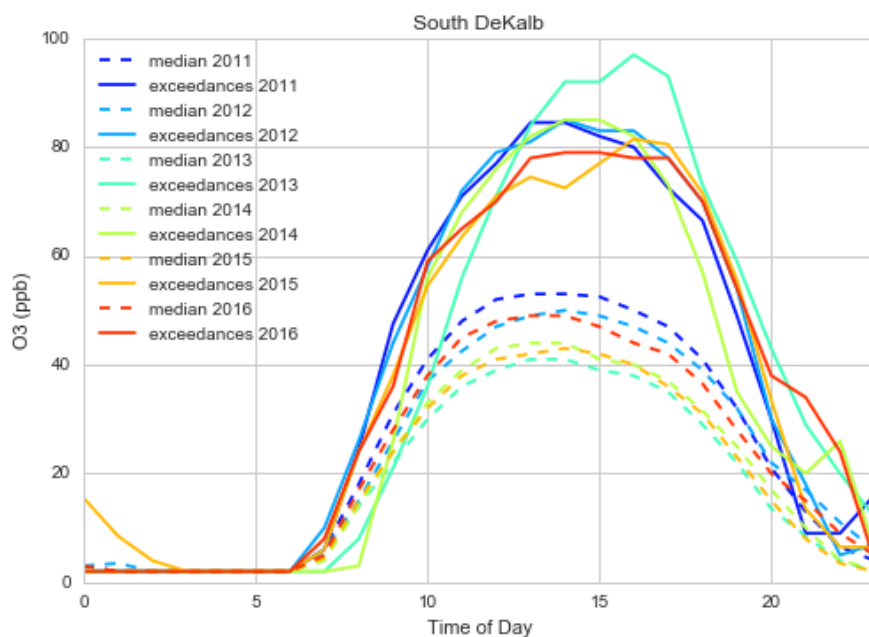


Figure 43. Diurnal profile of median ozone for each ozone season (dashes) and exceedance days (solid lines) during 2011-2016.

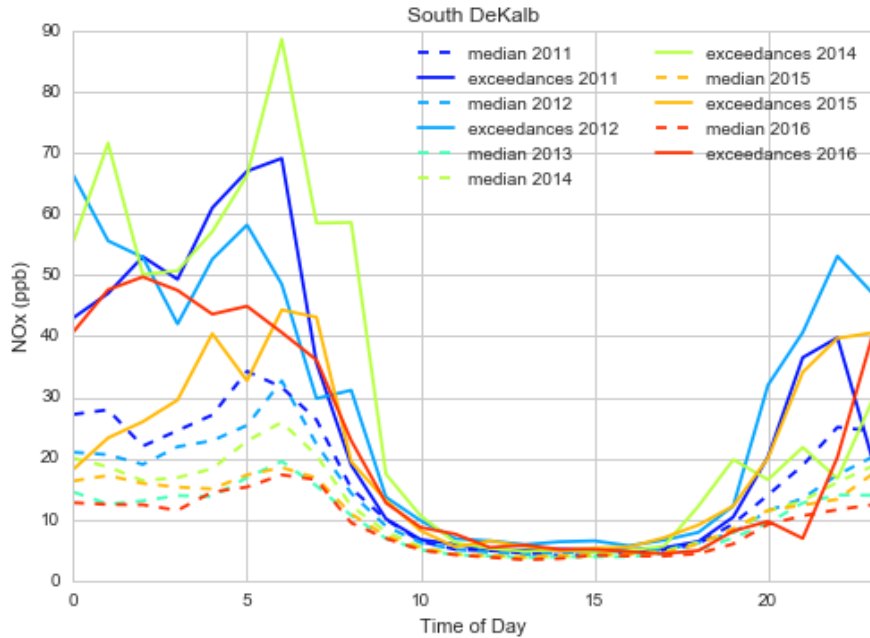


Figure 44. Diurnal profile of median NO_x for each ozone season (dashes) and exceedance days (solid lines) during 2011-2016. The profile for exceedance days during 2013 is missing since there is only one exceedance day in 2013 and some NO_x measurements for that day are missing.

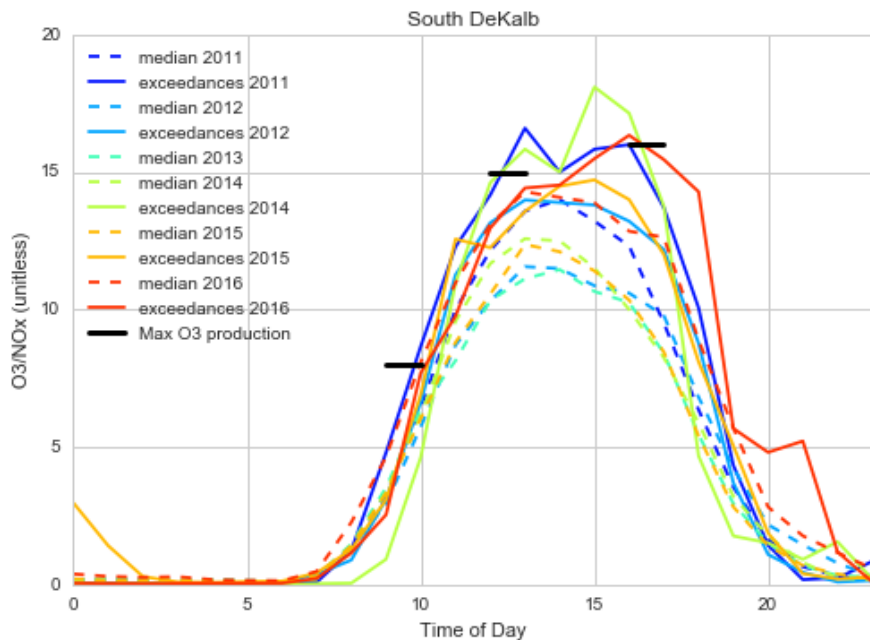


Figure 45. Diurnal profile of median O₃ to NO_x ratio for each ozone season (dashes) and exceedance days (solid lines) during 2011-2016. The black bars at 9 to 10 am, 12 to 1 PM and 4 to 5 PM represent the ratios where peak O₃ production occurs according to Tonnesen's 2010 study. The profile for exceedance days during 2013 is missing since there is only one exceedance day in 2013 and some NO_x measurements for that day are missing.

NO_x Trends Based on OMI Satellite Data

NO_x trends in Atlanta during 2005-2016 ozone seasons are evaluated using the daily tropospheric NO₂ columns by Ozone Monitoring Instrument (OMI) onboard NASA's Aura satellite. The polar orbit satellite has a 1:45 PM \pm 15 minute equator crossing time, which means OMI provides NO₂ information in early afternoon when local ozone production is near its daily peaks. Since there are large fractions of tropospheric NO₂ columns at the ground level as shown from in situ and aircraft measurements (e.g. Steinbacher et al., 2007; Heland et al., 2002; Martin et al., 2004), the tropospheric NO₂ columns can generally represent the surface NO_x conditions, especially at hot spots over urban areas. The standard tropospheric OMI NO₂ column product has a ground pixel size of 13 \times 24 km² (Bucsela et al., 2013), and was processed onto 0.1 degree \times 0.1 degree global grid (Lamsal et al., 2014). The Metro Atlanta area is defined in this study as 13 \times 13 grids centering at Five Points and covering 6 grids ($=0.6^\circ$) in all 4 directions (Figure 46).

Spatial distribution of the 12-year average OMI NO₂ columns during 2005-2016 over the Metro Atlanta area (Figure 46) shows the NO₂ gradient increases from the southwest to the northeast of the city, (Laughner et al., 2016). The hot spot of NO₂ columns clearly shows strong local NO_x emissions in the Metro Atlanta area.

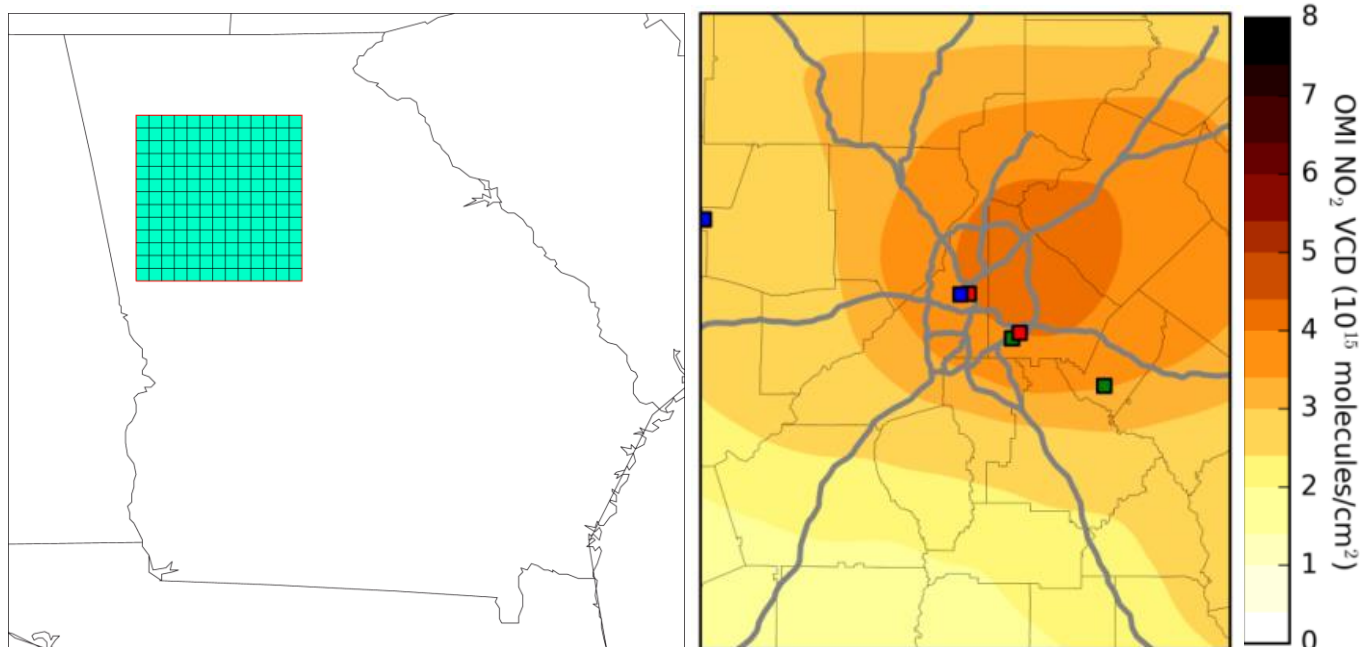


Figure 46. (a) Selected OMI NO₂ grids over the Metro Atlanta area. (b) Mean OMI NO₂ columns over the Metro Atlanta area during 2005-2016. Six Georgia monitoring sites are shown in squares (Blue: SEARCH, Red: Near road, Green: AQS).

The inter-annual comparison of NO₂ columns in ozone season shows significant decrease in NO₂ concentrations since 2005 (Figure 47 and Figure 48). NO₂ columns in warm months are much lower than in cold months (Figure 49) due to additional photochemistry during the warmer months. Therefore, only OMI NO₂ columns during the ozone season (April to October) were used to develop the inter-annual trend. The inter-annual NO₂ variation based on OMI data matches well with the large ozone decreasing trends in recent years. Day-of-week patterns of OMI NO₂ columns (Figure 50) show higher values during weekdays than weekends, consistent with findings based on NO₂ ground-based observations. In summary, OMI NO₂ columns and ground-based NO_x observations have shown similar inter-annual and day-of-week patterns, which is also consistent with the trend for the ozone concentrations, indicating that NO_x plays an important role in tropospheric ozone formation.

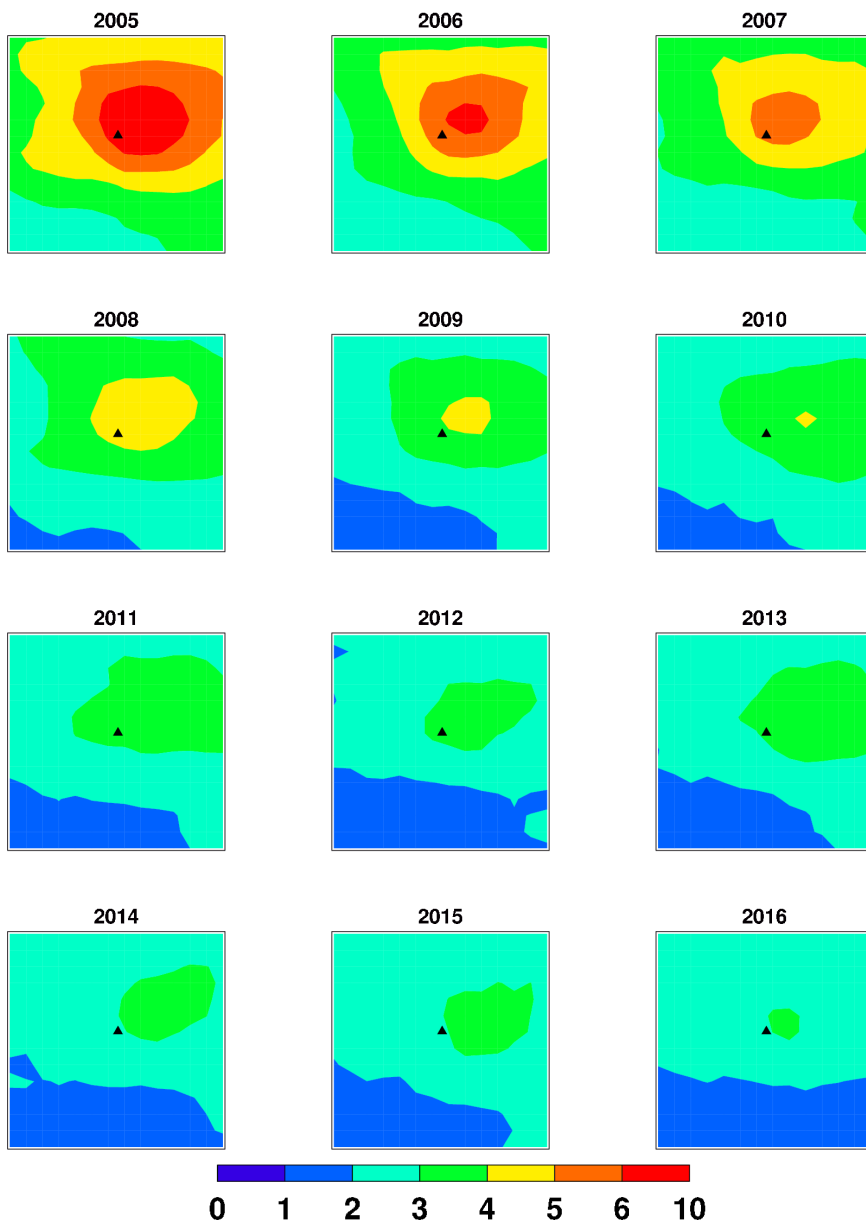


Figure 47. OMI NO₂ columns over the Metro Atlanta area during 2005-2016.

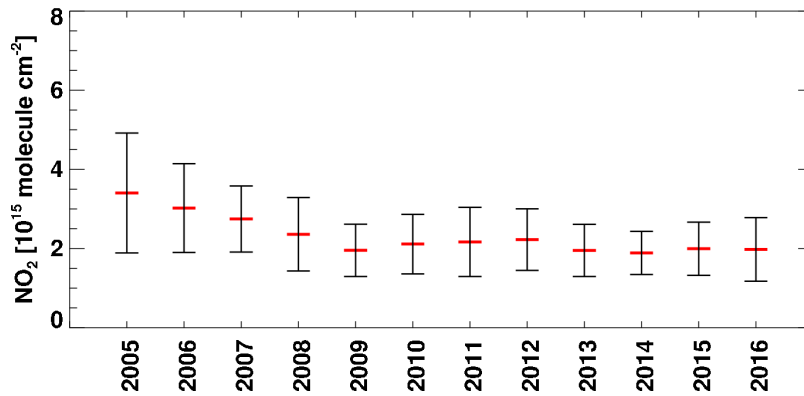


Figure 48. Annual spatial mean OMI NO₂ over the Metro Atlanta area during April-October of 2005-2016. The means (red bar) and its standard deviations (black bars) are shown.

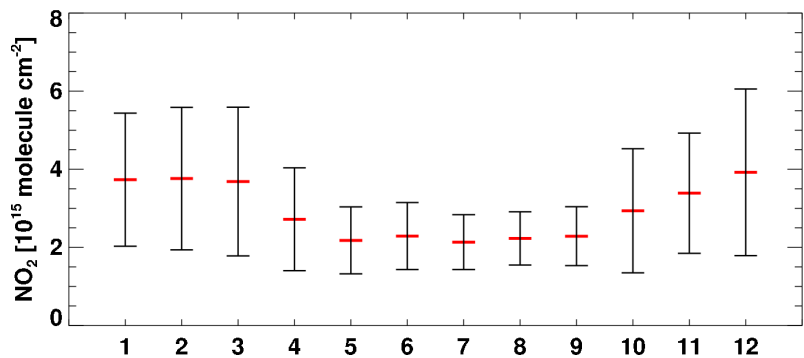


Figure 49. Monthly OMI NO₂ in 2005-2016 over the Metro Atlanta area. The means (red bar) and its standard deviations (black bars) are shown.

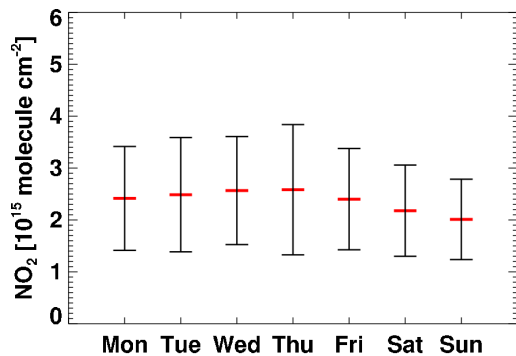


Figure 50. Mean OMI NO₂ columns on weekday over Metro Atlanta area in April-October, 2005-2016. The mean (red bar) and its standard deviations (black bars) are shown.

9. Ozone and VOCs precursors

Peak ozone concentrations in the Atlanta urban core can be sensitive to VOCs, although Atlanta is generally NO_x-sensitive according to previous work (Blanchard et al., 2010; Hidy et al., 2014). VOCs are emitted from a variety of sources, including motor vehicles, chemical manufacturing facilities, refineries, factories, consumer and commercial products, and natural (biogenic) sources (mainly trees). In the Metro Atlanta area during 2014, approximately 73% of VOC emissions are from biogenic sources and 13% from mobile (onroad + nonroad) sources (Figure 51). Both anthropogenic VOC emissions and ambient VOC concentrations have been decreasing (Hidy and Blanchard, 2015). In this study, impacts of VOCs on 2016 ozone exceedances in Atlanta are investigated using an observation-based method.

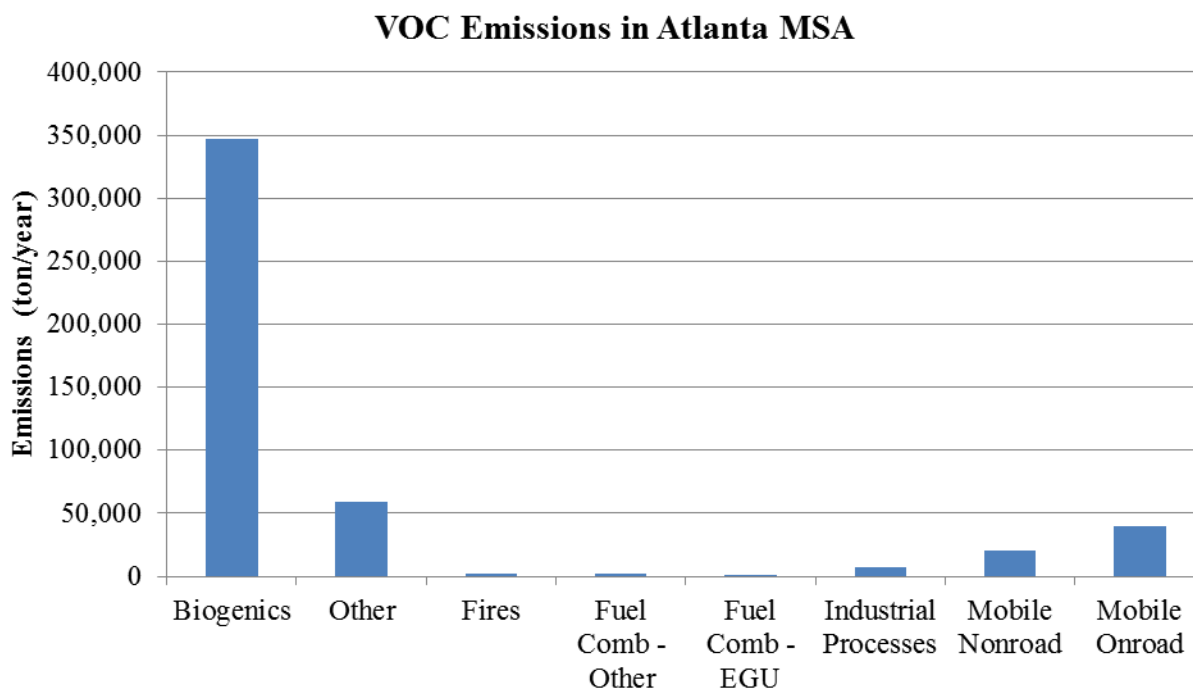


Figure 51. 2014 VOC emissions (tons/year) by source sectors in Metro Atlanta area.

Relationship between peak 8-hr ozone and anthropogenic VOC

The relationship between peak 8-hour ozone and anthropogenic VOC was assessed using a linear regression model. There are three Photochemical Assessment Monitoring Stations (PAMS) monitors (Figure 52) in the Metro Atlanta Area. In Atlanta, westerly winds are considered the long-term prevailing winds. Thus, the Yorkville monitor is typically used as the background monitor for the area. The South DeKalb monitor measures urban air quality conditions because it is located in the urban core. The Conyers monitor measures aged air masses transported from the urban core. The VOC measurements at the South DeKalb PAMS monitor are chosen for this analysis due to data availability and its existence inside of the Atlanta urban core.

The annual summer time average anthropogenic VOC concentrations are calculated using 1-hour VOC data measured daily at the South DeKalb monitor during June-August of 2010, 2011, 2013 and 2014 and obtained from AQS data retrieval system. Isoprene is considered biogenic and is

not included in the anthropogenic VOC calculation. Significant data are missing in 2012 and 2015, and 2016 data are not available; therefore, these years are not used in this analysis.

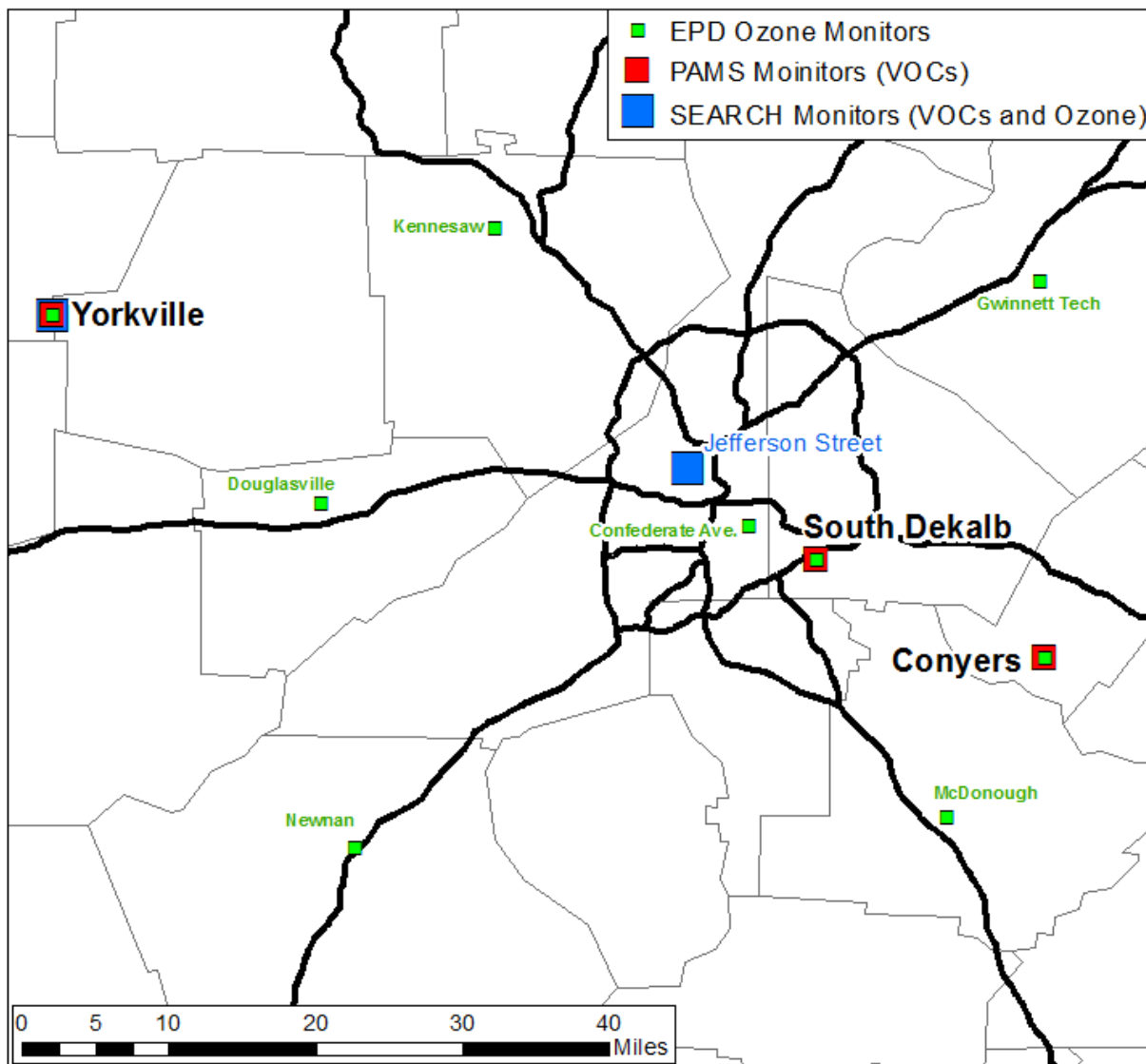


Figure 52. Locations of ozone, PAMS, and SEARCH monitors in the Metro Atlanta area.

Figure 53 figure shows a strong linear relationship (coefficients of determination, $R^2 \sim 0.99$) between ozone and anthropogenic non-methane organic carbon (aNMOC; defined as measured VOCs excluding methane and isoprene). This correlation has been found in previous work (Hidy and Blanchard, 2015). It is estimated that the annual 4th highest MDA8O3 concentrations can be reduced by 6.5 ppb if annual summertime average aNMOC concentrations are reduced by 10 ppbC assuming all photochemical conditions including reactivity of the total aNMOC and NO_x concentrations are relatively consistent with that in the period between 2010 and 2014. This result may indicate that the Atlanta ozone may have become more sensitive to aNMOC than in past years. However, it does not show any specific information about which VOCs are important and, in turn, which anthropogenic sources are potentially important for controlling the Atlanta ozone.

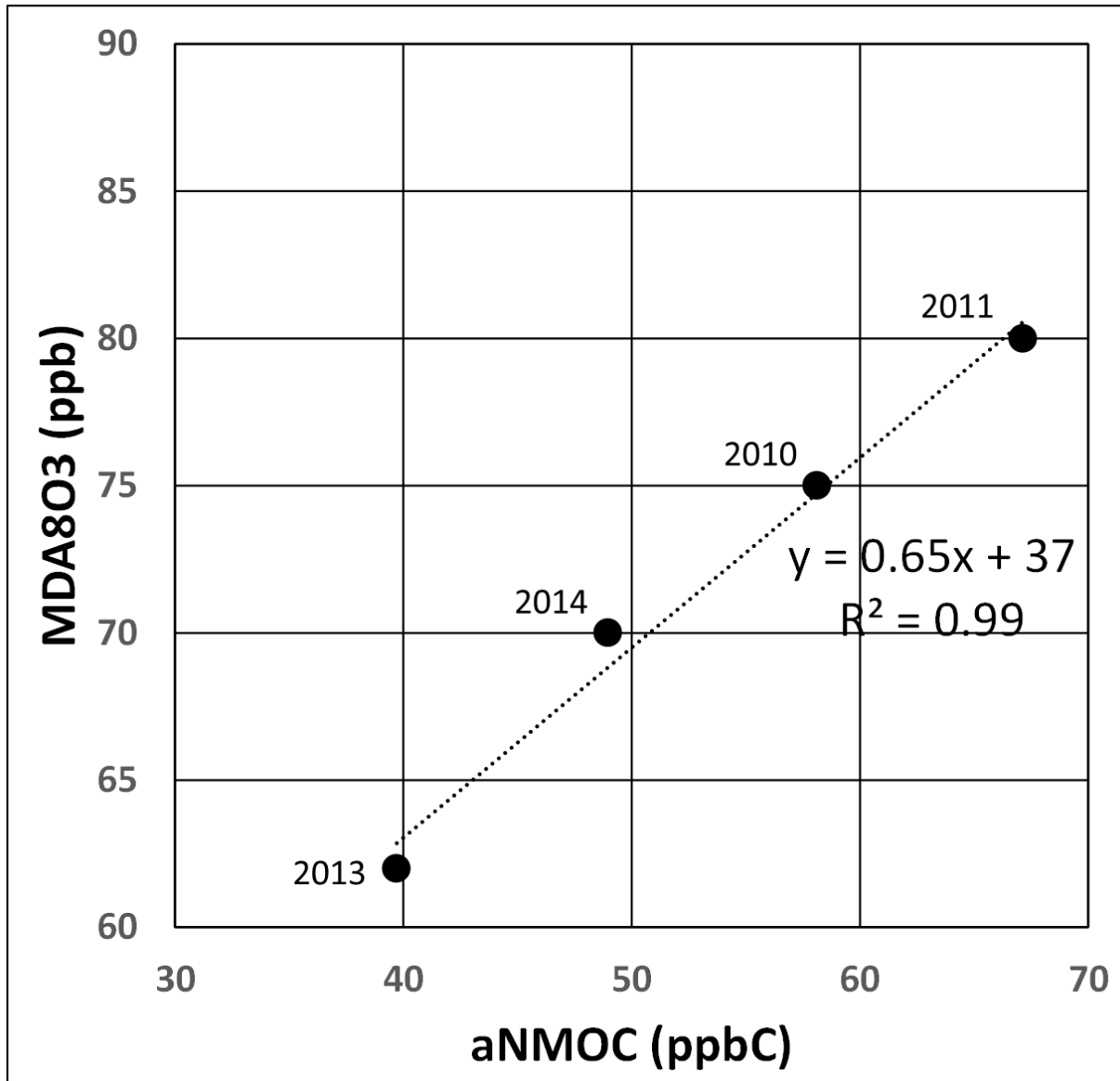


Figure 53. Univariate regression for the 4th highest MDA8O3 and summertime average aNMOC at the South DeKalb monitor during 2010, 2011, 2013 and 2014.

The correlation of MDA8O3 and total VOCs concentrations (Figure 54), as well as correlation of MDA8O3 and nine VOC species with high ozone effects (Figure 55 - Figure 57) are statistically significant no matter what types of average concentrations are used. The slopes of the fitted lines indicate the reactivity of a particular VOC species. The steeper slope is usually associated with a more reactive VOC species. These correlation results are generally consistent with the reactivity scales used in this study.

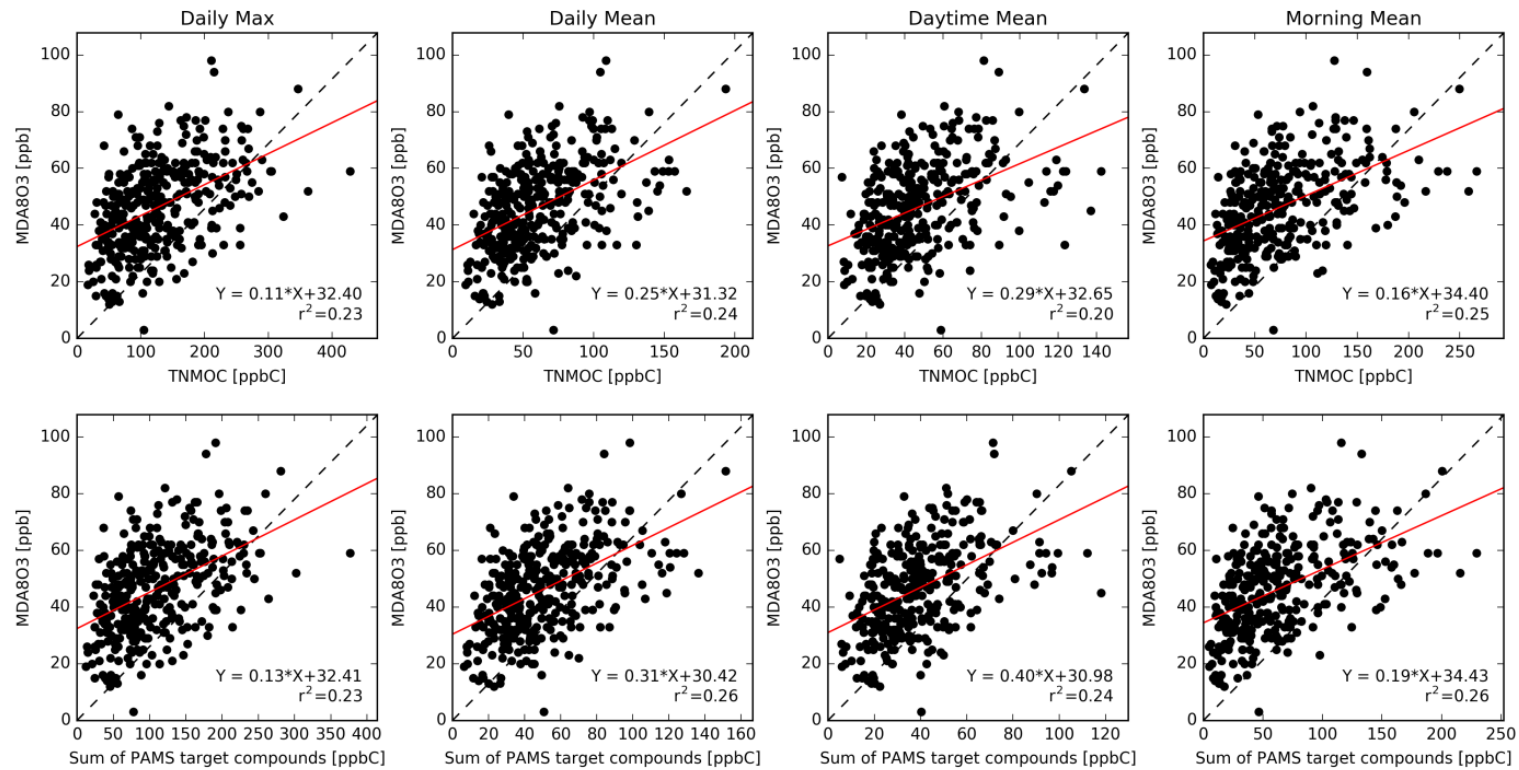


Figure 54. Correlation between MDA8O3 concentrations and VOCs concentrations averaged by different periods for Total NMOC (top) and Sum of PAMS species (bottom).

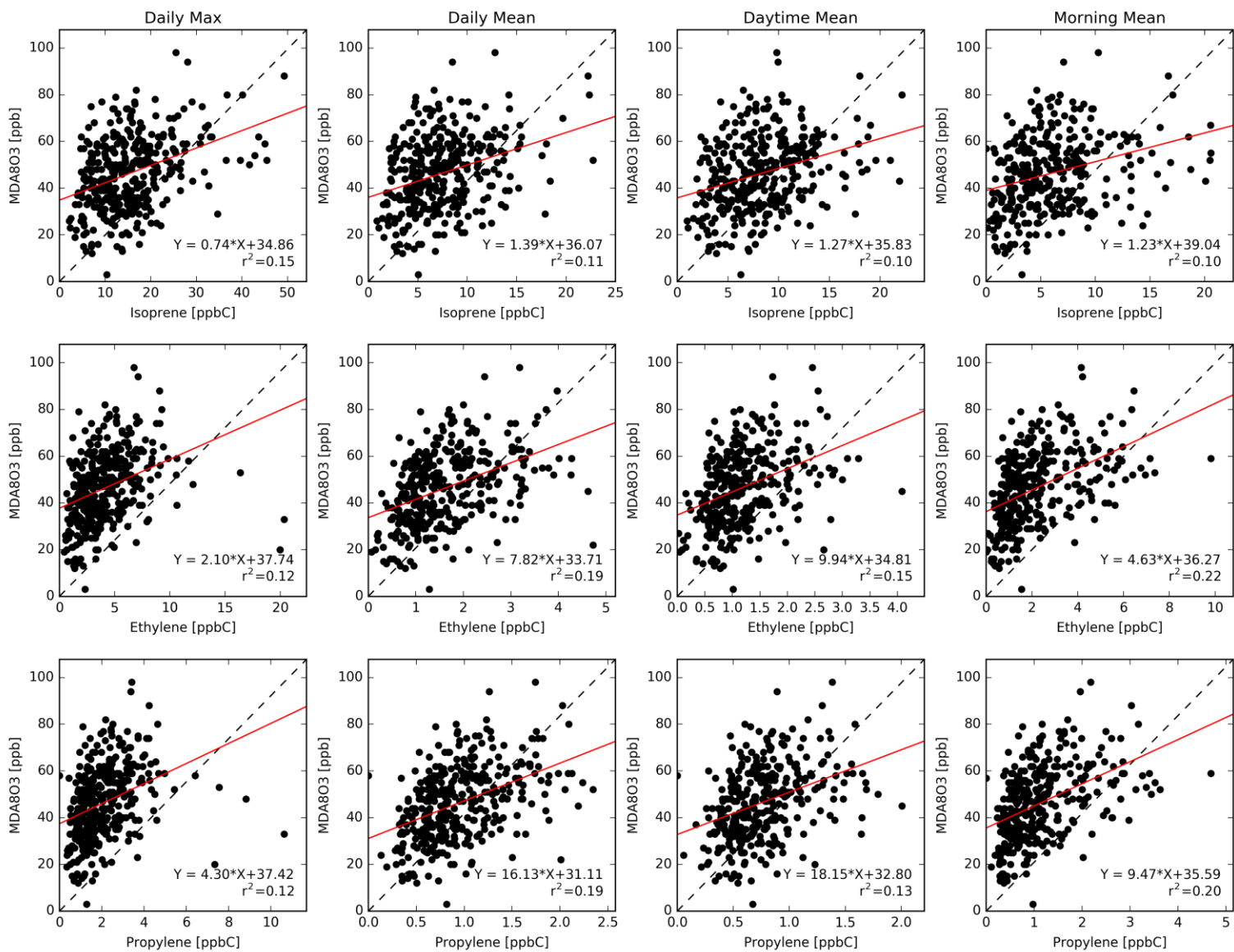


Figure 55. Correlation between MDA803 concentrations and VOCs concentrations averaged by different periods for isoprene (top), ethylene (middle), and propylene (bottom).

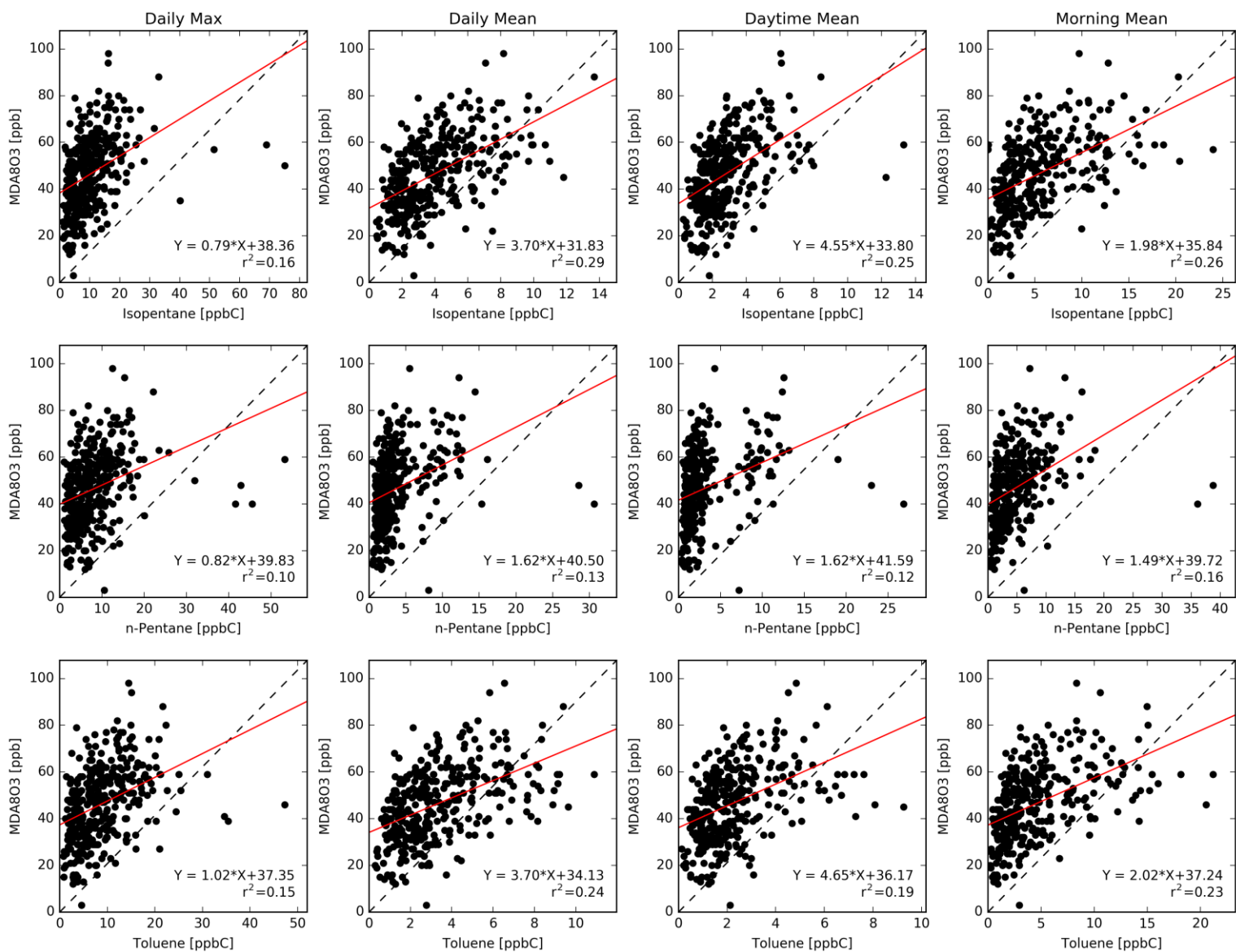


Figure 56. Correlation between MDA803 concentrations and VOCs concentrations averaged by different periods for isopentane (top), n-pentane (middle), and toluene (bottom).

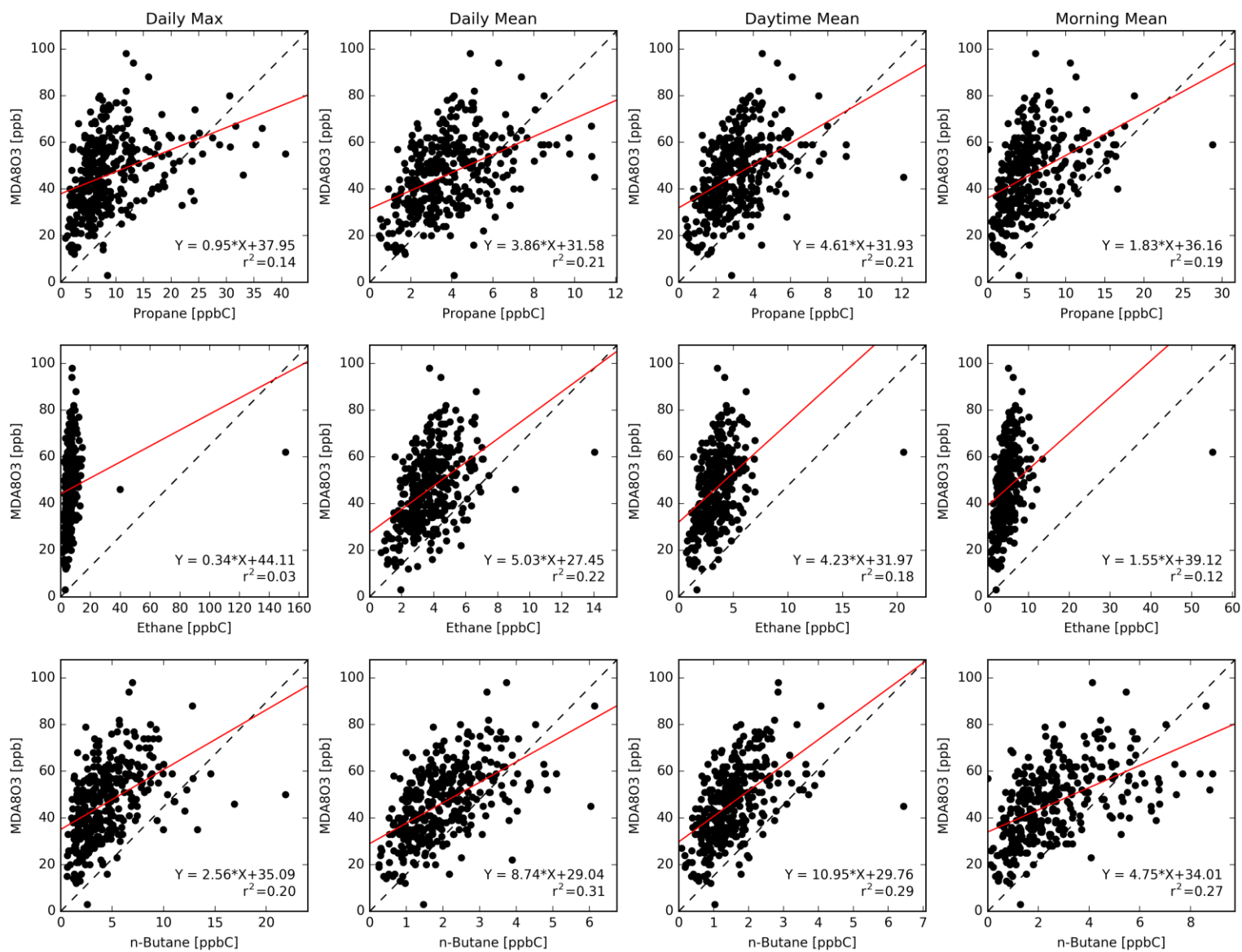


Figure 57. Correlation between MDA803 concentrations and VOCs concentrations averaged by different periods for propane (top), ethane (middle), and n-butane (bottom).

Comparison of reactivity-weighted concentrations of VOC species

Reactivity of VOC species has been used to describe their different effects on ozone formation, depending on ambient conditions, and is applied here to weight VOC measurements at the South DeKalb monitor using the Chemical Abstract Service (CAS) numbers in the pollutant matching table to calculate the corresponding ozone effects. The higher reactivity-weighted concentrations indicate higher ozone effects. The reactivity scale by VOC species developed by Bill Carter at the University of California at Riverside obtained from <http://www.engr.ucr.edu/~carter/SAPRC/saprc07.xls> is used in this study. It is “Incremental Reactivity” (IR) which is the estimated number of additional ozone molecules formed per VOCs molecule added to the existing environment. Three different scales are developed to account for different photochemical conditions (National Research Council, 1999):

- Maximum Incremental Reactivity (MIR): “Incremental reactivity of a VOC computed for conditions in which the compound has its maximum absolute IR value. This generally occurs at a low VOC-to-NO_x ratio”
- Maximum ozone incremental reactivity (MOIR): “Incremental reactivity computed for conditions that maximize the ozone concentration, i.e. representing conditions in which the VOC to NO_x ratio is moderate and the chemistry is approaching, or in, the transitional region between VOC limitation and NO_x limitation”
- Equal Benefit Incremental Reactivity (EBIR): “IR for the conditions in which the sensitivity of ozone to VOCs is equal to that of NO_x. Thus, the EBIR scale is calculated for conditions that lie midway between VOCs limitation and NO_x limitation (i.e., the transitional regime).”

EBIR is chosen in this study because the Metro Atlanta area is likely transitioning between NO_x-limited and VOC-limited conditions and VOC-to-NO_x ratio is relatively high in the Metro Atlanta as found in previous work (Blanchard and Hidy, 2014). Reactivity-weighted concentrations (RWC) are calculated as follows:

$$\text{RWC in ppb} = \frac{(\text{VOC concentrations in ppbC})}{(\text{Carbon Number})} \times (\text{EBIR Scale})$$

Table 12 lists average measured concentrations, number of carbons, EBIR scales, and reactivity-weighted concentrations of major PAMS VOC species for the analysis period, 2010-2014 excluding 2012. Table 12 clearly shows that each VOC species has differences in their abundance (i.e. concentrations) in the atmosphere and ozone forming capability per unit concentration (i.e. EBIR scale).

The ozone effects (i.e. the reactivity-weighted concentrations) of VOC species also vary with the types of average concentrations. Diurnal concentration patterns vary with VOC species which have different emissions characteristics and go through different photochemical reactions. For example, isoprene concentrations usually start to increase after sunrise and reach their peak in the afternoon, while emissions of VOC species related to mobile sources peak during morning and afternoon traffic hours. Morning measurements can be used to represent emission rates for anthropogenic species, and mid-day and afternoon measurements are related to photochemical formation. Therefore, four types of concentrations covering different periods are assessed in this

study: daily maximum, daily mean, daytime mean (6 AM – 6 PM), and morning (6 AM – 10 AM) mean.

Among all VOC species measured at the South DeKalb PAMS monitor, isoprene from biogenic sources has the highest reactivity-weighted concentrations, followed by ethylene, propylene isopentane, n-pentane, and toluene.

Table 12. Average concentrations, number of carbons, EBIR scale, and reactivity-weighted concentrations of major PAMS VOC species at the South DeKalb PAMS monitor during 2010-2014 excluding 2012. Isoprene (biogenic) is shaded in green and the top five anthropogenic values are shaded in yellow.

VOC Species	Concentration (ppbC)				Carbon Number	EBIR Scale (mole O ₃ /mole VOC)	Reactivity-weighted Concentration (ppb)			
	Daily Mean	Daily Max	Daytime Mean	Morning Mean			Daily Mean	Daily Max	Daytime Mean	Morning Mean
isoprene	7.41	15.44	8.34	6.02	5	2.51	3.72	7.74	4.18	3.02
ethylene	1.62	4.10	1.17	2.20	2	2.49	2.01	5.11	1.46	2.74
propylene	0.94	2.08	0.75	1.15	3	2.95	0.93	2.04	0.74	1.13
isopentane	3.93	10.12	2.77	5.35	5	0.66	0.52	1.34	0.37	0.71
n-pentane	3.62	7.94	2.98	4.50	5	0.56	0.40	0.88	0.33	0.50
toluene	3.31	8.87	2.21	4.59	7	0.68	0.32	0.86	0.21	0.45
propane	3.83	8.88	3.14	5.63	3	0.24	0.31	0.71	0.25	0.45
ethane	3.75	6.53	3.41	4.72	2	0.14	0.26	0.45	0.24	0.33
n-butane	1.98	4.39	1.52	2.62	4	0.52	0.26	0.57	0.20	0.34
m-ethyltoluene	1.64	4.47	0.84	1.96	9	1.28	0.23	0.63	0.12	0.28
1-butene	0.24	0.54	0.24	0.25	4	2.46	0.15	0.33	0.15	0.15
trans-2-butene	0.04	0.20	0.02	0.07	4	3.34	0.03	0.17	0.02	0.05
cis-2-butene	0.03	0.17	0.02	0.06	4	3.26	0.03	0.14	0.02	0.05
cis-2-pentene	0.02	0.12	0.01	0.03	5	2.52	0.01	0.06	0.01	0.02
trans-2-pentene	0.07	0.33	0.04	0.11	5	2.52	0.04	0.16	0.02	0.05
1,3,5-trimethylbenzene	0.22	0.78	0.11	0.28	9	2.17	0.05	0.19	0.03	0.07
1-pentene	0.04	0.19	0.03	0.05	5	1.84	0.01	0.07	0.01	0.02
1,2,4-trimethylbenzene	0.68	1.94	0.40	0.93	9	1.74	0.13	0.37	0.08	0.18
isobutane	1.02	2.51	0.71	1.44	4	0.52	0.13	0.33	0.09	0.19
2,2,4-trimethylpentane	1.30	3.46	0.83	1.71	8	0.45	0.07	0.19	0.05	0.10

Ozone-VOCs Time Series Analysis

Time series of hourly ozone and reactivity-weighted VOC concentration during 2016 for a Southeastern Aerosol Research and Characterization (SEARCH) monitor at Jefferson Street in Atlanta were developed. The time series were developed for all exceedance days in Atlanta when there is at least one ozone monitor exceeding the NAAQS and include the data for at least one day before the exceedance event. The 2016 VOC measurements at the Jefferson Street monitor are used in this study due to data availability and its existence in Atlanta urban core. These measurements are assumed to be representative of the photochemical conditions in the Atlanta urban area. The representativeness can be partially verified by the high correlation of ozone measurements at the Confederate Avenue and Jefferson Street monitors (Figure 58). Since the ozone data at the Jefferson Street monitor have not undergone through regular QA and have some abnormal values, such data are corrected before being used in the correlation analysis. The correction includes: (1) removing any values marked with “null”, (2) removing abnormally high ozone values (>200 ppb) on April 10 and 11, and (3) removing the negative ozone value on May 8.

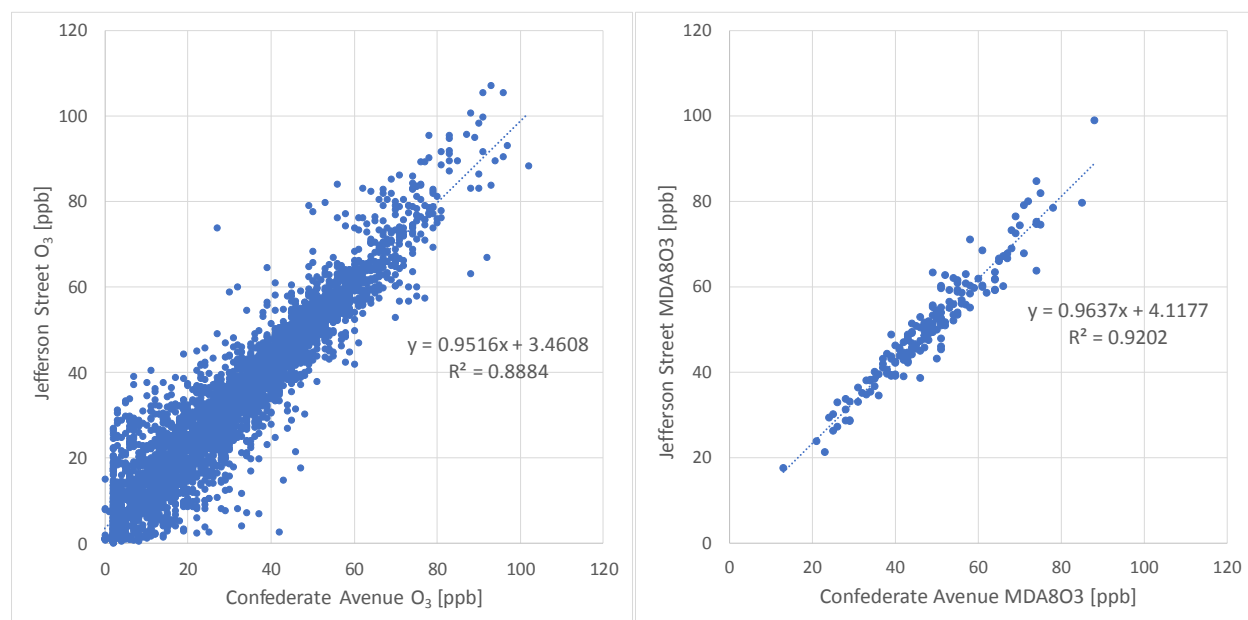


Figure 58. Correlation of 1-hour ozone concentrations (left) and MDA8O3 (right) between the Confederate Avenue and Jefferson Street monitors.

Time series for eleven time periods with ozone exceedance days at ozone monitors in Atlanta show different conditions of anthropogenic VOC species and isoprene on ozone exceedance days during different periods (Figure 59 - Figure 69). Isoprene levels during the daytime are significant during the months of June, July, and August, but less significant in April, May, and September. Ethylene concentrations are high during the evening and morning hours on most ozone exceedance days, followed by propylene, ethane, isopentane, and propane (Table 13). Ethylene, propylene, ethane, and isopentane are mainly emitted from gasoline mobile sources and other sources that use gasoline (Conner et al., 1995; National Research Council, 1999). The impacts of isoprene and the anthropogenic VOCs (i.e. ethylene, propylene, ethane, isopentane,

and propane) on ozone exceedance days are in line with the ranking of reactivity-weighted VOC concentrations. This demonstrates the importance of both biogenic and anthropogenic VOC emission sources on ozone exceedance days.

Table 13. Qualitative Summary of impacts of VOC species on ozone exceedance days. “-” means similar values between exceedance days and other days.

Exceedance Period (Exceedance Days)	Isoprene Impact	Ethylene Impact	Propylene Impact	Ethane Impact	i-Pentane Impact	Propane Impact
April 28-30 (29)	-	29	29	29	29	29
May 22-28 (23, 24, 25, 26, 28)	-	23, 24, 25, 26, 28	23, 24, 25, 26	23, 24, 25, 26	23, 25, 36	23, 24
June 7-13 (8, 9, 10, 11, 13)	10, 11, 13	8, 9, 10, 11, 13	8, 9, 10, 11, 13	9, 10, 11, 13	8, 9, 10, 11, 13	9, 10, 11
June 20-27 (21, 25, 27)	21, 25, 27	21, 25, 27	21, 25, 27	25, 27	-	21, 27
June 28-July 2 (29, 30, 1, 2)	29, 30, 1, 2	29, 30, 1, 2	29, 30, 2	29, 30, 2	29, 30, 2	29, 2
July 19-25 (20, 25)	20, 25	20, 25	20, 25	25	25	25
August 2-3 (3)	3	3	3	-	3	3
August 22-23 (23)	N/A	N/A	N/A	N/A	N/A	N/A
September 6-8 (7,8)	7, 8	7, 8	7, 8	-	7, 8	7, 8
September 14-15 (15)	15	15	15	15	15	15
September 24-25 (25)	25	25	25	25	25	25

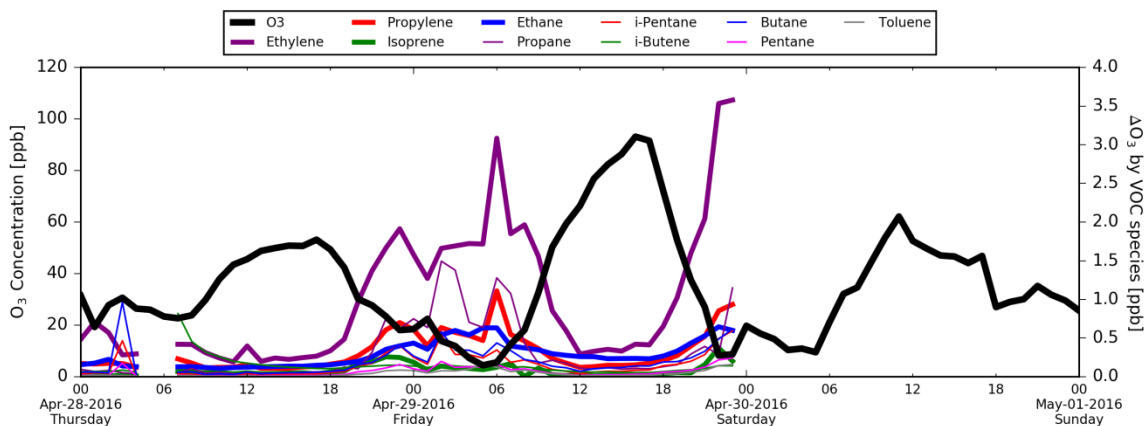


Figure 59. Time series of 1-hour ozone concentrations (left y-axis) and reactivity-weighted ozone concentration (right y-axis) for April 28-30, 2016.

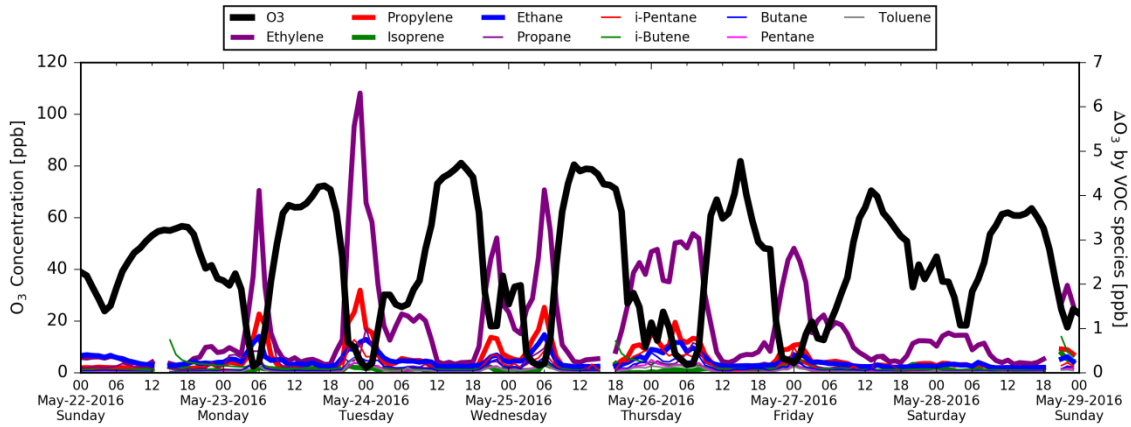


Figure 60. Time series of 1-hour ozone concentrations (left y-axis) and reactivity-weighted ozone concentration (right y-axis) for May 22-28, 2016.

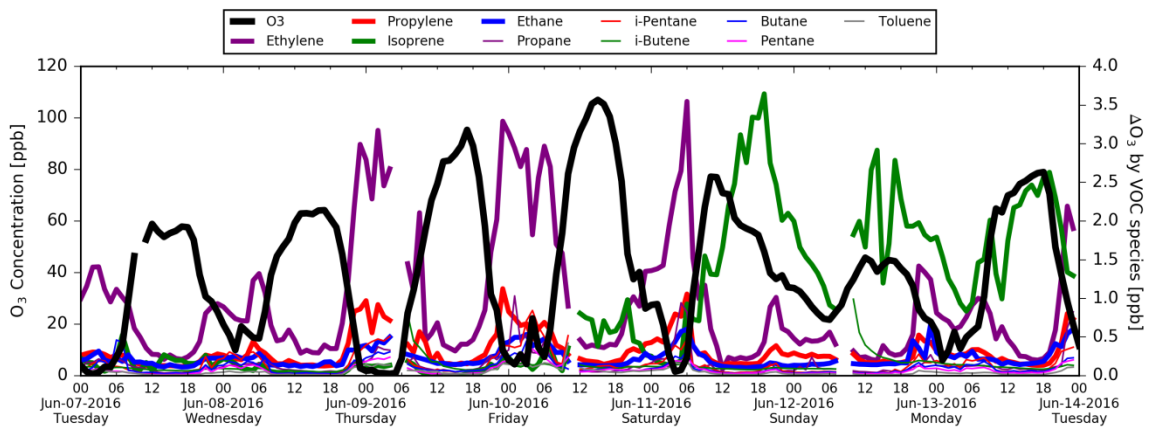


Figure 61. Time series of 1-hour ozone concentrations (left y-axis) and reactivity-weighted ozone concentration (right y-axis) for June 7-13, 2016.

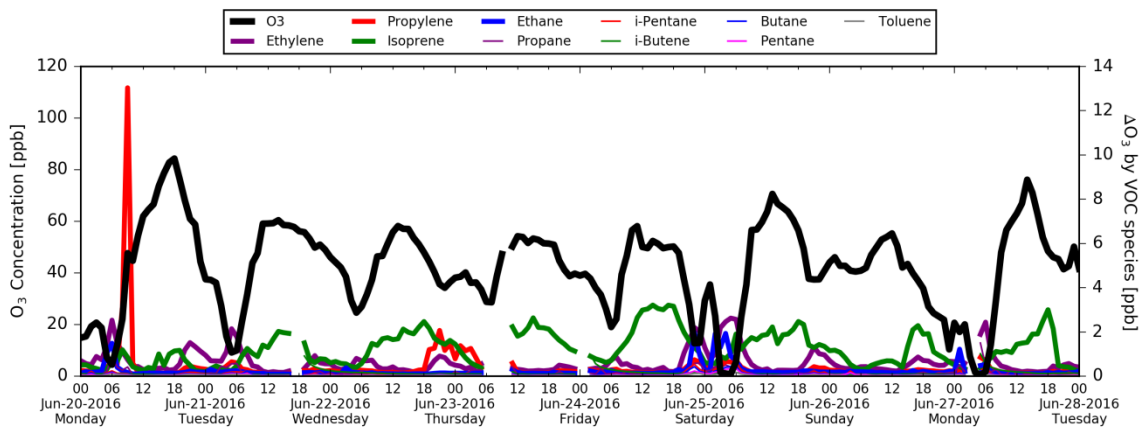


Figure 62. Time series of 1-hour ozone concentrations (left y-axis) and reactivity-weighted ozone concentration (right y-axis) for June 20-27, 2016.

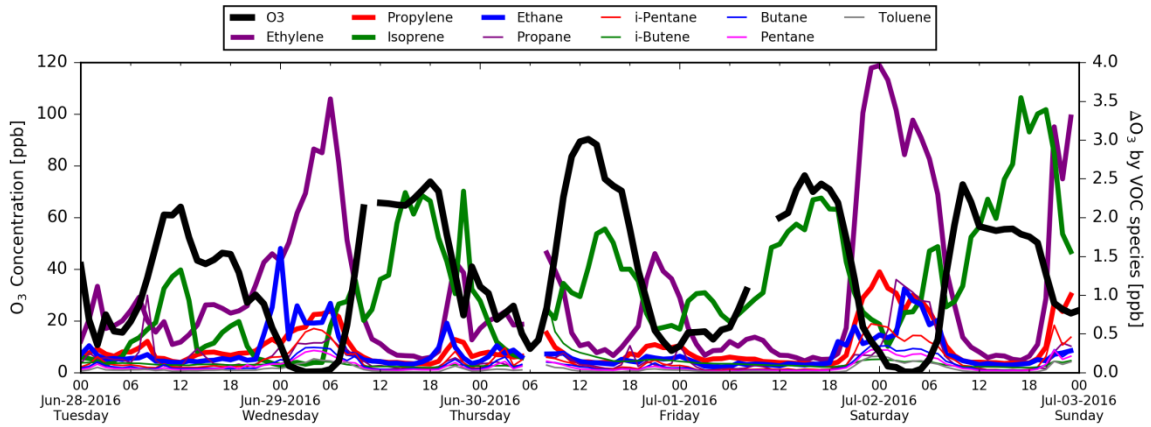


Figure 63. Time series of 1-hour ozone concentrations (left y-axis) and reactivity-weighted ozone concentration (right y-axis) for June 28-July 2, 2016.

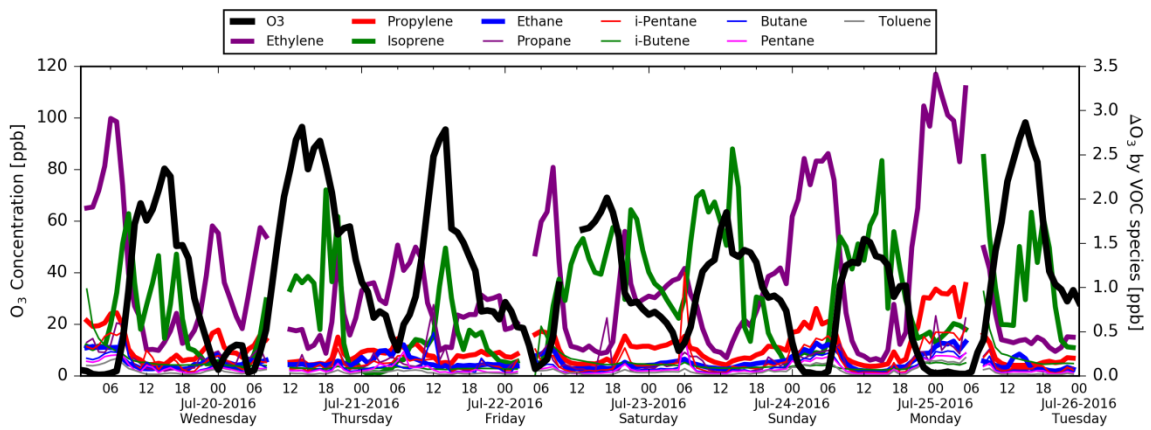


Figure 64. Time series of 1-hour ozone concentrations (left y-axis) and reactivity-weighted ozone concentration (right y-axis) for July 19-25, 2016.

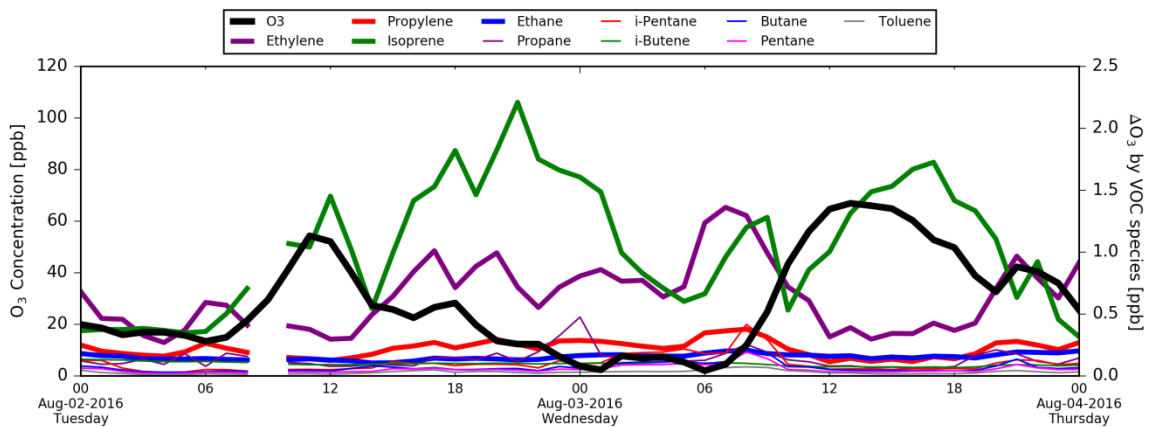


Figure 65. Time series of 1-hour ozone concentrations (left y-axis) and reactivity-weighted ozone concentration (right y-axis) for August 2-3, 2016.

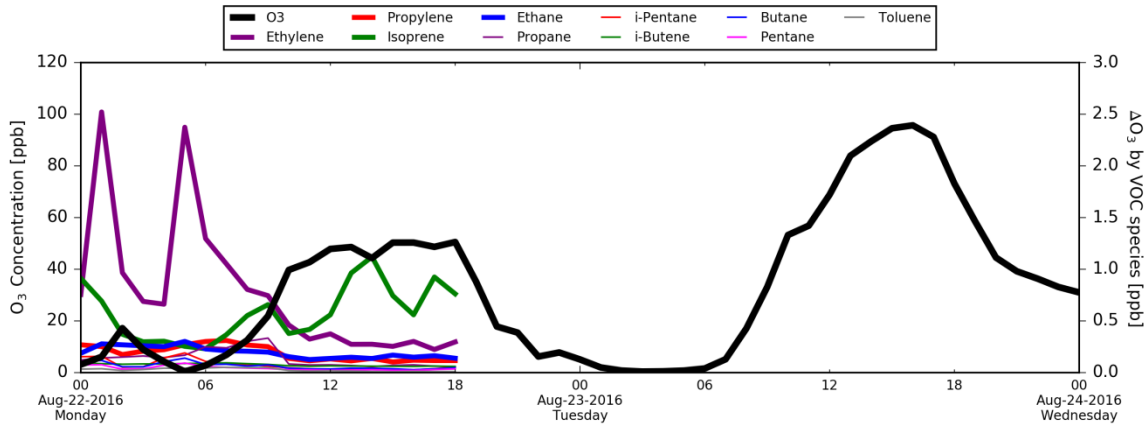


Figure 66. Time series of 1-hour ozone concentrations (left y-axis) and reactivity-weighted ozone concentration (right y-axis) for August 22-23, 2016.

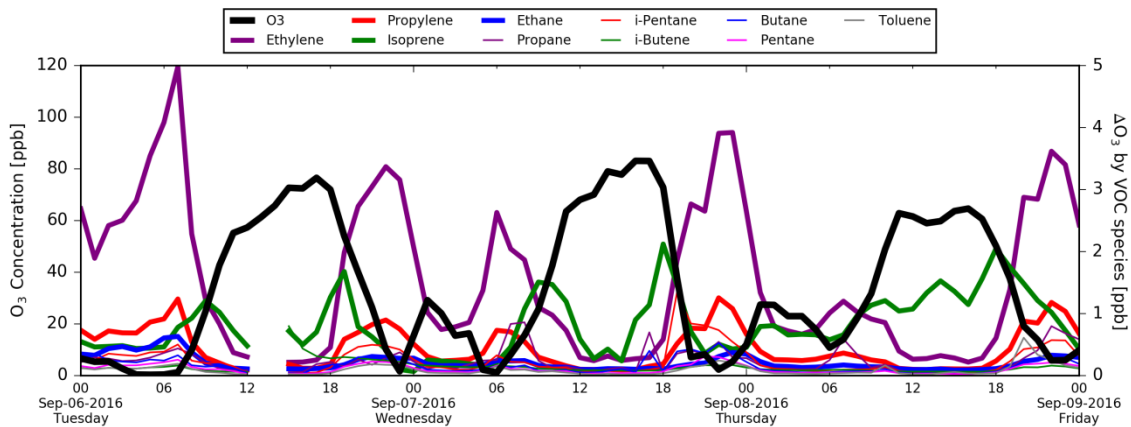


Figure 67. Time series of 1-hour ozone concentrations (left y-axis) and reactivity-weighted ozone concentration (right y-axis) for September 6-8, 2016.

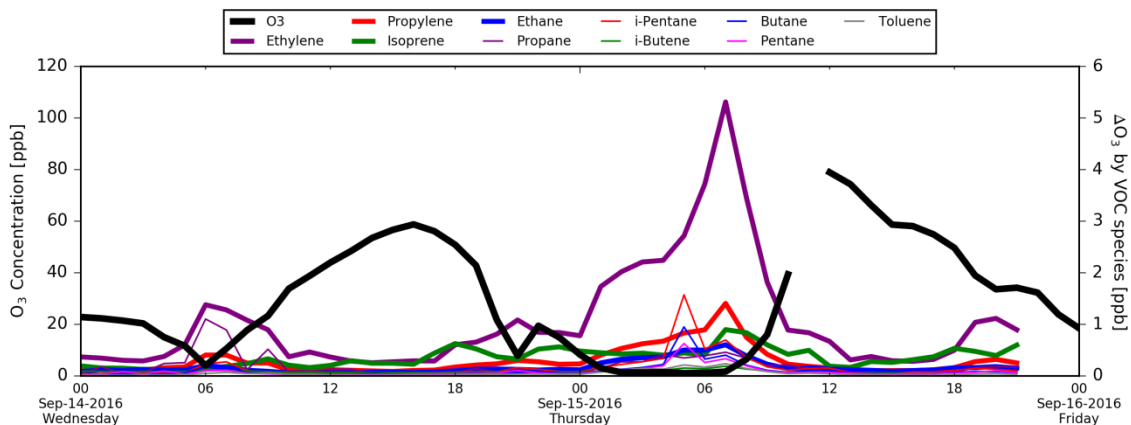


Figure 68. Time series of 1-hour ozone concentrations (left y-axis) and reactivity-weighted ozone concentration (right y-axis) for September 14-15, 2016.

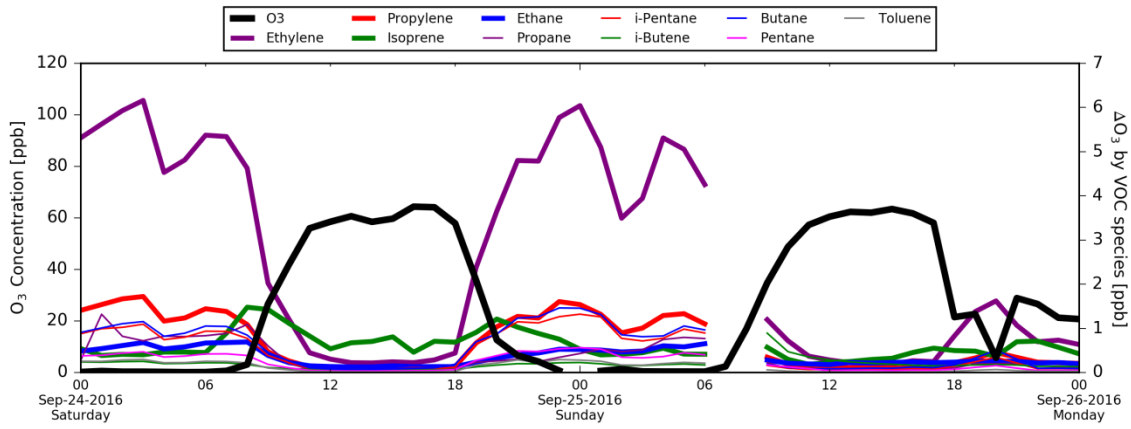


Figure 69. Time series of 1-hour ozone concentrations (left y-axis) and reactivity-weighted ozone concentration (right y-axis) for September 24-25, 2016.

10. Summary

Various in-depth analyses such as trend analysis of ozone exceedance and meteorological conditions in Atlanta during 1990-2016, multiple linear regression (MLR) analysis and classification and regression tree (CART) analysis to understand the relationship of Atlanta ozone and environmental variables, HYSPLIT back trajectory analysis to determine the origin of air masses and establish source-receptor relationships on ozone exceedance days, and analysis of VOCs and NO_x measurements to understand the impacts of precursors on ozone exceedance have been conducted to understand the causes of ozone exceedances in Atlanta during 2016. Both MLR and CART analyses have shown that ozone exceedances are likely to occur when relative humidity in the afternoon is low and daily maximum air temperature is high. These summertime meteorological conditions can occur in Atlanta under stable, stagnant conditions due to the presence of Bermuda and subtropical high pressure systems. The ozone exceedances are also associated with high ozone on previous days, low wind speed, and other meteorological variables with decreased correlation. HYSPLIT back trajectory analysis found that most 2016 ozone exceedances were linked to local air parcels. Also, the emissions from the Atlanta urban core area have been demonstrated to greatly impact local downwind monitors.

Analysis of NO_x measurements in the Atlanta urban core area along with ozone measurements found that ozone exceedance occurred more often on weekdays when the NO_x emissions from the dominant NO_x source (i.e. on-road mobile) in the Metro Atlanta area are higher. The morning time NO_x measurements on ozone exceedance days also tend to be higher due to the commuter traffic. The ratio of ozone and NO_x, an indicator of local ozone production efficiency, on exceedance days is close to previous studies, indicating a strong impact of NO_x on ozone formation. In addition, OMI NO₂ column data have similarly shown high NO₂ concentration on weekdays and a downward trend consistent with the trend in ozone concentrations.

Analysis of VOCs measurements in the Atlanta urban core area found a strong correlation of elevated ozone concentrations with biogenic VOCs and a moderate correlation with anthropogenic VOCs. Isoprene (from biogenic sources) is the top VOC species with high reactivity-weighted concentrations. Ethylene, propylene, and isopentane (all associated with gasoline use and mobile engines) are the top three anthropogenic VOC species with high reactivity-weighted concentrations.

In summary, the following factors likely contributed to 2016 ozone exceedances in Atlanta:

- 1) Low relative humidity in the afternoon;
- 2) High daily maximum air temperature;
- 3) Low cloud coverage;
- 4) High ozone on previous days;
- 5) Low wind speed;
- 6) NO_x emissions, mainly from local on-road mobile sources;
- 7) VOC emissions, mainly from biogenic sources in the summer months with additional contributions from local on-road mobile sources in the evening and morning hours; and
- 8) Local transport of emissions from the Atlanta urban core to monitors outside the urban core.

The following studies are recommended to further understand the causes of future ozone exceedances in the Metro Atlanta area:

- Co-located measurements of NO_x and VOC species at the five ozone monitors that are currently above the 2015 ozone standard;
- Aircraft measurements (ozone, NO_x, and CO) on elevated ozone days;
- Use of personal air sensors to understand spatial gradients;
- Ozone and NO₂ soundings to understand vertical profiles;
- Ozone profiles from LIDAR;
- Traffic studies using GPS speed data (Waze or Google maps) or GDOT “Navigator” speed and traffic data; and/or
- Modeling studies to examine the impact of various emission control strategies on ozone concentrations.

Such information may help us explore new options to prevent future ozone exceedances in the Atlanta area.

11. References

Blanchard, C.L., G.M. Hidy, S. Tanenbaum (2014). Ozone in the southeastern United States: An observation-based model using measurements from the SEARCH network, *Atmospheric Environment*, 88 192-200.

Blanchard, C.L., Hidy, G.M., Tanenbaum, S., 2010. NMOC, ozone, and organic aerosol in the southeastern United States, 1999–2007: 2. Ozone trends and sensitivity to NMOC emissions in Atlanta, Georgia. *Atmospheric Environment* 44, 4840–4849.
doi:10.1016/j.atmosenv.2010.07.030

Breiman, Leo, J. Friedman, R. Olshen, and C. Stone (1984). *Classification and Regression Trees*. Belmont, California: Wadsworth.

Bucsela, E. J., Krotkov, N. A., Celarier, et al. (2013). A new stratospheric and tropospheric NO₂ retrieval algorithm for nadir-viewing satellite instruments: applications to OMI, *Atmos. Meas. Tech.*, 6, 2607–2626, doi:10.5194/amt-6-2607-2013.

Cardelino, C., M. Chang, J. St. John, et al. (2011). Ozone Predictions in Atlanta, Georgia: Analysis of the 1999 Ozone Season, *J. Air & Waste Manage. Assoc.* 51:1227-1236.

Conner, T.L., Lonneman, W.A., Seila, R.L., 1995. Transportation-Related Volatile Hydrocarbon Source Profiles Measured in Atlanta. *Journal of the Air & Waste Management Association* 45, 383–394. doi:10.1080/10473289.1995.10467370

Heland, J., H. Schlager, A. Richter, and J. P. Burrows (2002). First comparison of tropospheric NO₂ column densities retrieved from GOME measurements and in situ aircraft profile measurements, *Geophys. Res. Lett.*, 29, 1983, doi:10.1029/2002GL015528, 2002.

Hidy, G.M., Blanchard, C.L., 2015. Precursor reductions and ground-level ozone in the Continental United States. *Journal of the Air & Waste Management Association* 65, 1261–1282. doi:10.1080/10962247.2015.1079564

Hidy, G.M., Blanchard, C.L., Baumann, K., Edgerton, E., Tanenbaum, S., Shaw, S., Knipping, E., Tombach, I., Jansen, J., Walters, J., 2014. Chemical climatology of the southeastern United States, 1999–2013. *Atmospheric Chemistry and Physics* 14, 11893–11914.
doi:10.5194/acp-14-11893-2014

Lamsal, L. N., N. A. Krotkov, E. A. Celarier, et al. (2014). Evaluation of OMI operational standard NO₂ column retrievals using in situ and surface-based NO₂ observations, *Atmos. Chem. Phys.*, 14, 11587–11609.

Laughner, J L., A. Zare, and R. C. Cohen (2016). Effects of daily meteorology on the interpretation of space-based remote sensing of NO₂, *Atmos. Chem. Phys.*, 16, 15247–15264.

Martin, R. V., D. D. Parrish, T. B. Ryerson, et al. (2004). Evaluation of GOME Satellite Measurements of Tropospheric NO₂ and HCHO Using Regional Data from Aircraft Campaigns in the Southeastern United States. *J. Geophysical Research* 109 (D24): D24307. doi:10.1029/2004jd004869.

National Research Council, 1999. Ozone-Forming Potential of Reformulated Gasoline. National Academies Press, Washington.

Therneau, T. M., E. J. Atkinson, M. Foundation (2015). An Introduction to Recursive Partitioning Using the RPART Routines, <https://cran.r-project.org/web/packages/rpart/vignettes/longintro.pdf>

Timofeev, Roman (2004). Classification and Regression Trees (CART), Theory and Applications, Master Thesis. <http://edoc.hu-berlin.de/master/timofeev-roman-2004-12-20/PDF/timofeev.pdf>

Tonnesen, Gail S., and Robin L. Dennis. 2000. “Analysis of Radical Propagation Efficiency to Assess Ozone Sensitivity to Hydrocarbons and NO_x : 1. Local Indicators of Instantaneous Odd Oxygen Production Sensitivity.” *Journal of Geophysical Research* 105(D7): 9213. http://apps.webofknowledge.com.proxy.lib.uiowa.edu/CitedFullRecord.do?product=WOS&colName=WOS&SID=4CFNLHuzDcKBGOYfWrU&search_mode=CitedFullRecord&isickref=WOS:000086586400025 <http://dx.doi.org/10.1029/1999JD900371>.

Seinfeld, J. H., S. N. Pandis (1998). Atmospheric chemistry and physics: from air pollution to climate change, Wiley.

Steinbacher, M., C. Zellweger, B. Schwarzenbach, et al. (2007). Nitrogen oxides measurements at rural sites in Switzerland: Bias of conventional measurement techniques, *J. Geophys. Res.*, 112, D11307, doi:10.1029/2006JD007971.

Zhang, Y., and Y. Wang (2016). Climate driven ground-level ozone extreme in the fall over the Southeast United States, *Proc. Natl. Acad. Sci.*, 113, 10025-10030, doi: 10.1073/pnas.1602563113.